REPRESENTATION AND ANALYSIS OF BIOMEDICAL SIGNALS USING FOURIER DECOMPOSITION METHOD

Thesis submitted in fulfilment of the requirements for the Degree of

Doctor of Philosophy

By

VIRENDER KUMAR MEHLA

Department of Electronics and Communication Engineering

School of Engineering and Applied Science

BENNETT UNIVERSITY

(Established under UP Act No 24, 2016)

Plot No's 8-11, Tech Zone II,

Greater Noida-201310, Uttar Pradesh, India.

November 2021

Declaration by the Scholar

I hereby declare that the work reported in the Ph.D. thesis entitled "**Representation and Analysis of Biomedical Signals using Fourier Decomposition Method**" submitted at **Bennett University, Greater Noida, India**, is an authentic record of my work carried out under the supervision of **Dr. Amit Singhal** and **Dr. Pushpendra Singh**. I have not submitted this work elsewhere for any other degree or diploma. I am fully responsible for the contents of my Ph.D. Thesis.

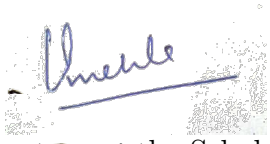

(Signature of the Scholar)

Virender Kumar Mehla

Enrolment No: E18SOE805

Department of Electronics and Communication Engineering

Bennett University, Greater Noida, India

Date: 18.11.21

Supervisor's Certificate

This is to certify that the thesis entitled "**Representation and Analysis of Biomedical Signals using Fourier Decomposition Method**" submitted by **Virender Kumar Mehla** at **Bennett University, Greater Noida, India** is a bonafide record of his original work carried out under our supervision. This work has not been submitted elsewhere for any other degree or diploma.

(Dr. Amit Singhal)
Assistant Professor
Department of ECE
Netaji Subhas University of Technology, Delhi
Date: 18.11.21

(Dr. Pushpendra Singh)
Assistant Professor
Department of ECE
National Institute of Technology Hamirpur
Date: 18.11.21

I would like to dedicate this thesis to my loving parents

Acknowledgements

My research work has been made possible through many blessings I received in my life. Firstly, I would like to thank God, the Almighty, for bestowing his blessings, without which I am nothing.

I would like to express my profound gratitude to my supervisors, Dr. Amit Singhal and Dr. Pushpendra Singh for their invaluable guidance, continuous encouragement, and support in every stage of the work. Their technical acumen, precise suggestions and guidance has been an invaluable source of inspiration and moral support.

I am deeply indebted to Prof. Rama S. Komaragiri and Dr. Manjeet Kumar whose encouragement helped me in all the time of the research. I would like to acknowledge Dr. Sanjay Kataria, Dr. Manoj Sharma and Dr. Urvashi Arora for their support.

I gratefully acknowledge the support provided by my fellow research scholars at Bennett University to get through the tough times during this work. My special thanks are due to Mr. Ramanna Ranganatham and Dr. Ashish Kumar for providing valuable suggestions and support whenever required. I am also grateful to all the members of ECE research lab for creating a joyful environment. I also thank all the staff members of Department of ECE, Bennett University for their help whenever needed.

Most importantly, my heartfelt gratitude to my family for their love and support throughout my life. With their blessings only, this work has been accomplished. I am indebted to my father, Shri Ishwar Singh and mother, Smt. Bimla Rani for their love and care. I would like to thank my wife Ms. Seema Mehla for all the support during these years. I regret for any inadvertent omissions because enlisting all the individuals whose contributions went into the making of the thesis is a very difficult task.

VIRENDER KUMAR MEHLA

Abstract

Due to rapid growth in the arena of health care sectors, various non-invasive tools, for instance electroencephalogram (EEG), electrocardiogram (ECG) and positron emission tomography (PET) have established their significance in the analysis and interpretation of various health issues such as brain disorders, heart diseases, sleep disorders and alcoholism identification. Epilepsy is one of the most prevalent neurological disorders in humans characterized by transient and hyper-synchronization movement of neuronal discharges in the brain cortex. Clinical information related to brain disorders is complex and multi-dimensional, and such information may produce an amalgamation of multiple research problems. Due to its low cost, high temporal resolution and non-invasive nature, EEG is the most frequently used technique for the analysis of various brain disorders. The detection of such abnormalities is usually performed by trained professionals using continuous monitoring of EEG recording, which is a tedious and challenging task that may produce inaccurate diagnosis results due to fatigue of trained experts. Therefore, numerous efforts have been made by the researchers towards the automatic detection of epileptic seizures.

The prime motive of this study is to develop automatic diagnosis and classification systems for the accurate detection of various brain abnormalities. Efficient and accurate classification of two class problems is explored, such as identification of seizure EEG signals, differentiation between alcoholic and non-alcoholic subjects, and localization of epileptogenic zones. The proposed study deals with various aspects including pre-processing of EEG signals, feature extraction and selection followed by classification. In pre-processing of EEG signals, various artifacts such as eye movements, baseline wander and power line interference are removed from the recorded EEG signals. Thereafter, decomposition of EEG signals is performed using Fourier decomposition method. Different levels and schemes for signal decomposition are investigated in this work. In the next stage, various time-domain, frequency-domain and statistical features

are extracted to analyze the dynamic behavior of the EEG signals. Further, Kruskal-Wallis approach is utilized to choose the significant features to reduce the size of the feature vector. Lastly, various learning algorithms are applied to assess the effectiveness of the proposed study. The simulation results show that the proposed work is an efficient technique for accurate classification of two class problems related to various brain disorders.

Contents

List of Figures

List of Tables

List of Abbreviations

ADC	Analog to Digital Converter
ALL	Accumulate Line Length
ANN	Artificial Neural Network
ANOVA	Analysis of Variance
ApEn	Approximate Entropy
AR	Auto Regressive
ASMF	Adaptive Switching Mean Filtering
AUC	Area Under Curve
BP	Band Power
BSS	Blind Source Separation
BW	Baseline Wander
CC	Centered Correntropy
CEEMD	Complete Ensemble Empirical Mode Decomposition
CNS	Central Nervous System
COV	Coefficient of Variation
CT	Computed Tomography
CV	Cross Validation
CWT	Continuous Wavelet Transform

DCT	Discrete Cosine Transform
DFT	Discrete Fourier Transform
DoG	Difference of Gaussian
DPE	Delay Permutation Entropy
DTCWT	Dual Tree Complex Wavelet Transform
DWT	Discrete Wavelet Transform
ECG	Electrocardiogram
EEG	Electroencephalogram
EEMD	Ensemble Empirical Mode Decomposition
EMD	Empirical Mode Decomposition
EMG	Electromyogram
EOG	Electrooculogram
EVD	Eigen Value Decomposition
EWT	Empirical Wavelet Transform
FAWT	Flexible Analytic Wavelet Transform
FD	Fractal Dimension
FDM	Fourier Decomposition Method
FFT	Fast Fourier Transform
FIBF	Fourier Intrinsic Band Function
FLP	Fractional Linear Prediction
fMRI	Functional Magnetic Resonance Imaging
FN	False Negative
FP	False Positive
FR	Fourier Representation

FS	Fourier Series
FT	Fourier Transform
FWHT	Fast Walsh Hadamard Transform
GMM	Gaussian Mixture Model
HMM	Hidden Markov Model
HMS	Hilbert Marginal Spectrum
HOS	Higher Order Spectra
HVD	Hilbert Vibration Decomposition
HWPT	Harmonic Wavelet Packet Transform
ICA	Independent Component Analysis
IF	Instantaneous Frequency
IMF	Intrinsic Mode Functions
IQR	Inter Quartile Range
kNN	k-Nearest Neighbor
KW	Kruskal Wallis
LBP	Local Binary Pattern
LDA	Linear Discriminant Analysis
LEE	Log Energy Entropy
LINOEP	Linearly Independent Non Orthogonal Yet Energy Preserving
LMS	Least Mean Square
LMT	Logistic Model Tree
LS-SVM	Least Square Support Vector Machine
MAD	Median Absolute Deviation
MDF	Median Frequency

MRLS	Modified Recursive Least Square
MSE	Mean Square Error
NCA	Neighborhood Component Analysis
NCRB	National Crime Records Bureau
NE	Norm Entropy
OWFB	Orthogonal Wavelet Based Filter Bank
PCA	Principal Component Analysis
PET	Positron Emission Tomography
PLI	Power Line Interference
PNS	Peripheral Nervous System
PSD	Power Spectral Density
RBF	Radial Basis Function
REM	Rapid Eye Movement
RNN	Recurrent Neural Network
ROC	Receiver Operating Characteristic
RP	Recurrence Plot
RQA	Recurrence Quantification Analysis
RSD	Resonance Based Signal Decomposition
RSI	Relative Sharpness Index
SD	Standard Deviation
SE	Sample Entropy
SNR	Signal to Noise Ratio
SSWT	Synchrosqueezed Wavelet Transform
STFT	Short-Time Fourier Transform

SVM	Support Vector Machine
TF	Time–Frequency
TFE	Time-Frequency-Energy
TN	True Negative
TP	True Positive
TQWT	Tunable-Q Wavelet Transform
VMD	Variational Mode Decomposition
WHO	World Health Organization
WPT	Wavelet Packet Transform
WT	Wavelet Transform
WVD	Wigner-Ville Distribution

Chapter 1

Introduction

A biological signal is a description of a physiological phenomenon. The human body is a system that is composed of several subsystems combined to perform myriad tasks. These subsystems include the nervous system, skeleton system, respiratory system, digestive system, muscular system and reproductive system. The human body functions properly due to the coordinated action of these systems. Each of the subsystems must work continuously and properly to keep people healthy. The human body is constantly communicating information about health in terms of some signals commonly known as biomedical signals.

1.1 Biomedical signals and their importance in healthcare

Biomedical signals are the source of information that aid in analyzing the physiological behavior of the living systems. The process by which significant information is extracted from these signals is called biomedical signal processing. The biomedical signals include electroencephalogram (EEG), electrocardiogram (ECG), electromyogram (EMG) and electrooculogram (EOG). The EEG records the electrical signals from the brain. The ECG, EMG and EOG signals capture the electrical activity of heart, muscles and eye movements, respectively. These signals play a significant role in monitoring and diagnosis of various health diseases such as cardiovascular diseases, epilepsy, sleep disorder, anesthesia, tumor, depression and Alzheimer's. Some of these disorders affect the functioning of the individual's brain. Therefore, it becomes important to understand the structure and functioning of the human brain before discussing

the diagnosis and effect of such diseases.

1.2 Human brain

The brain is a vital organ that is liable for observing and controlling numerous functions of the human body. It is an indisputable fact that everyone requires a healthy brain. The structure and functioning of a brain are highly complicated. This composite organ in association with the spinal cord and nervous system controls the information transmitted during various voluntary (reading, speaking) and involuntary (breathing, digestion) actions. It consists of four major parts: brain stem, cerebrum, diencephalon, and cerebellum. The cerebrum is the largest area of the brain which is sited on the upper portion of the brain. It is composed of four lobes, namely the parietal lobe, temporal lobe, occipital lobe and frontal lobe. The frontal lobe is responsible for cognitive functions, control of voluntary movement, emotion and problem-solving. The parietal lobe processes the information related to taste, touch and temperature. The occipital lobe is primarily responsible for vision. The temporal lobe has the responsibility to perform cognitive skills such as planning, organize, and controlling [1]. Fig. 1.1 represents various parts of the human brain [2].

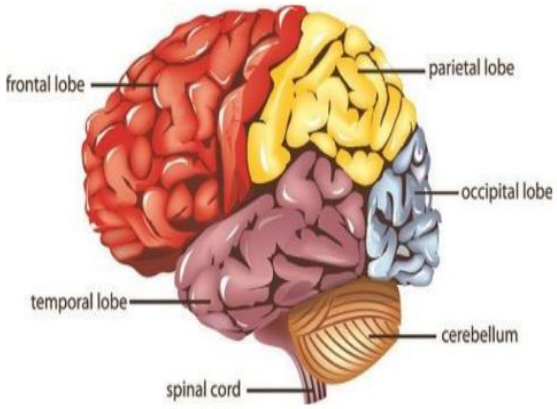

Figure 1.1: Parts of the human brain.

The brain is composed of numerous cells, including nerve cells and glial cells. These cells are the fundamental units of the nervous system that transmit the electrochemical signals between the brain and nervous system. The human nervous system can be divided into two parts: central nervous system (CNS) and peripheral nervous system (PNS) [3]. The main parts of the CNS are the spinal cord and the brain. The information is processed and controlled in this region. On the other hand, the PNS comprises all the nerves of the body associated with

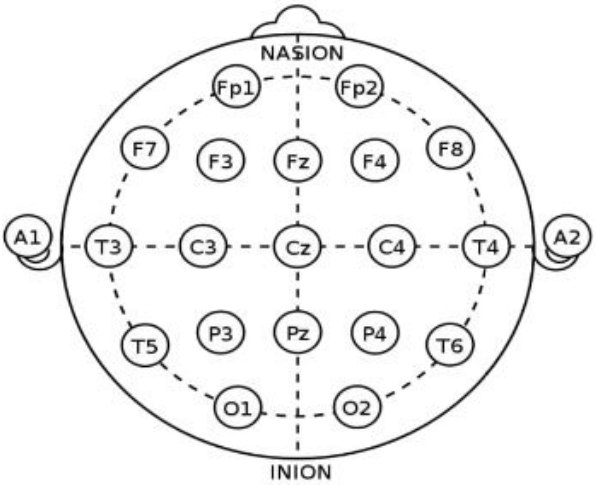

Figure 1.2: Electrode locations of International 10-20 system for EEG recording.

the CNS. A human brain is composed of approximately eighty-six billion nerve cells (neurons), which establish a huge number of connections with other neurons to build networks [4]. At rest, the neuron is negatively charged, having a potential of -70 millivolt (mV). When an excitation or a stimulus takes place, the neuron gets more positive ions. Once a neuron exceeds a certain level of threshold, i.e., -55 mV, an action potential is generated which enables the neuron to fire. Therefore, an electrical activity takes place among neurons within the brain. The information carried out by the neurotransmitters in terms of electric potential can be recorded using the EEG technique.

1.3 Electroencephalogram (EEG)

In 1924, a German physiologist, Hans Berger obtained the first human EEG signal. Subsequently, EEG has been adopted as one of the widely used non-invasive techniques in the field of medicine and research to record the biopotentials from the brain by mounting electrodes on the scalp. In comparison to other neuro-imaging methods, for instance, functional magnetic resonance imaging (fMRI), positron emission tomography (PET), and computed tomography (CT), EEG has high temporal resolution, relatively low cost, and measures the brain activity in milliseconds. EEG is employed to measure the spontaneous brain activity or the activity during an event [5]. Event-related potential refers to the activity associated with a particular event.

1.3.1 Acquisition of EEG signals

EEG is employed to capture brain information by mounting electrodes on the scalp. Monitoring of EEG has been an effective method for diagnosing many neurological illnesses and diseases. During an EEG test, several small sensors, called electrodes, are placed at different locations of the scalp using a special glue or paste. EEG electrodes are classified into two types: monopolar and bipolar. In monopolar electrodes, a potential difference is established between the scalp electrode and a reference electrode located close to the ear lobe. In bipolar electrodes, a potential difference is produced between two active electrodes located on the scalp. Each electrode is attached to an amplifier circuit and an EEG recording machine. The electrical signals from the brain are picked up by these electrodes and recorded on a computer [6]. There are two types of EEG recordings: scalp and intracranial EEG. A scalp EEG, a non-invasive technique, is used to record brain activity using electrodes attached to the different locations of the scalp using a conductive gel or paste. The intracranial EEG, an invasive technique, is obtained by applying special electrodes in the brain during surgery. In a normal adult, the amplitude of EEG recording is of the order of 10-100 microvolts when measured from the scalp. Since the structure of the human brain is not uniform, the EEG can vary depending upon the position of electrodes on the scalp. The standard method used to describe the location of scalp electrodes is the international 10-20 electrode system [7, 8]. Fig. 1.2 depicts the positions of the electrodes on the scalp according to this system. The location of the electrodes is determined by using two points: Nasion and Inion. The alphabets F, T, C, P and O refer to Frontal, Temporal, Central, Parietal and Occipital. The odd numbers shown in Fig. 1.2 refer to electrode locations on the left hemisphere, whereas the even numbers refer to electrode locations on the right hemisphere.

1.3.2 EEG brain rhythms

Signal morphology is adopted as an essential parameter for the recognition of various mental activities. The frequency of the EEG signals is affected by the mental activity of a person. These activities exhibit different wave patterns which are described using five frequency rhythms, i.e., delta, theta, alpha, beta and gamma rhythms as shown in Fig. 1.3 [9]. The description of these rhythms is as follows:

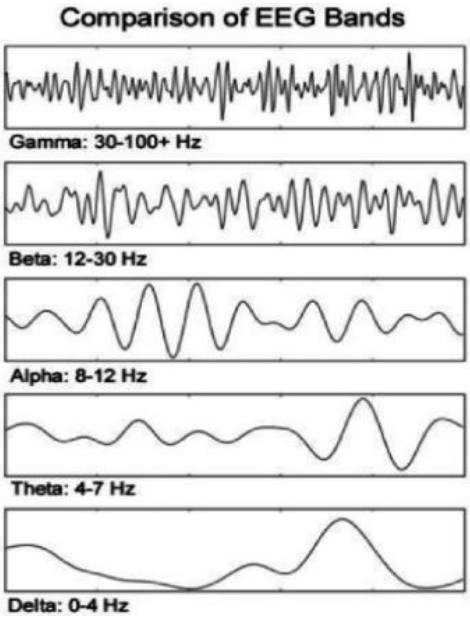

Figure 1.3: Five frequency rhythms of brain.

- Delta rhythms exist in the frequency range of 0-4 Hz having an amplitude of the order of 20-200 microvolt. These waves have low frequency and high amplitude. These waves are prominent in the occipital and temporal regions and appear during deep sleep in adults and children.

- Theta waves appear in the frequency range of 4-7 Hz and having an amplitude of less than 200 microvolts. These waves can be observed in the unconscious mind and they also exist during meditation and drowsiness.

- Alpha rhythms occur in the frequency range of 8-12 Hz and have an amplitude around 50 microvolts. These waves can be seen in the parietal and occipital regions during eye closed, wakefulness, very relaxed, and passive attention. These waves are mainly observed in adults. The frequency of alpha waves is impacted by various factors such as high blood glucose level, high body temperature and alert state. Alpha rhythms are abolished during thinking or alertness.

- Beta rhythms are high-frequency waves having a frequency range of 12-30 Hz and a low amplitude of 5-10 microvolts. These waves are irregular and variant. These waves can be recorded during various mental activities such as alertness, stress, fear and anxiety. Beta rhythms having high frequencies are associated with arousal states.

- Gamma waves possess a frequency range greater than 30 Hz. These waves are observed

during high mental activity such as cognition, learning and perception. These rhythms appear in each part of the brain.

1.3.3 Artifacts in EEG

Artifacts are defined as undesired signals which contaminate the actual shape of the recorded signal. These artifacts occur due to measurement from the recorded instruments or some movements of the human subject. They influence the utility of recorded EEG strongly and need to be removed for accurate analysis and diagnosis. They are mainly classified into two categories: extrinsic artifacts and intrinsic artifacts [10]. Both intrinsic and extrinsic artifacts are more relevant while accumulating vital information from the recording machine. The extrinsic artifacts arise due to defective electrodes, supply noise, and electrode contact noise. These artifacts may be minimized by designing a more accurate recording system and follow the precautions to avoid redundant motion-inducing artifacts. The intrinsic artifacts include all physiological artifacts such as eye movements, eye blinks, cardiac activity and muscle activity [10]. These physiological artifacts overlap with the activities of the neurons which may produce inaccurate results in clinical diagnosis. Therefore, it is essential to eliminate these artifacts from the recorded signals before being processed. However, these artifacts could be quite intricate to eliminate. Filter circuits can be employed to remove these artifacts if the frequency of these artifacts is not consistent with the desired signals. A summary of various kinds of physiological artifacts is provided below:

- Ocular Artifacts: The prime source of ocular artifacts is eye blinks and eye movements that disseminate through different electrodes located on the skull and get overlapped with the EEG activity. Artifacts caused by eye movements are generated due to variation in the orientation of the retina and cornea, while eye blinks artifacts happen because of the opening and closing of the eyelids during EEG activity. The signal generated by eye blinks and movements is measured using an EOG. The frequency of EOG signals resembles EEG signals, but its amplitude is much higher than the EEG signals.

- Muscular Artifacts: These artifacts happen due to muscle contraction or stretch during talking, sniffing, tongue movement, swallowing and chewing. The degree of muscle contraction is proportional to the amplitude of the artifacts. Low contraction provides low

amplitude artifact and vice versa. The muscular signals are recorded by EMG. These artifacts are mainly observed in the frontal and temporal lobes of the skull.

- Cardiac Artifacts: The electric potential produced by the human heart is measured using an ECG. This electric potential is transmitted to the skull, which gets mixed with the EEG activity. As a result, there exists a potential variation in the recorded EEG signal. There are two categories of cardiac artifacts: electrical and mechanical artifacts. The major cause of mechanical artifacts is slow and fast beats of the heart. The electrical artifacts primarily arise due to cardiac electrodes.

1.4 Need and motivation

Every human being in this universe wants to spend a healthy lifestyle. It is only possible if the person has a healthy brain. The brain is the most complex organ of the human body. The structure and functioning of the human brain are highly complicated. There could be various causes, such as brain injury, stroke, depression, tumor, epilepsy, dementia or Alzheimer's disease, for the occurrence of abnormalities in the human brain. Epilepsy is one of the most prevalent neurological disorders characterized by the transient and hyper-synchronization movement of neuronal discharges in the human brain [11]. According to a report by World Health Organization (WHO), approximately two percent of the total population are suffering from epilepsy worldwide [12]. Moreover, half of the epileptic cases are observed in youth or adolescence. It has been estimated that 80% of the people having epilepsy are residing in low and middle income countries. Around 70% of epileptic patients might spend their lives seizure-free if they are diagnosed and treated properly. Subjects suffered from epileptic seizures have a high chance of dying prematurely in comparison to a healthy person [12]. Epileptic seizures arise due to malfunctioning of the electrical and physiological activities in the brain which produces transient electrical activities in neurons present in the brain cortex. Therefore, the investigation of epilepsy has consistently been of the most extreme significance in the biomedical area of research. The diagnosis of epilepsy is mainly performed by the trained experts and neurologists when conducting continuous monitoring of the EEG recording, which is a time-consuming, tedious, and challenging task. It may result in inaccurate diagnosis results due to the fatigue of

trained experts. There is a need to develop an automated epileptic seizure detection technique for the accurate classification of EEG signals.

Alcoholism is considered the third highest risk factor for early death and disability which is caused by the excessive consumption of alcohol. Although a controlled consumption of alcohol might give some health benefits, yet excessive consumption of alcohol can lead to a variety of health problems, such as cancer, cardiovascular and liver diseases. According to a report published by WHO, approximately three million deaths occurred globally due to harmful use of alcohol, out of which 75% are among men [13]. Globally, nearly two billion people occasionally drink alcohol in their daily lives while 82 million people are severely addicted to alcohol. In recent years, the consumption of alcohol in India has increased to a great extent. According to a survey reported by National Crime Records Bureau (NCRB), in every two hours, one emergency related to destructive use of alcohol is recorded in India [14]. A large population residing in the rural region in India is highly addicted to alcohol due to scarcity of awareness. In the literature, the neuro experts confirmed that alcoholism is the prime cause for variation in neurological activities, which are accountable for various mental disorders. Alcoholism adversely affects the central nervous system and other organs of the human body [15]. The diagnosis of above stated neurological disorders is usually performed by neuro-experts and clinical professionals by the manual screening of EEG recording, which may produce inaccurate results. It is complex to analyze EEG signals in presence of artifacts for alcoholism detection. Hence, it becomes necessary to develop novel and efficient approach for automated alcoholism identification using machine learning techniques.

1.5 Identifying the research problem

Signal analysis plays a major role in biomedical applications. It is a transformation where meaningful information is captured from the biomedical signals using analytical and logical approaches. In the real-world, most of the signals such as biomedical signals, speech signals, seismic signals are non-stationary that are generated from non-linear systems. The non-stationary behavior of the EEG signal is analyzed using various decomposition techniques by segmenting the entire signal into several individual components and analyze each component separately. A computer-based signal processing technique is primarily divided into four sections namely:

pre-processing, feature extraction and selection, followed by classification. In the first stage, pre-processing has been employed to remove the unwanted artifacts and noise from the EEG signals and convert them into a suitable format for further processing. Further, a number of techniques based on time-domain [16, 17, 18], frequency-domain [19, 20], time-frequency domain [21, 22, 23, 24, 25, 26, 27] and non-linear approaches [28, 29, 30] have been presented to investigate various brain disorders. Time-domain analysis of the signals does not provide relevant information about the frequency components of EEG signals. Fourier transform (FT) has been employed to get information about frequency contents. FT is a popular technique used to analyze stationary signals. Since EEG signal has non-stationary behavior in nature, FT is not an efficient tool for analyzing EEG signals.

Various time-frequency methods such as short-time Fourier transform (STFT) [31], wavelet transform (WT), multi-wavelet transform [27] and synchrosqueezed wavelet transform (SSWT) [32] have been employed for analysis of non-stationary behavior of EEG signals. Since STFT uses a fixed window size, it is not possible to obtain high resolution for the low and high frequency components of the signal simultaneously. This resolution problem is resolved using WT because it has the provision to adjust the window size. The analysis is carried out with a scaled and shifted version of a basic function called wavelet. The wavelet could be scaled and shifted in time during signal analysis to provide a variable resolution in time and frequency. WT method provides good frequency resolution for low frequencies and good time resolution for high frequency components. When applying the WT method, it is somewhat difficult to select the most appropriate kernel function as well as the number of decomposition levels. Further, several adaptive signal decomposition frameworks such as eigenvalue decomposition (EVD) [33], variational mode decomposition (VMD) [34], empirical mode decomposition (EMD) [35] and resonance-based signal decomposition (RSD) [36] have been developed to analyze the non-linear and non-stationary behavior. Out of these techniques, EMD is the most popular method across various applications such as artifacts' removal, seizure detection, recognizing driver fatigue, detection of Alzheimer's disease and sleep stage classification. However, this technique suffers from the mode-mixing problems, end-effects artifacts, inaccurate results in presence of noise and loss of significant information while removing artifacts from biological signals. In most of the research works, the authors have designed and evaluated algorithms on a single dataset.

The epilepsy detection system is designed based on only five subjects' database which makes the algorithm not reliable for clinical use. Many works are based on uneven training dataset without considering the problem of class imbalance. Hence, the evaluation metrics such as sensitivity, specificity, and accuracy are not reliable. Also, there do not exist methods that are clinically validated on the data collected from various resources. To address these problems, a novel signal decomposition method, known as the Fourier decomposition method (FDM) in conjunction with machine learning approach is proposed to analyze EEG signals for automated disease detection.

1.6 Objectives of the work

Based on the above-mentioned brief overview, the following are identified as objectives of the proposed work:

- To develop a novel signal decomposition technique for the pre-processing of the EEG signals that suppresses the artifacts and noise.
- To develop an efficient feature extraction technique to recognize the patterns that characterize the dynamic non-stationary behavior of the brain.
- To develop a suitable machine learning approach that utilizes the extracted features to monitor, diagnose, and classify various brain-related disorders.
- Comparing the performance analysis of the proposed algorithm with the existing state-of-the-art methods for widely used and publicly available databases for EEG signals.

1.7 Outline of thesis

The proposed study is comprised of seven chapters. Chapter 1 presents the basic introduction of biomedical signals, description of the human brain, acquisition of EEG signals, EEG rhythms, artifacts encountered during EEG recordings, needs and motivation, and finally, the objectives of the work and the organization of the thesis. Chapter 2 provides a detailed literature review of various techniques used for automatic detection and classification of various brain abnormalities such as epileptic seizure detection, alcoholism detection and identification of epileptogenic

regions. In Chapter 3, a detailed study about the pre-processing of the EEG signals has been presented. In Chapter 4, a novel approach for the identification of brain abnormality such as alcoholism detection is presented using the Fourier decomposition method. In Chapter 5, an efficient method for automatic epileptic seizure detection from EEG signals using Fourier analysis is discussed. In Chapter 6, an accurate technique for the classification of focal and non-focal EEG signals using the Fourier decomposition method is discussed. In Chapter 7, we summarize the contributions of this thesis and present the future scope of the study and also outline some directions for proposed future work.

Chapter 2

Literature survey

Due to fast growth and developments in the healthcare sector, neuroscience becomes an emerging area of research that deals with monitoring, analysis and diagnosis of various brain disorders such as epilepsy, sleep disorder, tumor, stroke, Alzheimer's, alcoholism and brain death, using EEG signals. The role of EEG in clinical applications is quite significant and there exist plenty of research articles that have explored novel ideas and concepts in the EEG analysis, interpretation and related applications. It is impracticable to discuss all the research efforts for building diagnostic systems using different biomedical signals such as EEG, ECG and EMG. However, a comprehensive review related to the topic of the thesis has been presented. The current review is mainly focused on the techniques employed for analysis of various brain abnormalities such as epilepsy detection, alcoholism detection and identification of epileptogenic zone in the brain.

2.1 Epilepsy detection

In the last few decades, various attempts have been made by researchers for the automatic detection of epileptic seizures using EEG signals. Liu et al. in [37] identify periodic discharges in EEG signals using the autocorrelation method for neonatal seizure detection, but this approach is not accurate for patients of all ages. The fractional linear prediction (FLP) technique, explored in [38], utilized signal energy as a feature to differentiate between ictal and seizure-free EEG signals. In [39], various entropy-based features are considered to extract information from the EEG signals. Since these techniques consider the time-domain signal, hence the frequency information does not get captured completely. Fourier transform (FT) is used in [40] to extract

EEG rhythms for the classification of EEG signals. From the literature, it has been estimated that EEG signals exhibit a non-stationary behavior [41, 42, 43] which means the frequency content of EEG signals changes with time. Hence, conventional approaches based on FT are not efficient tools to precisely obtain the attributes of EEG signals, because they are widely used for analyzing stationary signals. Fourier-Bessel expansion series has been considered in [42, 44]; however, it does not provide complete time-frequency information of the signal. Tzallas et al. in [43] employed a time-frequency-based method using different time and frequency smoothing windows for the automatic diagnosis of the seizure by computing fractional energy from various EEG segments in the time-frequency plane. Srinivasan et al. in [45] performed an experiment by computing time-domain and frequency-domain features from the pre-processed EEG signal and passed these features to the recurrent neural networks (RNN) for the automatic diagnosis of an epileptic seizure. Tzallas et al. in [46] demonstrated the STFT method for the localization of epilepsy. Power spectral density (PSD) has been computed from each segment of the EEG signal and used as input features to artificial neural network (ANN) for the classification of epileptic seizures. Using a short window in the time domain leads to poor frequency resolution and vice-a-versa. It is difficult to obtain a good resolution in both the time and frequency domain simultaneously.

Wavelets transform (WT) is applied in [47, 48] for seizure detection as it offers flexibility in varying the window size as per requirements. Subasi in [49] introduced the discrete WT (DWT) method and a mixture of experts network for the accurate identification of epileptic seizures. In [50, 51], the DWT technique is applied to decompose the EEG signals into several frequency bands for the classification of EEG signals. Rafiuddin et al. in [52] computed two features, namely, interquartile range (IQR) and median absolute deviation (MAD) using a wavelet-based approach for the demarcation of seizure and seizure-free events. In [53], the authors explored multi-wavelet transform for automatic epileptic seizure detection where approximate entropy is derived as an input feature, but this method has a higher dependency on the signal length and suffers from a bias because of self-counting. The proper choice of mother wavelet and the number of decomposition levels is difficult to select while implementing the wavelet method. Further, several attempts [54, 55, 56, 57] have been made to analyze the non-stationary behavior of EEG signals using the EMD technique. In [54], Alam et al. have used third order and higher-order

moments of intrinsic mode functions (IMFs) as features for the detection of epileptic seizures. Spectral centroid and skew are obtained as features in [55], while the phase space representation of IMFs is considered in [56]. The ellipse area covered by the second-order difference plot of IMFs is utilized in [57] for the classification of ictal and seizure-free EEG signals. Dash et al. in [58] considered three features, i.e., PSD, variance, and fractal dimension (FD) of IMFs to classify seizure and non-seizure events using the hidden Markov model (HMM).

Hassan et al. in [59] presented a popular variant of the EMD method for the identification of epileptic seizures. An adaptive boosting algorithm is adopted to discriminate between normal and epileptic EEG signals. Hilbert Huang transform (HHT) is applied in [60, 61] to decompose the signal using EMD and extract instantaneous frequency using Hilbert transform to identify seizure EEG signals. Alickovic et al. in [62] considered both EMD and wavelet-based signal decomposition for the accurate detection of seizures. The original EMD, although popular, has many limitations such as mode mixing, detrend uncertainty, end effect artifacts, non-orthogonality of IMFs, non-uniformity, and scale alignment of IMFs. The mode mixing and detrend uncertainty issues were resolved in ensemble EMD (EEMD) [63] and complete ensemble EMD (CEEMD) [64], however, they increase the computational complexity many times. The orthogonality issue has been resolved by orthogonal and energy preserving EMD algorithm [65]. Further, the non-uniformity and scale alignment problem of IMFs is resolved in multivariate EMD [66]. In all these variants of EMD, there is a lack of mathematical background for the EMD algorithm, for example, the dependence of IMFs on number of sifting and the stopping criteria, convergence and also the stability to noise perturbations.

2.2 Identification of alcoholism

Alcoholism is considered a neurological disease characterized by excessive consumption of alcohol, where a person has no control over alcohol intake [67]. Alcoholism is mainly classified into three categories: mild, moderate, and severe. Although mild or moderate consumption of alcohol provides some health benefits, including reduced risk of diabetes and heart diseases, yet excessive consumption of alcohol might cause various health problems, such as stroke, liver diseases, cardiovascular diseases, cancers and cirrhosis. According to the report published by WHO, approximately eighty-two million people are severely addicted to alcohol [68, 69]. The

excessive use of alcohol is responsible for economic losses to individuals and society as well. Among various neuroimaging techniques, EEG is the most popular technique for studying the complex dynamics of brain functioning. It is suitable for real-time recognition of mental disorders and provides a better correlation with the complex functioning of the human brain [70, 71]. The data recorded by EEG signals are non-linear and non-stationary, hence, it is not reliable to interpret the data by visualization. Also, evaluation using a questionnaire-based approach could involve miscalculation during screening and estimating the actual amount of alcohol consumption unless handled by neuroimaging techniques such as EEG [72, 73]. Initially, time-domain and frequency-domain-based methods are employed for analysis and interpretation of recorded EEG signals [74, 75]. These methods do not provide complete information about the non-stationary behavior of the EEG signals effectively. To overcome this problem, time-frequency (TF) based frameworks, namely, STFT, WT, wavelet packet transform (WPT) and empirical wavelet transform (EWT) are discussed.

In [76], continuous wavelet transform (CWT) is used to decompose EEG signals for extracting TF features. Four statistical features are computed from wavelet coefficients and passed as inputs to several models of classification for alcoholism detection. In [77], the tunable-Q wavelet transform (TQWT) is explored to compute centered correntropy (CC) based features for the diagnosis of alcoholism using EEG signals. Faust et al. in [78] discussed the WPT method for the detection of alcoholic and non-alcoholic EEG signals. Detailed and approximation coefficients up to the third level are extracted from the decomposed EEG signals. After that, energy from each sub-band is calculated as a feature. Acharya et al. in [79] tested non-linear features for the discrimination of alcoholic and normal EEG signals using a support vector machine with different kernel functions. In [80], the author introduced an autoregressive (AR) model to classify normal and alcoholic EEG signals using gamma-band visual evoked potential signals. Using a linear discriminant (LD) classifier, the proposed method achieved the best discrimination performance. Faust et al. in [81] applied fast Fourier transform (FFT) and AR model for computing PSD from the stationary segment of the recorded EEG signals to recognize various mental states such as healthy, alcohol and epilepsy. In [82], the authors adopted two non-linear methods, known as recurrence plot (RP), and recurrence quantification analysis (RQA), for discriminating three classes, namely, normal, epilepsy and alcoholic using

six different classifiers. The result showed that the Gaussian mixture model (GMM) produces the best result in comparison to all other classifiers. In [83], power and coherence estimates computed from the recorded EEG signals are utilized as input features to three different classifiers for the classification of alcohol and healthy EEG signals. Mumtaz et al. in [84] applied machine learning technique on EEG data acquired from three different classes of participants for the classification of alcohol abusers, normal and alcoholic EEG signals. The classification is carried out using four different classifiers, where the logistic model tree (LMT) classifier achieved the best classification accuracy among these classifiers. Faust et al. in [85] adopted an automated system for discrimination of alcoholic and healthy EEG signals by computing non-linear features such as higher-order spectra (HOS) from the recorded EEG signals.

2.3 Identification of epileptogenic zone

The authors in [86] examined the localization of the epileptogenic zone by observing the asymmetries in the delta activity using EEG signals captured from epileptic and control subjects. Zhu et al. in [87] employed delay permutation entropy (DPE) as a feature to classify epileptogenic and non-epileptogenic zones. This feature is fed to an SVM classifier to recognize the epileptogenic zone. It has been revealed that the DPE index was found to be smaller for the epileptogenic zone in comparison to the non-epileptogenic zone. In [88], a compressed EEG display based on relative sharpness index (RSI) is presented to highlight epileptogenic sites in the multichannel intracranial EEG recordings. The authors in [89] explored various wavelet functions namely non-orthogonal, orthogonal and bi-orthogonal basis for the identification of epileptic events by computing the wavelet coefficients' energy at different scales. The authors in [90] applied the EWT technique for the discrimination of focal (F) and non-focal (NF) EEG signals by computing entropy-based attributes from the EEG rhythms. Using 10-fold cross validation (CV) scheme, high classification accuracy is obtained using the SVM classifier. In [91], the authors applied the DWT method for the discrimination of F and NF EEG signals and observed that high decomposition levels of wavelet coefficients degrade the performance of the proposed method. In [92], a novel method is presented based on the dual-tree complex wavelet transform for accurate detection and classification of F and NF EEG signals by computing mean and standard deviation from the wavelet coefficients. Chen et al. in [93] applied DWT

for the localization of epileptogenic focus by discriminating F and NF classes. Wavelet coefficients are obtained by decomposing the EEG signals into various frequency bands using DWT. Nine features, elicited from the wavelet coefficients, are supplied as input features to the SVM classifier to identify F EEG signals. Another research work by Acharya et al. in [94] adopted wavelet packet decomposition (WPD) to detect epileptic activity using the Gaussian mixture model algorithm. In [95], the authors have designed an automated system based on flexible analytic wavelet transform (FAWT) for the detection of focal epilepsy. Three entropies, drawn out from sub-bands signals, are applied as input features to the least squares SVM (LS-SVM) classifier for the accurate diagnosis of focal epilepsy. Sharma et al. in [96] deploy TQWT for the detection of F EEG signals. Nine features, computed from sixteen sub-bands, are employed as input features to the LS-SVM classifier to reveal the complex behavior of the EEG signals.

Chapter 3

Pre-processing of EEG signals

3.1 Introduction

The prime objective of the signal processing techniques in real-time applications is to investigate the characteristics of the recorded signals by analyzing their elementary building blocks or individual components. The signal processing aims is to extract significant information from the recorded data using transformation techniques and utilize those techniques that enhance our perception of information and structure present in the signal. Due to low cost and high temporal resolution, EEG is one of the most widely used non-invasive tools for the analysis and diagnosis of various brain abnormalities in neuroscience. The prime disadvantage of this technique is that various physiological and non-physiological artifacts get intermingled with the recorded EEG signals. The physiological artifacts include eye blinks, eye movements, heart activity, sweating, muscle activity and many more. The non-physiological artifacts arise due to faulty electrodes, supply noise, ventilation and other similar factors. As the frequency of the ocular artifacts resembles that of the EEG signals, it is highly complex to identify and eliminate these artifacts from the recorded EEG data. Therefore, it is an essential step to eliminate these artifacts before being utilized for further processing of the recorded signals. For this, numerous artifacts removal techniques, namely regression method, filtering methods, blind source separation (BSS) approaches such as principal component analysis (PCA) and independent component analysis (ICA), WT, EMD and hybrid methods have been investigated by many researchers in the literature [97] - [106].

The traditional method for removing the undesired signals from the recorded EEG signal

is the regression method. It is a commonly used approach to eliminate ocular artifacts from the recorded EEG data in both time-domain and frequency-domain. Gratton [97] suggested a time-domain regression method for reducing the eye movement artifacts from the raw EEG signals. Woestenburg [98] implemented a novel method based on frequency-domain regression analysis for the removal of eye movement artifacts from the signal of interest. Later, Jung et al. [99] observed that this method is not suitable for eliminating muscle artifacts and supply noise as these artifacts do not possess any reference channel. Also, this method has an inherent issue that movement of excitation exists between EOG artifacts and EEG is bidirectional. Jung et al. [100] proposed the PCA approach, a type of BSS technique, for the separation of eye movement artifacts from the multichannel EEG recordings. Although the BSS method outperformed the regression approach, this technique was not appropriate for the complete removal of eye artifacts from the signal of interest, especially when both the waveforms have similar amplitudes. An advanced version of PCA, known as ICA, is investigated by Vigario [101] to extract artifacts due to eye activity from the recorded EEG signals. Romero et al. [102] applied the ICA technique for the reduction of EEG artifacts during different sleep stages such as awakeness, rapid eye movement (REM) sleep and delta sleep. Further, Kher et al. [103] described the adaptive filtering method using the least mean square (LMS) algorithm for eliminating eye movement artifacts from the recorded EEG data. Mosquera et al. [104] presented a novel approach based on adaptive filtering using a recursive least square algorithm and ICA for removing EOG artifacts from the recorded EEG signals. Chen et al. [105] explored an efficient hybrid method using DWT and Kalman filter to remove ocular artifacts from the signal of interest by minimizing mean square error (MSE). Ghandeharion et al. [106] applied an approach based on ICA and WT for the identification and removal of ocular artifacts.

In [107], authors applied the Hilbert vibration decomposition (HVD) approach in the pre-processing stage for the removal of baseline wander noise. A hybrid approach based on discrete-time oscillator, adaptive notch filter and modified recursive least square (MRLS) is reported in [108] for the elimination of powerline interference (PLI) noise from various biomedical signals. The authors in [109] applied a finite impulse response (FIR) filter to eliminate low frequency baseline wander (BW) and high frequency PLI noise components from the recorded ECG signals.

3.2 Empirical mode decomposition (EMD)

The empirical mode decomposition (EMD) proposed in [110] is an effective approach for the decomposition and analysis of non-stationary signals. EMD is a simple, adaptive and data-dependent algorithm that is used to analyze nonlinear and non-stationary signals. EMD algorithm decomposes any real signal into several band-limited oscillatory components, which are known as intrinsic mode functions (IMFs) [111]. Every IMF has to satisfy the following two basic conditions:

1. The number of extrema (i.e., local minima and maxima) are equal to the number of zero-crossings or at most differ by one.

2. The mean value of envelope, obtained by averaging of the upper and lower envelopes obtained from extrema, is zero at any instant of time.

To decompose a non-stationary signal using EMD algorithm, the following steps may be followed:

1. Identify local maxima and local minima in the signal.

2. Obtained an upper and a lower envelope by using cubic spline interpolation of the local maxima and minima, respectively.

3. Subtract the mean envelope from the signal.

4. Iterate until the number of extrema is equal to the number of zeros or utmost differ by one.

5. Subtract the obtained IMF from the signal.

6. Repeat the above steps until the final residue is a constant value or no more IMFs can be obtained from it.

The original time-series $s[n]$ after decomposition, can be expressed as:

$$s[n] = \sum_{i=1}^{M} y_i[n] + r_M[n], \tag{3.1}$$

where M represents the number of IMFs, $y_i[n]$ is the i^{th} IMF and $r_N[n]$ denotes the final residue. After extracting IMFs from the real signal $s[n]$, the next step is to obtain the corresponding analytical signal $z_i[n]$ as follows:

$$z_i[n] = y_i[n] + j\hat{y}_i[n], \tag{3.2}$$

where $\hat{y}_i[n]$ represents Hilbert transform of $y_i[n]$ which is defined as: $\hat{y}_i[n] = y_i[n] * \frac{1}{\pi n}$. Equation (3.2) can be written in polar representation as

$$z_i[n] = a_i[n].e^{j\phi_i[n]}, \tag{3.3}$$

where $a_i[n] = \left(y_i^2[n] + \hat{y}_i^2[n]\right)^{1/2}$ is the instantaneous amplitude of the analytical signal, and $\phi_i[n] = \tan^{-1}\left(\hat{y}_i[n]/y_i[n]\right)$ is the instantaneous phase.

Since EMD is an adaptive time-series decomposition algorithm, it is employed for the analysis of various non-stationary signals and non-linear systems. In recent years, this algorithm has become very popular in numerous fields such as healthcare sectors, medical studies, meteorology, geophysical studies and image analysis. In [112], the authors applied a new EMD based approach and Hurst exponent for the cancellation of BW noise from the ECG signals. Anapagamini et al. in [113] suppressed the first IMF of the EMD decomposed signal for the cancellation of the PLI noise. Rakshit et al. in [114] introduced a hybrid method based on EMD and adaptive switching mean filtering (ASMF) for the removal of high-frequency noises and upgrading the signal quality. The validity of the proposed technique is carried out on a publicly available MIT-BIH arrhythmia database. Even though the EMD approach possesses considerable success in many applications, this algorithm is mainly reliant on empirical, heuristic procedures which make it hard to analyze mathematically. The EMD may suffer from detrend uncertainty, mode mixing, end effect artifacts, non-uniformity, non-orthogonality of IMFs and scale alignment of IMFs. Despite all these problems, the EMD algorithm is still a widely-used and most successfully adaptive data analysis tool for nonstationary signals [110, 111]. Therefore, we use EMD in this thesis as a reference to establish the validity and calibration of the proposed studies. In [115], the authors presented various signal decomposition approaches such as EVD, normalized sign least mean square (NSLMS), MRLS, EMD-WT and Fourier

decomposition method (FDM) for the pre-processing of ECG signals. It has been observed that out of these techniques, the FDM technique suppressed the BW and PLI noises from the recorded ECG signals most effectively, for the accurate diagnosis of the patients. The FDM has shown better performance than state-of-the-art methods at different levels of signal-to-noise ratio [115]. Recently, FDM method has been employed for the analysis of speech signal, seismic signals [116, 117, 118], sleep apnea [119], gravitational wave analysis [120], image decomposition [121], diagnosis of dementia disease [122], and also for the modeling, prediction and continuous monitoring of COVID-19 pandemic [123]. In this thesis, we investigate and use the FDM for the analysis of nonlinear and non-stationary time-series signals such as EEG signals for automatic identification of alcoholism and identification of epileptic seizures.

3.3 Fourier Decomposition Method (FDM)

In this section, we discuss a recently proposed algorithm based on the Fourier representation (FR), known as the FDM, for the analysis of nonlinear and non-stationary time-series signals [116]. In the classical Fourier series representation, an infinite set of sine and cosine functions of constant amplitudes and constant frequencies form the basis functions, and a periodic signal can be represented as

$$s(t) = \sum_{k=-\infty}^{\infty} C_k \exp(j2\pi k f_0 t), \tag{3.4}$$

where $f_0 = 1/T$ is the fundamental frequency, and

$$C_k = \frac{1}{T}\int_0^T s(t)\exp(-j2\pi k f_0 t)\mathrm{d}t. \tag{3.5}$$

From (3.5), one can observe that for a real signal $s(t)$, $C_k = C_k^*$, where $(^*)$ denotes complex conjugate operation. Hence, one can write analytic signal (AS) representation as [117, 124],

$$z(t) = s(t) + j\hat{s}(t) = C_0 + 2\sum_{k=1}^{\infty} C_k \exp(j2\pi k f_0 t), \tag{3.6}$$

where the imaginary part $\hat{s}(t)$ is the Hilbert transform of the real part $s(t)$ and C_0 is the mean value of $s(t)$.

FDM is an adaptive signal processing technique used to analyze the non-stationary charac-

teristics of real-time signals by mapping the prior sine/cosine basis functions into a set of finite, and generally small number of band-limited analytic FIBFs as [116, 117],

$$C_0 + 2\sum_{k=1}^{\infty} C_k \exp(j2\pi k f_0 t) = C_0 + \sum_{i=1}^{M} a_i(t)\exp(j\phi_i(t)), \tag{3.7}$$

where $a_1(t)\exp(j\phi_i(t)) = 2\sum_{k=1}^{K_1} C_k \exp(j2\pi k f_0 t)$, $a_2(t)\exp(j\phi_i(t)) = 2\sum_{k=K_1+1}^{K_2} C_k \exp(j2\pi k f_0 t)$, $\ldots$, $a_M(t)\exp(j\phi_i(t)) = 2\sum_{k=K_{M-1}+1}^{\infty} C_k \exp(j2\pi k f_0 t)$. From (3.6) and (3.7), one can obtain

$$z(t) = a_0 + \sum_{i=1}^{M} y_i(t) + j\hat{y}_i(t) = C_0 + \sum_{i=1}^{M} a_i(t)\exp(j\phi_i(t)), \tag{3.8}$$

where $a_0 = C_0$ and M FIBFs are denoted as $y_i(t) = a_i(t)\cos(\phi_i(t))$, $1 \leq i \leq M$, with instantaneous amplitude (IA) $a_i(t) = \sqrt{y_i^2(t) + \hat{y}_i^2(t)}$ and instantaneous phase (IP) $\phi_i(t) = \tan^{-1}(\hat{y}_i(t)/y_i(t))$. The signal $s(t)$ can be expressed as,

$$s(t) = a_0 + \sum_{i=1}^{M} y_i(t) = a_0 + \sum_{i=1}^{M} a_i(t)\cos(\phi_i(t)). \tag{3.9}$$

The FDM generates FIBFs that are complete, local, adaptive, and orthogonal. The locality is achieved by amplitude modulated-frequency modulated (AM-FM) representation of FIBFs where both amplitude and frequency are varying with time, and thus provide local features of the signal. The FIBFs are derived from the data and as data changes, FIBFs would change accordingly, thus they are adaptive and depend on the data itself. The set of FIBFs is complete because the sum of FIBFs and a constant produces the original signal.

The FIBFs, $y_i(t) \in \mathbb{C}^{\infty}[p, q]$, are defined in the time interval over which the original signal is defined, and satisfy the following conditions:

1. The FIBFs, $y_i(t)$, $1 \leq i \leq M$, are zero mean functions, i.e.,

$$\int_p^q y_i(t)dt = 0. \tag{3.10}$$

2. The FIBFs satisfy the orthogonality condition, i.e.,

$$\int_p^q y_\ell(t)y_k(t)dt = 0, \forall \ell \neq k. \tag{3.11}$$

3. The FIBFs provide analytic FIBFs representation with instantaneous frequency (IF)

$$f_i(t) = \frac{\omega_i(t)}{2\pi} = \frac{1}{2\pi}\frac{d}{dt}\phi_i(t) \geq 0 \qquad \text{and IA} \qquad a_i(t) \geq 0, \forall t. \tag{3.12}$$

The Hilbert spectrum, i.e., time-frequency-energy representation, can be obtained from the EMD and FDM by plotting $\{t, f_i(t), a_i^2(t)\}$ for $i = 1, 2, \ldots, M$.

3.3.1 Discrete-time analytic signal representation of FIBFs

Practically, all signals are acquired in the analog domain and converted to discrete signals through an analog to digital converter (ADC). Therefore, in this subsection, we present the discrete version of the FDM which is implemented using the fast Fourier transform (FFT) algorithms, making it computationally efficient. Let $s[n]$ be any discrete-time real signal having length L. The discrete Fourier transform (DFT) of $s[n]$ can be defined as

$$s[n] = \sum_{k=0}^{L-1} S[k] \exp(j2\pi kn/L), \tag{3.13}$$

where

$$S[k] = 1/L \sum_{k=0}^{L-1} s[n] \exp(-j2\pi kn/L) \tag{3.14}$$

is the DFT of $s[n]$. If L is considered an even number, then $S[0]$ and $S[L/2]$ are real terms, therefore $s[n]$ can be written as,

$$\begin{aligned} s[n] = S[0] + \sum_{k=1}^{L/2-1} S[k] \exp(j2\pi kn/L) + S[L/2] \exp(j\pi n) \\ + \sum_{L/2+1}^{L-1} S[k] \exp(j2\pi kn/L). \end{aligned} \tag{3.15}$$

As $s[n]$ is real signal, therefore, second term in this equation is the complex conjugate of the fourth term and we can rewrite

$$s[n] = S[0] + 2Re\{z[n]\} + S[L/2](-1)^n, \tag{3.16}$$

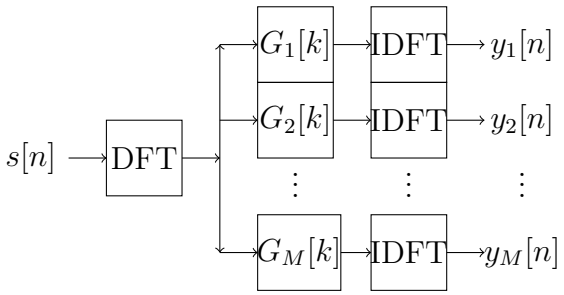

Figure 3.1: A block diagram of the FDM based on the DFT to decompose a signal $s[n]$ into a set of FIBFs $\{y_1[n], y_2[n], \cdots, y_M[n]\}$ with desired frequency bands.

where $Re\{z[n]\}$ represents the real part of the analytic signal $z[n]$. Therefore, we can write $z[n]$ as

$$z[n] = \sum_{k=1}^{L/2-1} S[k] \exp(j2\pi kn/L) = \sum_{i=1}^{M} a_i[n] \exp(j\phi_i[n]), \tag{3.17}$$

where $M << L$. This relation represents the generalized Fourier expansion of a time series. The real parts of terms $a_i[n] \exp(j\phi_i[n])$ are referred to as FIBFs, where $a_i[n]$ and $\phi_i[n]$ represent the IA and IP, respectively.

A block diagram of the FDM method using DFT based zero-phase filter-bank is illustrated in Fig. 3.1. The FDM decomposes a signal, $s[n]$, into a set of zero-mean components $y_1[n], y_2[n], ..., y_M[n]$ or $b_1[n], b_2[n], ..., b_M[n]$, such that

$$s[n] = b_o + \sum_{i=1}^{M} y_i[n] = b_o + \sum_{i=1}^{M} b_i[n], \tag{3.18}$$

where b_o representing the mean value of the signal $s[n]$; $y_i[n]$ and $b_i[n]$ represent orthogonal and linearly independent non-orthogonal yet energy preserving (LINOEP) FIBFs, respectively. Thus obtained FIBFs are complete, local, adaptive and orthogonal or LINOEP.

The FDM approach is preferred over the EMD algorithm due to the following reasons [116]:

1. The FDM possesses a complete mathematical background in comparison to EMD, which is largely based on an empirical approach, making it difficult to analyze mathematically.

2. Unlike the EMD, FDM eliminates various artifacts such as detrend uncertainty, mode mixing problem, and end effects during extraction of FIBFs.

3. As compared to EMD, FDM provides better time-frequency-energy (TFE) estimation and the ability to effectively separate frequency bands during the extraction of FIBFs from

the signal.

4. The FDM can decompose a signal into a set of FIBFs with desired cutoff frequencies, which cannot be obtained by the EMD algorithm. Moreover, FDM is implemented with the fast Fourier transform (FFT) algorithm, making it computationally more efficient.

A comparative analysis among various time-frequency analysis techniques [117] is presented in Table 3.1.

Table 3.1: A comparative analysis among various time-frequency analysis techniques

Attributes	Fourier Transform	Wavelet Transform	EMD	FDM
basis	a priori	a priori	adaptive	adaptive
frequency	convolution: global	convolution: regional	differentiation: local	differentiation: local
uncertainty	yes	yes	no	no
presentation	frequency-energy	frequency-time-energy	frequency-time-energy	frequency-time-energy
nonlinear	no	no	yes	yes
non-stationary	no	yes	yes	yes
harmonics	yes	yes	no	no
Theoretical base	complete	complete	empirical	complete

3.4 Summary

In this chapter, the pre-processing methods of the biomedical signals such as ECG and EEG are presented using decomposition techniques EMD and FDM. It has been observed from the literature that EMD is one of the most widely used techniques for the removal of artifacts and noises during the pre-processing of non-stationary signals. However, this technique suffers from some drawbacks (as discussed in Section 3.2). To overcome these drawbacks, a novel approach, based on Fourier theory, known as FDM, is considered for the analysis of non-stationary signals. The FDM has shown better performance as compared to state-of-the-art methods available in the literature.

Chapter 4

Identification of alcoholism

4.1 Introduction

Alcoholism is a neurological disease caused by excessive consumption of alcohol. It is responsible for economic losses to individuals and society as well. It has a wide range of parameters: the amount of alcohol consumed, age at which subject started drinking, duration of drinking, subject's age, gender, genetic background, and education level. It adversely affects the central nervous system and other organs of the human body. Therefore, it is important to distinguish alcoholic subjects from normal subjects efficiently and reliably, which reduces not only the economic losses and social problems but also provides a rapid and easy method for neurologists in clinical settings. Among various neuroimaging techniques [125, 126, 127] such as EEG, CT, PET and fMRI, analysis of EEG signals is a non-invasive tool and is the most popular technique for studying the complex dynamics of brain functioning.

Only time or frequency based methods are not suitable for analysis and interpretation of the non-stationary behavior of the recorded EEG signals. In [128], the STFT method is employed to translate EEG signals into time-frequency (TF) images. The texture of these images is analyzed for feature extraction and used as inputs to a non-negative least square model to classify between alcoholic and normal EEG signals. However, the prime drawback of the STFT approach is that it does not provide optimum time and frequency resolution simultaneously due to fixed window size. On the contrary, wavelet transform can vary window size by using translation and dilation parameters. M. Sharma et al. in [129] used dual-tree CWT (DT-CWT) to decompose EEG signals into nine sub-bands. Two features, namely L_2 norms (L2N)

and log-energy entropy (LEE), are extracted from these sub-bands and by applying feature ranking and selection techniques, relevant features are fed to various classifiers to estimate their performances. In [130], a flexible analytic wavelet transform (FAWT) approach is proposed. Using this approach, fractal dimension (FD) is computed in each sub-band after decomposing the EEG signals and least-squares support vector machine (LS-SVM) is used to discriminate the two groups. Further, EWT and its variant algorithms have also been proposed [131, 132] for the classification of physiological signals and images. In [133, 134], Fourier-Bessel series expansion (FBSE)-based EWT is used for better TF representation as compared to the traditional EWT method. In another study presented by Anuragi et al. in [134], narrow sub-band signals are computed after decomposition of EEG signals by applying FBSE-EWT. Three attributes, such as accumulate line length (ALL), LEE, and norm entropy (NE), are extracted from these sub-bands. To select appropriate features, various feature ranking techniques are utilized, followed by different classifiers to assess the performance and efficacy of the proposed methods.

Several adaptive signal decomposition frameworks like EVD, VMD, EMD, RSD and time-varying vibration decomposition (TVVD) [135] have been developed to analyze non-linear and non-stationary signals. Out of these methods, EMD is the most popular technique across various applications, including time-frequency analysis [124], artifacts removal from biological signals [136], epilepsy seizure detection [137], recognizing driver fatigue [138], sleep stage classification [139, 140], alcoholism detection [141, 142] and diagnosis of Alzheimer's disease [143], yet it suffers with the following problems: i) inaccurate time-frequency representation in presence of noise, ii) loss of significant information while removing noise from the biological signals. To address these problems, an adaptive signal decomposition approach, known as the Fourier decomposition method (FDM), is presented in [116, 144]. In this chapter, we have proposed FDM-based method for alcoholism detection using EEG signals. This technique segments the given signal into a limited number of orthogonal components referred to as FIBFs. The variability and complexity of each FIBF are evaluated using linear and non-linear time-domain features such as Hjorth parameters (activity, complexity, and mobility), kurtosis, median frequency (MDF), and inter-quartile range (IQR). These features are considered as inputs to various machine learning algorithms for the classification of normal and alcoholic EEG recordings.

4.2 Methodology

The flow chart of the proposed work is illustrated in Fig. 4.1. The dataset [145] consists of two classes of recorded EEG signals, obtained from normal and alcoholic subjects. The FDM is applied to decompose the EEG recordings into a set of desired orthogonal components (FIBFs), and six FIBFs are generated by dividing the complete bandwidth of EEG signals into equal frequency bands. The FIBFs for alcoholic and normal EEG signals are shown in Fig. 4.2 and Fig. 4.3, respectively. Hjorth parameters, kurtosis, IQR and MDF, utilized as features, are extracted from FIBFs to interpret the EEG signals. Thereafter, significant features are selected using Kruskal-Wallis (KW) statistical test and applied as inputs to various machine learning models such as k-nearest neighbor (kNN), support vector machine (SVM) and linear discriminant analysis (LDA) for classification of alcoholic and normal EEG signals. The proposed methodology is discussed in the following sub-sections: EEG dataset, feature extraction followed by the feature selection process, and finally, a brief introduction of several classifiers used for alcoholism identification and their performance measures.

4.2.1 Dataset

The dataset used in this work is obtained from the UCI machine learning repository and is publicly available online [145] for research. It is composed of two groups, normal and alcoholic, with a total of 122 subjects. The data is recorded using 64 electrodes placed on the subject's scalp and sampled at a frequency of 256 Hz. Out of 64 electrodes, 61 electrodes are used for signal acquisition, while the remaining electrodes are considered as reference. The position of all electrodes is as per 10-20 electrode system [146]. Each subject is exposed to two different stimuli, which are pictures selected from 1980 Snodgrass and Vanderwart set [147]. Various artifacts such as eye blinking, body movements (> 73.3 μV) introduced during EEG recording have been removed in the baseline itself. The recorded EEG signals are divided into four segments, each having a duration of 8 seconds (2048 samples). A total of 240 segments, i.e., 120 segments (30 signals) each of normal and alcoholic subjects are used in this work.

EEG signals exhibit a non-stationary behavior, which means the frequency content of EEG signals changes with time. The intrinsic mode functions (IMFs) obtained using EMD, which are also AM-FM components, are widely used and well-established for nonlinear and non-

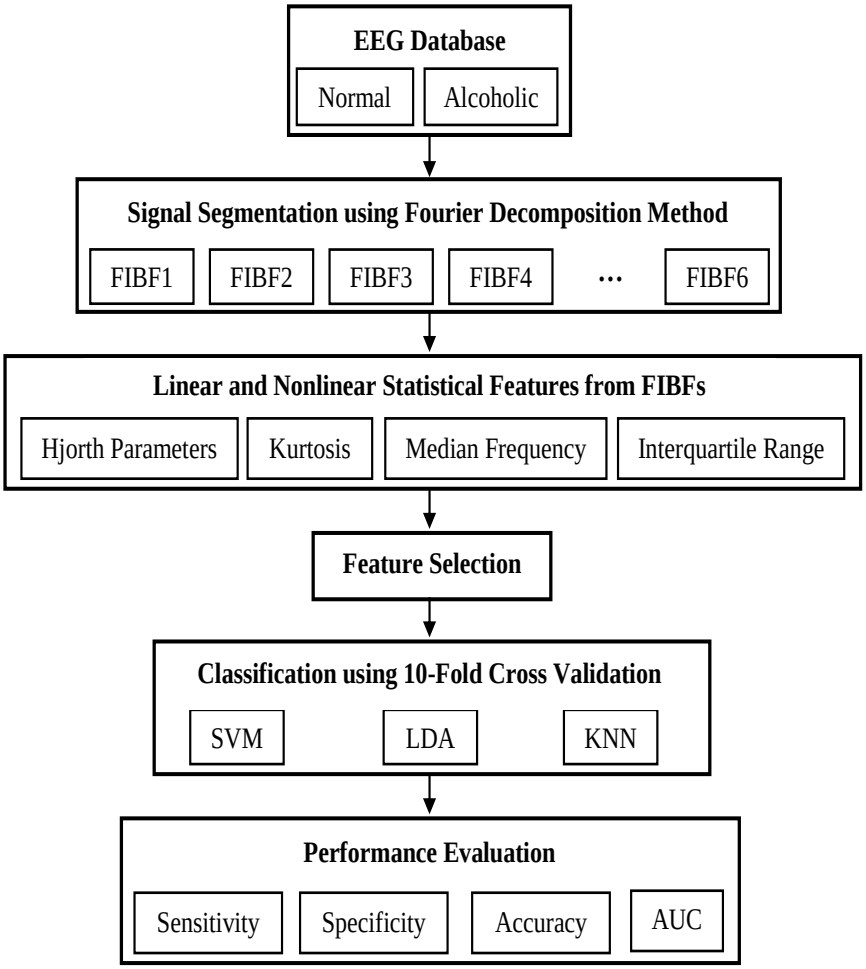

Figure 4.1: Flow chart of the proposed methodology for automated alcoholism detection.

stationary data analysis. Similarly, FIBFs are suitable for nonlinear (i.e., data generated from the nonlinear systems like a brain) and non-stationary data analysis. Moreover, the time-varying nature of the amplitude and phase of each FIBF captures the complexity, nonlinear and non-stationary dynamics of the brain system, as shown in Fig. 4.2 and 4.3.

4.2.2 Feature extraction

In this work, features such as kurtosis, MDF, IQR and Hjorth parameters (activity, complexity and mobility) [148, 149] obtained from FIBFs of both normal and alcoholic EEG signals have been computed. As these features play a vital role in detecting epileptic seizures using EEG signals [148, 150, 149], therefore, in our present work, we are trying to assess the significance of these features for the identification of alcoholism. A brief overview of these features is presented as follows:

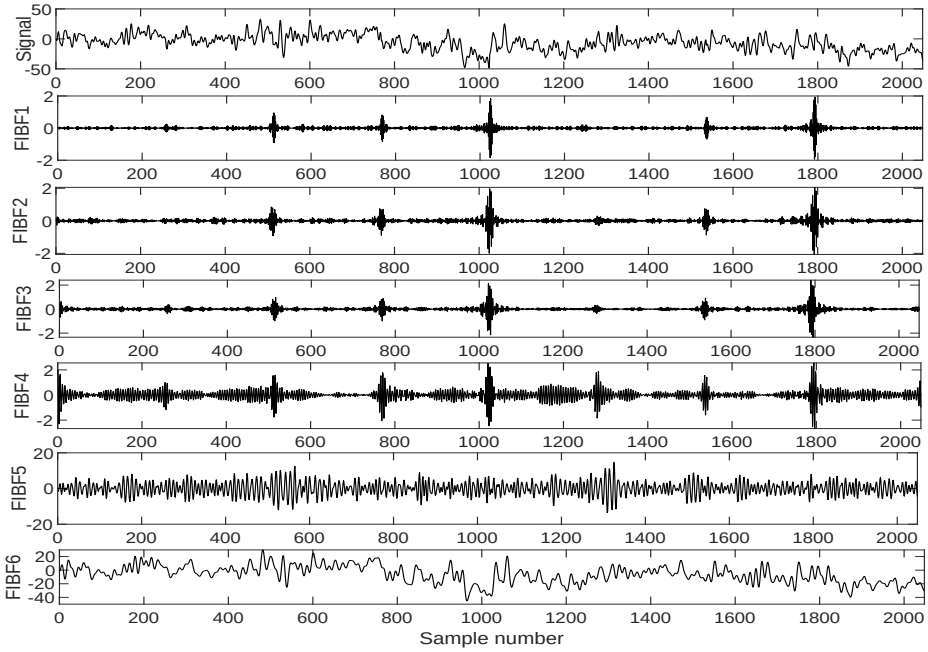

Figure 4.2: Fourier decomposition process of alcoholic EEG signal using equal frequency bands: FIBF6: 0-21.33 Hz, FIBF5: 21.33-42.66 Hz, FIBF4: 42.66-63.99 Hz, FIBF3: 63.99-85.32 Hz, FIBF2: 85.32-106.65 Hz, and FIBF1: 106.65-128 Hz.

1. Kurtosis is a statistical measure of peakedness or flatness of a frequency distribution. It is used to measure the outliers present in the distribution. A large number of outliers present in the dataset indicates heavy tails and hence a high value of kurtosis, while lack of outliers in the data indicates light tails and has a low value of kurtosis. It is also known as the fourth-order moment in statistics, and it is defined as:

$$a_4 = \frac{\frac{1}{N}\sum_{n=0}^{N-1}(y[n]-\mu)^4}{\left(\frac{1}{N}\sum_{n=0}^{N-1}(y[n]-\mu)^2\right)^2}, \quad \text{where mean,} \quad \mu = \frac{1}{N}\sum_{n=0}^{N-1} y[n] \tag{4.1}$$

   and $y[n]$ denotes a FIBF obtained from the signal.

2. Hjorth parameters are widely used for the analysis of biomedical signals like ECG and EEG for the extraction of relevant information. These parameters include activity, mobility, and complexity. The activity parameter measures the variance of the signal, which is defined as:

$$activity = var(y[n]) = \frac{1}{N}\sum_{n=0}^{N-1}\left(y[n]-\mu\right)^2. \tag{4.2}$$

   The second parameter, mobility, is defined as the ratio of the standard deviation of the

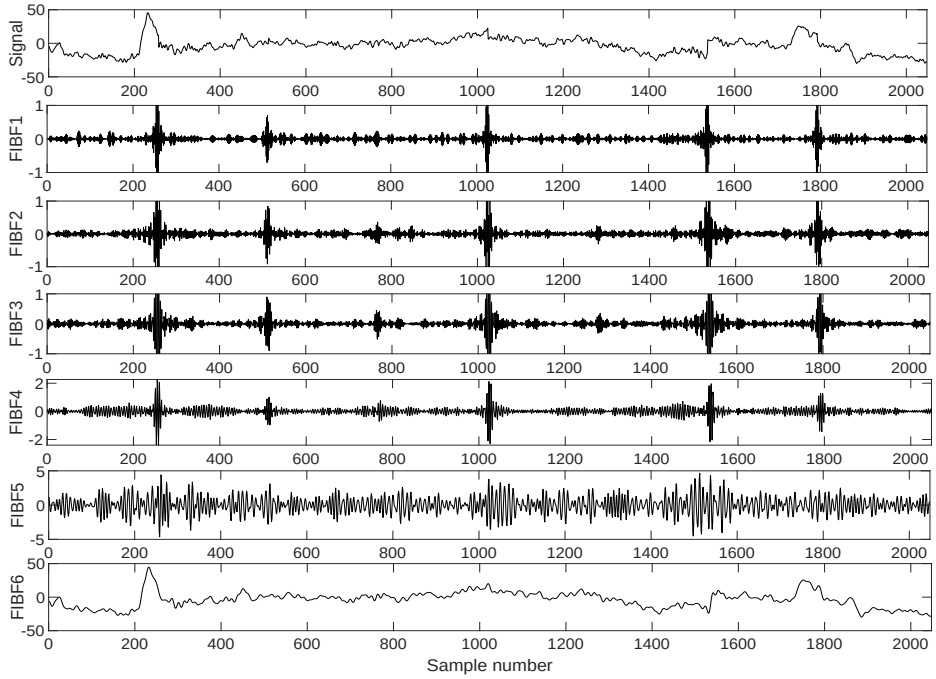

Figure 4.3: Fourier decomposition process of normal EEG signal using equal frequency bands: FIBF6: 0-21.33 Hz, FIBF5: 21.33-42.66 Hz, FIBF4: 42.66-63.99 Hz, FIBF3: 63.99-85.32 Hz, FIBF2: 85.32-106.65 Hz, and FIBF1: 106.65-128 Hz.

first derivative of the signal to the standard deviation of the signal. It represents the mean frequency of the signal. It is defined by the following relation:

$$mobility(y[n]) = \sqrt{\frac{var(y[n] - y[n-1])}{var(y[n])}}. \tag{4.3}$$

The third parameter, complexity, indicates any variation in the signal frequency. In other words, it represents whether the pattern of the given signal resembles a pure sine wave or not. It is obtained as:

$$complexity(y[n]) = \frac{mobility(y[n] - y[n-1])}{mobility(y[n])}. \tag{4.4}$$

3. The interquartile range (IQR) of a signal is defined as the difference between the upper (third) quartile and lower (first) quartile of the EEG dataset. The upper quartile is 75 % percentile of the dataset and the lower quartile is 25 % of the dataset. The IQR is defined as

$$IQR = Q3 - Q1, \tag{4.5}$$

where $Q3$ and $Q1$ denote the third and first quartile, respectively.

4. The median frequency (MDF) is defined as the frequency which divides the area under the power spectrum of EEG signal into two equal regions.

4.2.3 Feature selection

After extracting the features from FIBFs, the next step is to select the most significant features. Various feature selection techniques such as student t-test, Chi-square test, Kruskal-Wallis (KW) test, correlation attribute, and gain ratio attribute have been presented in the literature [151, 149] for finding the most relevant features. These approaches reduce not only the complexity of the classifiers but also improve their performance. In this work, one of the commonly used statistical tests, the KW method, is used for finding the most significant features at a 95% significance level using MATLAB statistical toolbox. KW test is a non-parametric method employed to determine whether given features are originated from the same distribution or not. This technique is utilized to check whether two or more groups have an equal median and also returns the value of p. The p-value can be viewed as the probability of the null hypothesis being true, which states that the medians are equal. The value $(1-p)$ indicates the significance level, i.e., the null hypothesis is rejected at a 95% significance level by considering $p < 0.05$. The smaller the p-value, the larger is the significance of the given feature. KW test is preferred over other feature selection techniques as it is simple to use and computationally less complex. In this work, the original signal, $s[n]$, is considered as a position vector. The first derivative of position, i.e., velocity vector in continuous time-domain is synonymous with the first-order difference in discrete-domain, and differentiation shows the same response as high pass filtering. A combination of 12 FIBFs is drawn out after decomposition of the original signal as well as the first derivative of the original signal.

Table 4.1: The obtained p-values of various FIBF-based features of the original signal using Kruskal-Wallis test

FIBFs	*Activity*	*Mobility*	*Complexity*	*Kurtosis*	*MedianFrequency*	*InterquartileRange*
FIBF1	0.0025	**0.5631**	$7.0550e-41$	**0.2685**	**0.6261**	0.0004
FIBF2	0.0026	**0.3913**	$7.0550e-41$	**0.4186**	**0.508**	$9.7169e-05$
FIBF3	0.0006	$3.3689e-06$	$7.0550e-41$	**0.5456**	0.0002	$4.2531e-08$
FIBF4	$2.2426e-15$	$6.3928e-22$	$7.0550e-41$	$9.9560e-08$	$1.1046e-20$	$1.2058e-20$
FIBF5	$3.3175e-37$	$7.9193e-16$	$7.0550e-41$	$4.2804e-28$	$1.5252e-14$	$1.4878e-38$
FIBF6	$1.6514e-06$	$7.0550e-41$	$7.0550e-41$	**0.5272**	$7.6820e-16$	$5.5087e-07$

Table 4.2: The obtained p-values of various FIBF-based features of the first derivative of the signal using Kruskal-Wallis test

FIBFs	*Activity*	*Mobility*	*Complexity*	*Kurtosis*	*MedianFrequency*	*InterquartileRange*
FIBF1	$7.0550e-41$	**0.6156**	$7.0550e-41$	**0.2661**	**0.5164**	0.0003
FIBF2	$7.0550e-41$	**0.3781**	$7.0550e-41$	**0.3872**	**0.3496**	$4.6171e-05$
FIBF3	$7.0550e-41$	$1.7948e-06$	$7.0550e-41$	**0.4175**	$8.8597e-05$	$4.0372e-07$
FIBF4	$7.0550e-41$	$2.3957e-22$	$7.0550e-41$	$1.6210e-06$	$8.2318e-22$	$7.1183e-21$
FIBF5	**0.1924**	$3.1146e-15$	$7.0550e-41$	$6.9172e-30$	$3.8374e-14$	$1.0027e-37$
FIBF6	**0.3593**	$7.5147e-38$	$7.0550e-41$	$1.5490e-10$	$1.4406e-35$	$1.3786e-36$

Table 4.3: Fold-wise accuracies of SVM, kNN and LDA classifiers

Number of Fold Used	SVM (%)	kNN (%)	LDA (%)
Fold 1	89.4	89.4	89.4
Fold 2	100	100	100
Fold 3	100	100	100
Fold 4	100	100	100
Fold 5	100	100	100
Fold 6	100	100	100
Fold 7	100	98.5	100
Fold 8	100	100	100
Fold 9	100	99.5	100

4.2.4 Classification

In this subsection, several classifiers namely SVM, kNN and LDA are discussed to classify normal and alcoholic EEG signals.

Support vector machine (SVM)

SVM is an elegant and powerful machine learning tool. It is used in many applications, such as face recognition, text, and image classification and bioinformatics [152]. It generates a hyperplane that maximizes the distance of the separating boundaries between two classes by maximizing the distance of the separating plane from each of the feature vectors. The optimal hyperplane can be considered as follows:

$$w.s_i + b \geq 1, \quad \text{if} \quad z_i = +1$$

$$w.s_i + b < 1, \quad \text{if} \quad z_i = -1, \tag{4.6}$$

where s_i represents the training data, z_i represents the desired classification, and w represents a vector perpendicular to the hyperplane. Here, b is referred to as the bias term representing the position of a hyperplane in higher-dimensional space. In this work, we have used MATLAB

software package 2018b for simulation. Radial basis function (RBF) kernel is used for SVM and the hyperparameters for the classifier model are optimized inherently by the in-built library functions.

k-nearest neighbor (kNN)

kNN is a supervised machine learning algorithm mainly used for classification and regression analysis [153]. The classifier searches for k data points of the training set to find the label (or class) of any data point that is not included in the training set. The symbol 'k' in kNN is a positive integer that indicates the number of nearest neighbors participating in the bulk voting process. Smaller k may increase sensitivity to noise while a larger value may provide a smooth decision boundary at the cost of higher computational complexity. The commonly used matrices for calculating the distances between two data points are Euclidean, Hamming, Minkowski and Manhattan [154]. In this work, we use the standard Euclidean distance measure to obtain the nearest neighbors and choose $k = 10$ as it provides a better accuracy with a minimum error rate.

Linear discriminant analysis (LDA)

LDA is a simple classification approach, originally developed in 1936 by R. A. Fisher, commonly used for dimensionality reduction [153, 155]. This classifier is used to optimize the number of features which improves the ratio of inter-class variance to the intra-class variance for two classes of EEG signals. A hyperplane is drawn to segregate the features related to the two categories of signals. Here, the two categories to be discriminated against are alcoholic and normal EEG signals.

In this study, the data is divided into 10 equal blocks. Forward training and testing is done as follows:

* fold 1 : training [1], test [2],

* fold 2 : training [1 2], test [3],

* fold 3 : training [1 2 3], test [4] ... and so on.

This way, the trained model gets validated on one (unknown) block of data, before testing on the next (unknown) block. This process is repeated ten times to obtain average classification results. Five performance indexes, i.e., specificity, sensitivity, accuracy, precision, and f-measure

are computed for measuring the performance of the classifiers. These parameters are defined as:

$$\begin{aligned} sensitivity &= \frac{TP}{TP+FN} \times 100\% \\ specificity &= \frac{TN}{TN+FP} \times 100\% \\ accuracy &= \frac{TP+TN}{TP+TN+FP+FN} \times 100\% \\ precision &= \frac{TP}{TP+FP} \times 100\% \\ f\text{-}measure &= 2 \times \frac{precision \times recall}{precision + recall} \times 100\%, \quad \text{with} \\ recall &= \frac{TP}{TP+FN} \times 100\%, \end{aligned} \tag{4.7}$$

where TP denotes true positive events, which are defined as the total number of events that are detected as alcoholic correctly by the algorithm and the neurologist. TN represents true negative events which are defined as the total number of events that are recognized as normal or healthy by the expert and the algorithm. FP denotes the false positive events detected incorrectly and FN represents the false negatives, i.e., alcoholic events which the algorithm fails to detect. F-measure is represented as the harmonic mean of recall and precision achieved by the classifier. It is a statistical measure commonly employed to assess classification problems in machine learning. The receiver operating characteristic (ROC) curve, an efficient tool to assess the performance of a classifier, is a graphical plot that describes the tradeoff between true positive rate ($sensitivity$) and false positive rate ($1 - specificity$). The sixth performance index, area under ROC curve (AUC) is obtained as:

$$\text{AUC} = \int_0^1 sensitivity(x)dx\,, \tag{4.8}$$

where $x = 1 - specificity$.

4.3 Results and Discussion

In this work, a total of 120 EEG segments containing 2048 samples from normal and alcohol classes have been used to compute the simulation results. FDM method is applied to decompose

EEG signals into six FIBFs from which various time-domain features such as Hjorth parameters, kurtosis, MDF and IQR are obtained. KW statistical test is performed to assess the significance level of the extracted features for the discrimination of alcoholic and normal EEG recordings. Table 4.1 demonstrates the p-values obtained for these features by computing FIBFs from the original signal, while Table 4.2 illustrates the p-values of features obtained from FIBFs of the first derivative of the signal. The insignificant features (p-values greater than or equal to 0.05) are shown in bold letters in Table 4.1 and Table 4.2.

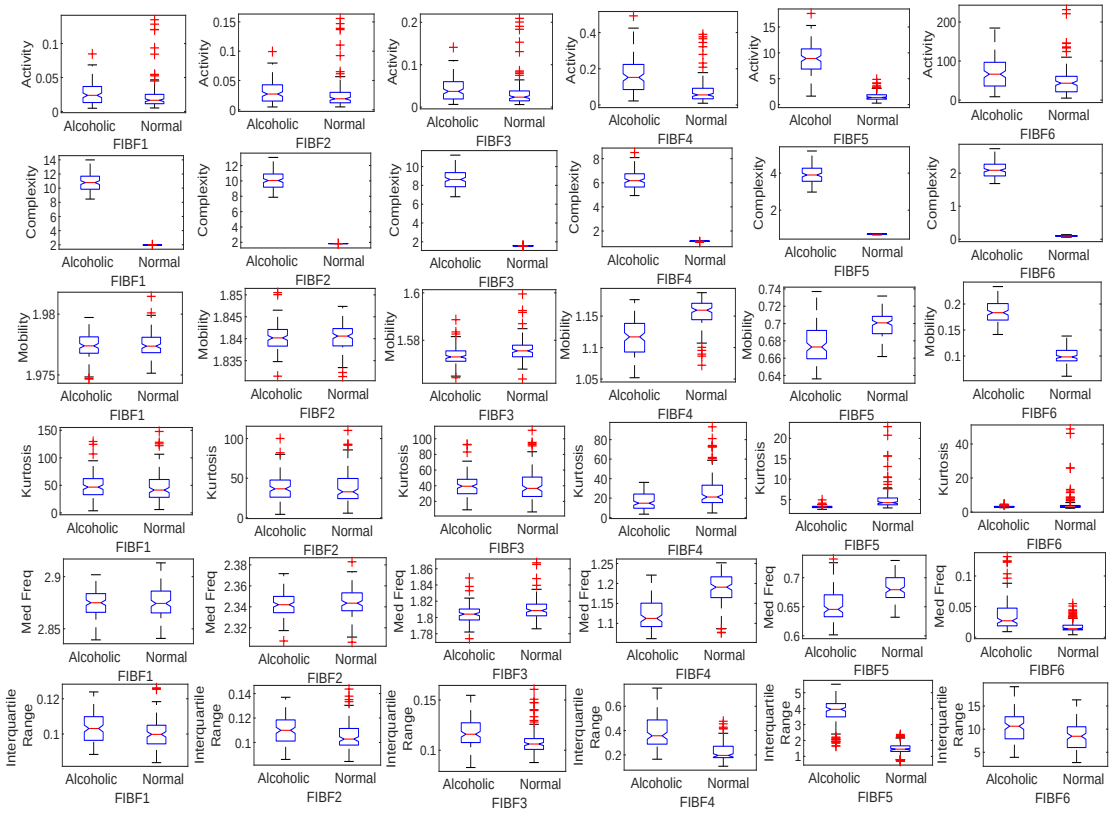

Figure 4.4: The box plots corresponding to KW test (first row: activity, second row: complexity, third row: mobility, fourth row: kurtosis, fifth row: MDF, sixth row: IQR of alcoholic and normal EEG signals)

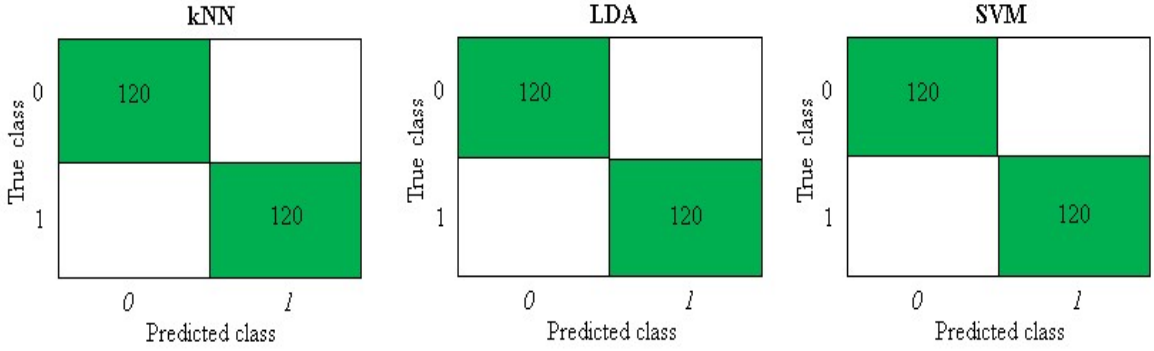

Figure 4.5: Confusion matrices for kNN, LDA, and SVM classifiers.

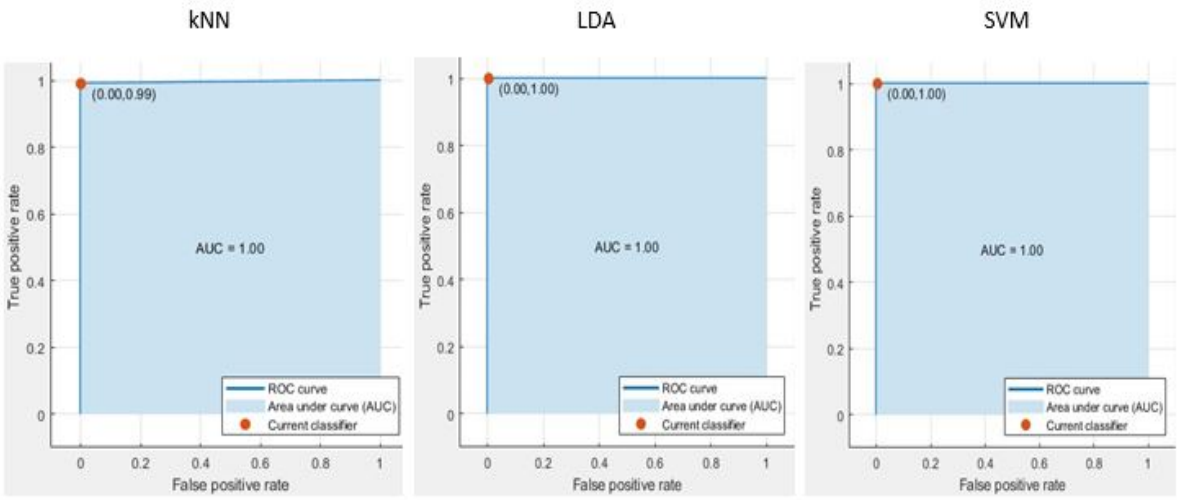

Figure 4.6: Receiver operating characteristics of kNN, LDA, and SVM classifiers.

It is evident that activity, complexity, and IQR are the most significant features for the discrimination of two groups of EEG signals because these features correspond to the lowest p-values. Further, kurtosis is found to be the least significant feature with p-values greater than 0.05. By applying the KW test, the box plots of these features obtained from the original signal are drawn in Fig. 4.4 for both alcoholic and normal EEG signals. The box plot assists in visualizing the discriminative ability of a given feature for classification. It shows the range of values obtained for a feature and its comparison for different classes. Higher is the separation of box plots corresponding to the distinct classes, better is the discrimination offered by the feature. It is evident from Fig. 4.4 that box plots corresponding to most of the features for normal and alcoholic EEG signals are well-separated and yield very low p-values, as shown in Table 4.1. The complexity feature has the highest discriminative ability with the lowest p-values corresponding to each FIBF while the kurtosis feature is insignificant for some FIBFs. Each signal is decomposed into 6 FIBFs. Considering the original signal and its first derivative, a total of 12 FIBFs are obtained, and 6 features are extracted from each FIBF, giving a feature matrix of dimension 72×1. After selection, we retain 55 features out of the total 72 to obtain a feature matrix of dimension 55×1. The significant features are used as input to SVM, kNN, and LDA models for the classification of normal and alcoholic EEG recordings. Using forward training and testing, fold-wise accuracies are reported in Table 4.3. It is evident that high accuracies are obtained for folds 3–9.

The performance of the proposed approach as a function of several FIBFs are depicted

in Table 4.4. The proposed technique achieves an optimum classification accuracy of 99.44% for 6 FIBFs. The confusion matrix provides the total number of occurrences correctly and incorrectly classified, as shown in Fig. 4.5. Further, it helps in evaluating various indexes, including, sensitivity, specificity, accuracy, precision, and f-measure of the used classifiers.

Table 4.4: Performance of SVM classifier with different levels of FIBFs

Number of FIBFs	4	6	8	10	12	15	20	25
Accuracy (%)	98.41	99.44	98.77	98.40	97.00	93.12	86.05	77.36

Table 4.5: A comparison of performance metrics for three classifiers

Performance metrics	SVM	kNN	LDA
accuracy (%)	99.44	98.73	95.6
sensitivity (%)	99.29	97.47	93.42
specificity (%)	99.58	100	97.74
precision (%)	99.58	100	97.85
f-measure (%)	99.43	98.71	95.58
AUC	1	1	0.99

Table 4.6: Effect of signal-to-noise ratio (SNR) of input signal on the accuracy of SVM, kNN and LDA classifiers

SNR (in dB)	SVM	kNN	LDA
-10	87.5	50.0	65.4
-5	90.3	51.3	70.2
0	94.7	61.4	75.6
5	97.2	80.1	80.1
10	99.1	91.2	85.2
15	99.5	97.0	90.3
20	99.8	98.1	92.4
25	99.9	98.7	94.4
30	99.9	99.0	95.0

Fig. 4.6 depicts the ROC curves of kNN, LDA, and SVM classifiers to discriminate between alcoholic and normal EEG signals. It is noticed that the AUC is one for all the classifiers. It is observed from Table 4.5 that SVM classifier produces best values of accuracy (99.44%), sensitivity (99.29%), specificity (99.58%), precision (99.58%) and f-measure (99.43%). Further, Table 4.6 shows the effect of the signal-to-noise (SNR) ratio on the performance of various classifiers considered in this work. While the performance of all the classifiers degrades with a reduction in SNR, SVM produces decent accuracy even at low values of SNR.

In recent years, various techniques have been explored in the literature to discriminate alcoholic subjects from normal subjects. Table 4.7 depicts the work done by various researchers

Table 4.7: Comparison of recent studies for the identification of alcoholism using same dataset (N.A. indicates that no decomposition technique has been used)

Authors and Year	Decomposition Technique	Features	Accuracy
Anuragi et al. [134] 2020	FBSE-EWT	ALL, LEE, NE	98.8%
Anuragi et al. [158] 2018	FAWT	Mean, SD, Kurtosis, Skewness, SE	99.17%
Taran et al. [141] 2018	EMD	MAD, IQR, COV, Entropy, Neg-entropy	97.92%
Priya et al. [35] 2018	EMD	Kurtosis, Skewness, Entropy, Neg-entropy	97.92%
Sharma et al. [159] 2017	Three-Band OWFB	Log-energy (LE)	97.08%
Patidar et al. [77] 2017	TQWT	Centered Correntropy	97.02%
Sharma et al. [129] 2018	DT-CWT	L2N, LEE	97.91%
Thilagaraj et al. [142] 2019	EMD	BP, FD	98.91%
Acharya et al. [79] 2012	N.A.	ApEn, LLE, SE, HOS	91.7%
Shah et al. [160] 2019	OWFB	Log-energy (LE)	94.2%
Proposed method	FDM	Hjorth parameters, kurtosis, MDF, IQR	99.44%

using the same UCI KDD dataset as considered in our study. A set of 240 EEG segments and 10-fold cross-validation (CV) scheme is used in [157]. Taran et al. in [141] used the EMD algorithm to decompose EEG signals into a set of intrinsic mode functions (IMFs). Further, instantaneous frequency (IF), computed from the analytic form of IMFs, is used to assess various frequency bands of EEG signals. Five features, namely, IQR, mean absolute deviation (MAD), entropy, coefficient of variation (COV) and neg-entropy have been drawn out from each frequency band and used as inputs to two different classifiers for the discrimination of alcoholic EEG signals. This system has obtained the best classification accuracy of 97.92%. Thilagaraj et al. in [142] used EMD algorithm to recognize the impact of alcoholism on the human brain. IMF coefficients based on band power (BP) are computed. A feature reduction technique is employed to reduce the number of features followed by the classification stage, achieving an accuracy of 98.91%. Anuragi et al. [158] applied the FAWT method to decompose EEG signals into as set of detailed and approximate coefficients. These wavelet coefficients are utilized to extract five different features which are fed to various classifiers for training and testing purposes. The simulation results showed better classification accuracy of 99.17%. In [159, 160], the authors presented an orthogonal wavelet-based filter bank (OWFB) approach for the classification of normal and alcoholic EEG recordings. They achieved accuracies of 97.08% and 94.20%, respectively. On the other hand, the authors in [161] have employed a Butterworth filter to differentiate various EEG rhythms. A combination of linear feature (absolute band power), non-linear features (Hjorth mobility and complexity), approximate entropy (ApEn), sample entropy (SE), and statistical features (kurtosis, variance, skewness) are utilized as inputs to kNN classifier, to achieve a classification accuracy of 98.25%. It is concluded from Table 4.7

that the current work has attained the highest classification accuracy of 99.44%, highlighting a superior performance in comparison to the existing methods. Further, the proposed study has considered less number of features, therefore, the computational complexity is also less.

4.4 Summary

This work presents a novel approach for the automated identification of alcoholic and normal subjects using EEG signals. A set of six FIBFs of equal frequency bands are generated using the FDM method. Thereafter, Hjorth parameters, kurtosis, median frequency and inter-quartile range features are extracted from each FIBF using the FDM approach. The KW test indicates that activity, complexity and inter-quartile range are the most significant features in differentiating normal and alcoholic EEG recordings. Three classifiers, namely SVM with RBF kernel, kNN and LDA, are employed for testing and training, and the SVM classifier attains the best classification performance. The proposed approach produces better results as compared to the existing schemes. It is also recommended to validate and verify current study on a large dataset before applying it to real-time systems to detect alcoholism. Further, the proposed approach could be investigated for the diagnosis of various other neurological abnormalities.

Chapter 5

Epilepsy detection

5.1 Introduction

Epilepsy is ranked amongst the most prevalent neurological disorders in humans. In terms of occurrence, it occupies the fourth position behind stroke, Alzheimer's, and migraine. It involves transient and hyper-synchronization movement of neuronal discharges in the brain cortex. According to the report published by the WHO, approximately fifty million people are affected by epilepsy worldwide. A large percentage of people suffering from epilepsy are residing in developing regions. Numerous efforts have been made by the researchers towards the automatic detection of epileptic seizures.

Local binary patterns (LBP) extracted from the signal are used for the classification of EEG signals in [162, 163, 164]. Authors in [163] use Gabor filters for pre-processing the signals. Key-points of a signal are identified using the difference of Gaussian (DoG) filters before extracting LBP in [164]. In [165], various EEG rhythms are extracted using a discrete cosine transform (DCT). Alam et al. [166] employed two time-frequency methods known as STFT and Wigner-Ville distribution (WVD) techniques for the analysis of non-stationary signals using multipath fading channel. Using a short window in the time-domain leads to poor frequency resolution and vice-a-versa. In [167], a modified version of STFT known as frequency slice wavelet transform (FSWT) is presented to monitor the signals dynamics using Gaussian window. WT is applied in [168, 169, 170, 171] for seizure detection as it offers flexibility in varying the window size as per requirements. Authors in [168, 169] use a linear phase wavelet filter bank, while features such as mean, variance, median, maximum, minimum are extracted from wavelet coefficients in

[170, 171]. In [172], the DWT technique is applied to decompose the EEG signals into several frequency bands for the classification of EEG signals. Local graph structures are explored in [173] and DWT is used for pooling. Harmonic WPT technique is used in [174] to decompose the given signal into subsequent levels and spectral features are extracted. The proper choice of mother wavelet and the number of decomposition levels are difficult to select while implementing the wavelet method.

Hilbert marginal spectrum (HMS) analysis is performed in [175] to extract spectral entropies and energy features from IMFs. In [176], a modified version of EMD based on peak selection criteria has been used to decompose the EEG signals. Another modified version of EMD known as complete ensemble EMD is employed in [177] to decompose the signal and statistical features such as mean, variance and kurtosis are computed from the IMFs.

In this study, FDM is used to decompose the EEG signal into a finite number of FIBFs. Further, L^p norms are extracted from these FIBFs, which are used as features and fed to the classifiers to distinguish between seizure and healthy/non-seizure/seizure-free EEG signals. The L^p norms help in emphasizing smaller sample values for $p < 1$ and larger sample values for $p > 1$, thereby capturing the relation between the magnitude of signal samples.

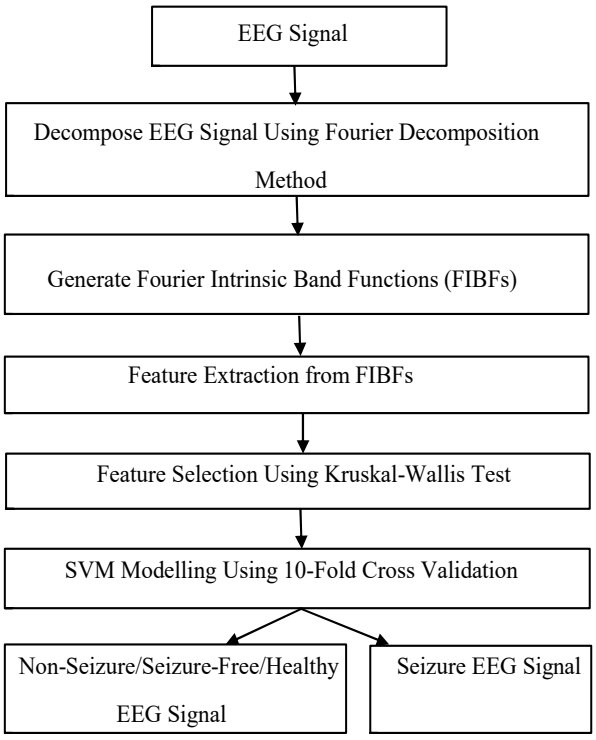

Figure 5.1: Flow chart for the proposed method.

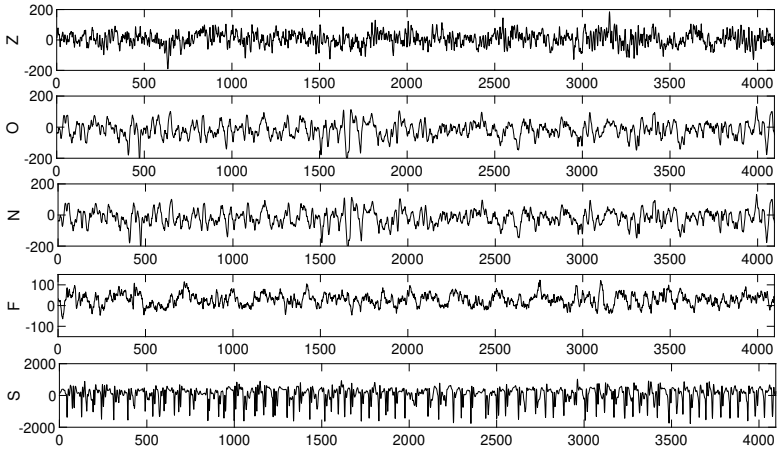

Figure 5.2: Sample of EEG signals from the BONN dataset showing the five subsets Z, O, N, F and S.

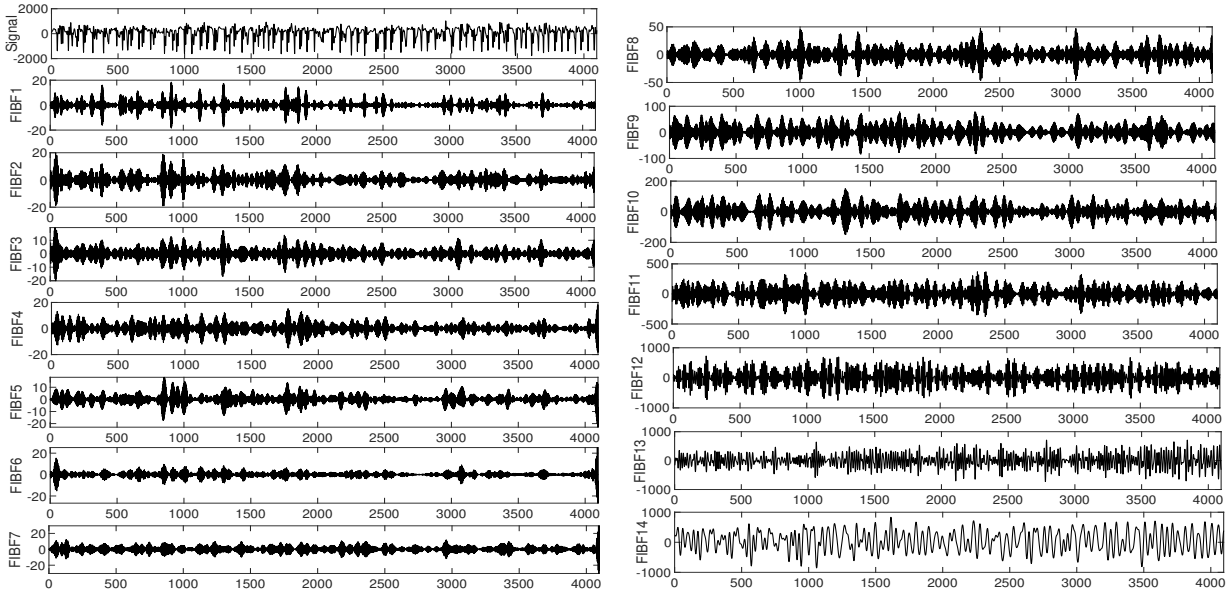

Figure 5.3: Fourier decomposition process of seizure EEG signal having duration of 23.6 seconds using uniform frequency bands.

5.2 Methodology

Fig. 5.1 describes the flow chart for the proposed method. The datasets and the various steps of the algorithm are discussed in detail as follows.

5.2.1 Datasets

BONN EEG dataset, utilized in this work, is managed by the Epileptology Department, University of Bonn, Germany, and is available online [178]. The dataset is composed of five subsets of data, labeled as Z, O, N, F and S each including 100 single-channel EEG signals. Subsets Z

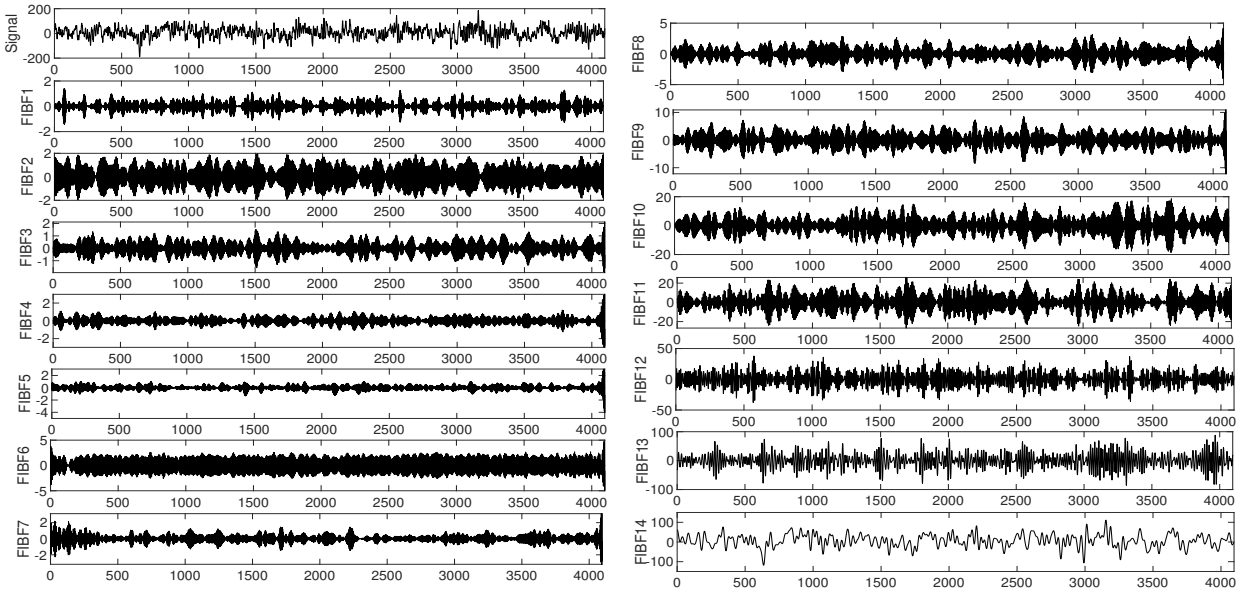

Figure 5.4: Fourier decomposition process of healthy EEG signal having duration of 23.6 seconds using uniform frequency bands.

and O contain surface EEG segments captured from five healthy people, using an international standard 10/20 electrode system, with their eyes in open and closed conditions. Subsets N, F and S are obtained from five epilepsy patients using an intracranial electrode placement system. Subsets N and F are recorded during seizure-free activity, while subset S is obtained during seizure intervals. The signals recorded in the digital system are sampled at 173.61 Hz. Each signal segment has a duration of 23.6 seconds. Fig. 5.2 shows sample EEG signals from the five subsets. In each segment, there are a total of $173.61 \times 23.6 \approx 4097$ sample points. The decomposition of seizure EEG signal into FIBFs with uniform frequency bands is depicted in Fig. 5.3. Fourier decomposition of healthy and seizure-free EEG signals into FIBFs is shown in Fig. 5.4 and Fig. 5.5, respectively.

We have also employed CHB-MIT EEG dataset [179, 180], which consists of 686 scalp EEG recordings collected from 23 pediatric patients, chb01-chb23 comprising 5 males and 18 females having ages between 1.5 and 22 years, suffering from an intractable seizure at Children's Hospital Boston, to check the efficacy of the proposed model. Out of 686 EEG records, 198 records correspond to seizure events. Most of the records are segmented into 1 hour duration while few records vary between 2-4 hours. The records that include one or more seizures are labeled as seizure events while the rest of the records are called non-seizure events. As subject chb24 was introduced to this database in 2010, the etiology of this subject is unknown and is

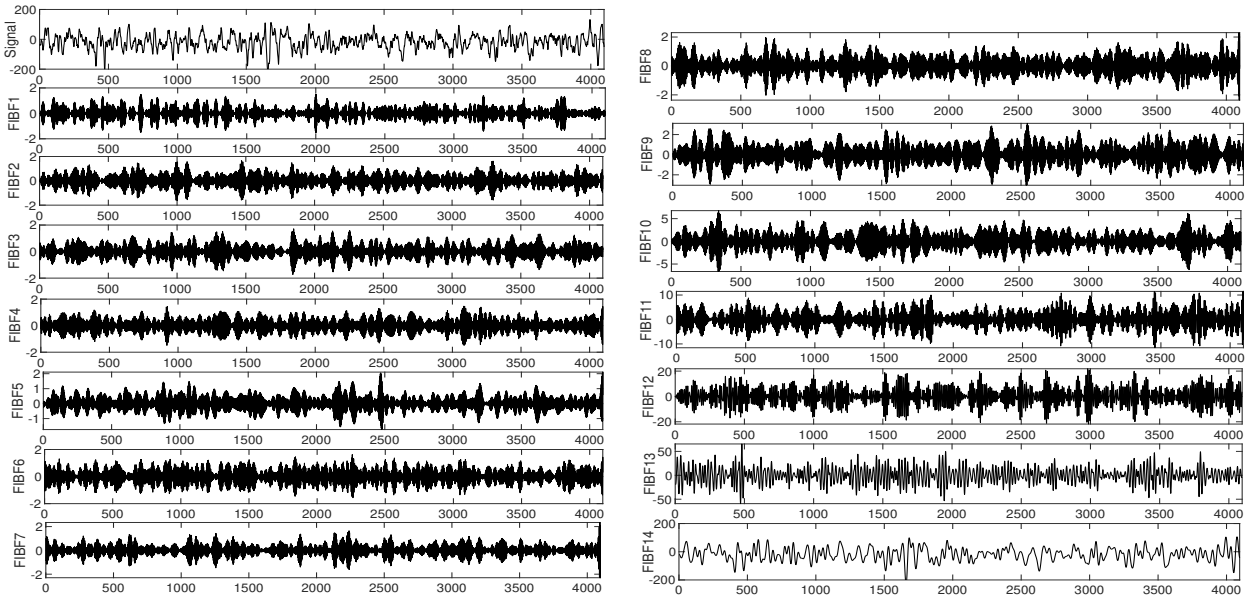

Figure 5.5: Fourier decomposition process of seizure-free EEG signal having duration of 23.6 seconds using uniform frequency bands.

discarded in this study. The sampling frequency of the EEG signals is 256 Hz with a resolution of 16-bit. The EEG signals are recorded using a 10/20 electrode placement system. The database considered in this work is constructed by dividing 1-hour long EEG records into EEG segments having a window size of 2560 samples (10 seconds), which are extracted from 182 seizure events and 182 data blocks randomly selected from the non-seizure files.

Table 5.1: Statistical analysis using Kruskal-Wallis test for two-class problem (healthy versus seizure)

FIBFs	$L^{0.1}$	$L^{0.25}$	$L^{0.5}$	L^{1}	L^{2}	L^{3}	L^{5}
FIBF1	$2.52394e-34$	$4.83203e-32$	$3.79644e-08$	**0.0702**	$1.99791e-07$	$6.80293e-09$	$2.53388e-08$
FIBF2	$2.52394e-34$	$2.52394e-34$	$4.7285e-20$	0.0186	0.026	0.0001	$6.53353e-07$
FIBF3	$2.52394e-34$	$1.15895e-32$	$4.24088e-07$	**0.0904**	$2.46374e-07$	$9.17533e-10$	$3.43808e-11$
FIBF4	$2.52394e-34$	$1.50806e-32$	$2.69589e-05$	0.0139	$1.48078e-08$	$1.56965e-11$	$3.75266e-13$
FIBF5	$2.52394e-34$	$2.99457e-33$	$1.025e-06$	**0.0773**	$1.30801e-07$	$2.05283e-11$	$5.97931e-14$
FIBF6	$2.52394e-34$	$2.52394e-34$	$2.10348e-31$	$8.18142e-23$	$2.21206e-09$	0.0325	0.0385
FIBF7	$2.52394e-34$	$7.24861e-33$	$7.28445e-10$	**0.5741**	$2.4994e-05$	$1.28378e-08$	$3.09049e-10$
FIBF8	$2.52394e-34$	$7.4647e-33$	0.0049	$3.63512e-07$	$3.3928e-16$	$2.38144e-19$	$2.20192e-21$
FIBF9	$2.52394e-34$	$4.55976e-32$	0.0421	$5.63287e-11$	$1.5822e-20$	$7.37314e-24$	$3.89231e-26$
FIBF10	$2.52394e-34$	$3.9062e-33$	**0.0899**	$3.09049e-10$	$4.75894e-21$	$2.71619e-24$	$2.36951e-26$
FIBF11	$2.52394e-34$	$2.35916e-31$	**0.4061**	$2.13689e-13$	$2.2024e-25$	$3.33184e-28$	$1.37666e-29$
FIBF12	$2.52394e-34$	$3.6419e-22$	0.0069	$5.52134e-19$	$3.45033e-27$	$1.00426e-28$	$2.03086e-29$
FIBF13	$2.52394e-34$	$6.27115e-32$	0.04	$1.02227e-17$	$2.45678e-24$	$1.83991e-25$	$3.50676e-26$
FIBF14	$2.52394e-34$	$4.6596e-13$	$3.07062e-20$	$1.1255e-33$	$2.52394e-34$	$2.52394e-34$	$2.52394e-34$

Table 5.2: Statistical analysis using Kruskal-Wallis test for two-class problem (seizure-free versus seizure)

FIBFs	$L^{0.1}$	$L^{0.25}$	$L^{0.5}$	L^{1}	L^{2}	L^{3}	L^{5}
FIBF1	$2.5239e-34$	$5.7495e-32$	$5.8174e-08$	**0.0823**	$9.0515e-07$	$7.0412e-08$	$1.056e-07$
FIBF2	$2.5239e-34$	$1.0308e-32$	$5.2756e-11$	**0.7434**	$4.6874e-05$	$5.0068e-07$	$1.2073e-07$
FIBF3	$2.5239e-34$	$5.7495e-32$	$1.0091e-05$	0.0168	$5.1424e-08$	$8.8979e-10$	$2.9946e-10$
FIBF4	$2.5239e-34$	$6.4552e-32$	0.0002	0.0029	$1.1025e-09$	$3.2177e-11$	$2.9873e-12$
FIBF5	$2.5239e-34$	$4.5597e-32$	0.0002	0.0026	$3.1893e-10$	$6.7917e-13$	$8.3582e-14$
FIBF6	$2.5239e-34$	$2.5239e-34$	$5.2038e-24$	$1.9622e-06$	**0.1249**	$9.6328e-07$	$3.9891e-11$
FIBF7	$2.5239e-34$	$2.6456e-31$	0.0027	$5.2516e-06$	$2.5391e-15$	$8.2656e-18$	$1.5037e-16$
FIBF8	$2.5239e-34$	$5.3889e-25$	0.0298	$7.4740e-17$	$6.7364e-23$	$6.6752e-24$	$4.0544e-24$
FIBF9	$2.5239e-34$	$1.8476e-17$	$1.2960e-06$	$7.0720e-23$	$5.4194e-27$	$4.6220e-27$	$8.2763e-27$
FIBF10	$2.5239e-34$	$1.3488e-11$	$7.0389e-13$	$1.6425e-28$	$3.7292e-31$	$2.7225e-31$	$1.0391e-30$
FIBF11	$2.5239e-34$	$1.6127e-08$	$2.7464e-15$	$6.4826e-30$	$5.2709e-32$	$4.9741e-32$	$2.7225e-31$
FIBF12	$2.5239e-34$	0.0006	$1.1917e-19$	$4.0629e-31$	$2.0194e-32$	$4.4293e-32$	$2.1646e-31$
FIBF13	$2.5239e-34$	$1.1033e-13$	$1.9662e-15$	$5.7961e-30$	$3.8310e-32$	$5.5854e-32$	$2.0439e-31$
FIBF14	$2.5239e-34$	$1.3090e-24$	$2.9145e-08$	$3.9410e-27$	$8.7643e-31$	$6.9821e-31$	$1.9917e-30$

5.2.2 Feature extraction from FIBFs

The EEG signal $s[n]$ is pre-processed and divided into FIBFs using FDM as discussed in Chapter 3. In this work, L^p norms for various values of p, i.e., $p = 0.1, 0.25, 0.5, 1, 2, 3, 5$ have been utilized to extract the features from the FIBFs. The L^p norm of a signal can be defined as [181]

$$\|y\|_p = \left(\sum_{n=0}^{L-1} |y[n]|^p \right)^{1/p}, \tag{5.1}$$

where $y[n]$ represents a FIBF. The length L of FIBF is same as the original signal $s[n]$. For $p < 1$, the sample values $|y[n]| < 1$ get more highlighted in regard to other samples. This impact becomes stronger for smaller values of p. On the other hand, $p > 1$ results in a higher emphasis on sample values $|y[n]| > 1$. It should be noted that the emphasis increases further with an increase in the value of p. For large values of p, the smaller sample values get suppressed to a great extent and the L^p norm is dictated by the larger samples of the signal. In this work, we thus restrict the maximum value of $p = 5$. For $p = 2$, the square of the L^2 norm would give the total energy of the signal.

The 7 values of L^p norms, obtained for each FIBF, are tested using Kruskal-Wallis (KW) test at a 95% significance level. To investigate the statistical significance of the selected features, a one-way analysis of variance (ANOVA) is employed. The statistical test is performed using MATLAB statistical toolbox. The p-values which are less than 0.05 identify the relevant features that can be applied to the classifier for achieving good classification results. In this study, we

have considered the original signal, $s[n]$, as the position vector. The first derivative of position is referred to as velocity and the second derivative of position is considered as acceleration. Differentiation produces an effect similar to high-pass filtering and is approximated in the discrete domain by the first-order difference [182, 183], i.e.,

$$\begin{aligned} s_{d1}[n] &= s[n] - s[n-1] \\ s_{d2}[n] &= s_{d1}[n] - s_{d1}[n-1], \end{aligned} \tag{5.2}$$

where $s_{d1}[n]$ and $s_{d2}[n]$ correspond to first and second order derivatives, respectively. Similarly, integration produces an effect similar to low-pass filtering and is approximated as a cumulative sum, i.e.,

$$\begin{aligned} s_{l1}[n] &= \sum_{k=0}^{n} s[k] \\ s_{l2}[n] &= \sum_{k=0}^{n} s_{l1}[k], \end{aligned} \tag{5.3}$$

where $s_{l1}[n]$ and $s_{l2}[n]$ denote the integrations of first and second order, respectively.

We consider the original EEG signal in combination with the high-pass versions, $s_{d1}[n]$ and $s_{d2}[n]$. The FIBFs are obtained for all three signals before extracting the features from each FIBF, giving a total of $3 \times M \times 7$ features, with M representing the number of FIBFs. In this work, we have taken $M = 14$, as it provides the best results. Further, we also consider a combination of the original signal and its low-pass versions, $s_{l1}[n]$ and $s_{l2}[n]$.

5.2.3 Classification

Considering the FIBF-based features, binary classification of EEG signals is performed for the following cases:

1. Non-seizure (Z, O, N, F) and seizure (S) classes
2. Seizure-free/inter-ictal (N, F) and seizure/ictal (S) classes
3. Healthy (Z, O) and seizure (S) classes

From the given BONN dataset, subsets Z and O are joined together to form healthy EEG

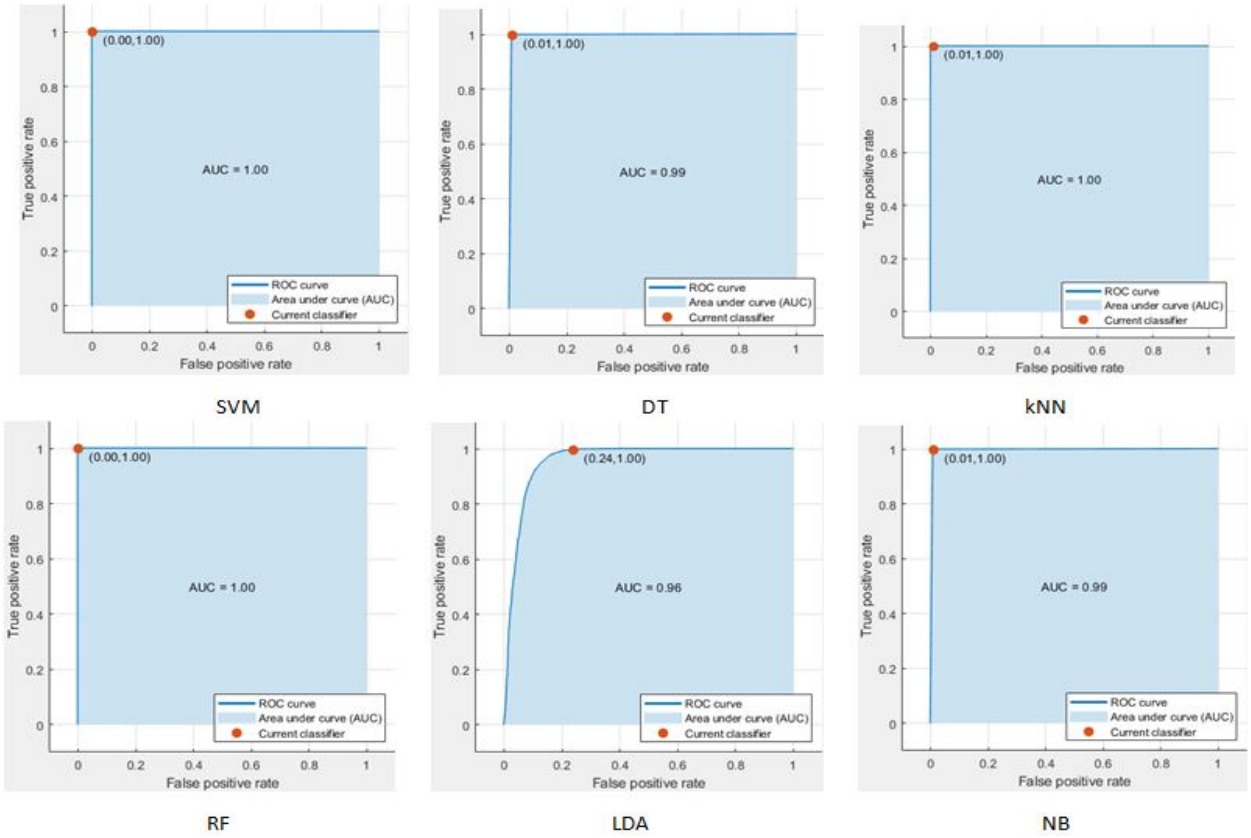

Figure 5.6: Receiver operating characteristics of SVM, DT, kNN, RF, LDA, and NB classifiers for the BONN dataset.

data, while subsets N and F are combined to represent seizure-free EEG signals. Non-seizure EEG signal is obtained by combining subsets Z, O, N and F. Subset S represents a seizure EEG signal. The data samples are arranged randomly before classification and 10-fold cross validation (CV) is performed. In this scheme, the data is partitioned randomly into ten equal parts and the performance of the classifier is measured ten times. For each measurement, one part of the data, i.e., 10% of the data is used for testing purposes while the remaining 90% is used to train the classifier. The process of data randomization followed by 10-fold CV is repeated ten times and average results are obtained using MATLAB software package R2018b. To discriminate the EEG signals, various machine learning algorithms are considered, such as kNN, LDA, random forest (RF), decision tree (DT), naive bayes (NB) and SVM. Out of these classifiers, three classifiers namely, SVM, kNN and LDA have been described in Chapter 4. The three other classifiers, i.e., RF, DT and NB classifiers are discussed here. The typical kernels used in SVM are linear, polynomial and radial basis function (RBF) [184, 185]. In this work, we use the RBF kernel function as it produces the best results.

Table 5.3: Effect of window size on the performance of SVM classifier for the BONN dataset

classification	window size	sensitivity (%)	specificity (%)	accuracy (%)
Healthy versus seizure	4096	100	100	100
	2048	100	100	100
	1024	100	99.99	99.99
	512	100	99.99	99.99
	256	100	99.99	99.99
Seizure-free versus seizure	4096	100	99.99	99.96
	2048	99.84	99.94	99.89
	1024	99.83	99.98	99.89
	512	99.79	99.99	99.89
	256	99.86	99.91	99.87
Non-seizure versus seizure	4096	100	99.99	99.99
	2048	99.86	99.94	99.96
	1024	99.85	99.96	99.95
	512	99.89	99.95	99.95
	256	99.84	99.97	99.91

Random forest (RF)

RF classifier is one of the most commonly used supervised machine learning algorithms capable of performing both classification and regression problems [186]. RF model employs an ensemble learning method in which the predictions are based on the combined results of various individual models. This classifier operates by creating a set of decision trees from randomly selected subsets of training data. The votes from different decision trees are combined to decide the class of the test sample. The main advantage of the RF classifier is that it overcomes overfitting problems by taking an average of all the predictions by canceling out the biases.

Decision tree (DT)

DT classifier is another supervised learning approach that is employed to solve both regression and classification problems [187]. This classifier builds classification models in the form of a tree structure. DT is a graphical representation of all the possible solutions to a decision on the basis of certain conditions. It takes a vector of attribute values as inputs and a decision is returned as a single output value. A DT classifier is comprised of three main parts: root node, branch, and leaf node. A root node represents the entire dataset used to perform tests by calculating the entropy and information gain of every attribute. It divides the complete dataset into two or more subsets. A branch corresponds to an attribute value while the leaf node represents the outcome.

Naive bayes (NB)

NB is a simple and powerful machine learning model employed for predictive modeling [188]. It is a linear classifier based on the Bayes theorem with the independent assumption that the effect of one feature in a particular class is not dependent on the values of the other features. The main advantage of NB classifier is that it needs only small training dataset to assess the parameters predetermined for the classification. It is commonly used in many applications, for instance fraud detection, text classification, medicine and target market analysis.

Table 5.4: Comparative analysis of state-of-the-art methods with proposed scheme for classification between non-seizure and seizure EEG signals from the BONN dataset

Authors and Year	Classifier	Features used	Accuracy (%)
Guo et al. [53] 2010	MLPNN	Approximate entropy (ApEn)	98.27
Peker et al. [171] 2016	CVANN	Statistical features	99.33
Hassan et al. [64] 2015	ANN	Statistical features	98.87
Tzallas et al. [43] 2007	ANN	Energy	97.73
Vidyaratne et al. [174] 2017	RVM	Spectral and fractal features	99.8
Kaleem et al. [176] 2013	1-NN	Energy, amplitude spectrum	98.20
Fu et al. [175] 2015	SVM	Entropy, sub-band energy	98.80
Wang et al. [170] 2017	SVM	Statistical features, Entropy	99.25
Hassan et al. [59] 2019	Adaboost	Normal inverse Gaussian	99.2
Tiwari et al. [164] 2017	SVM	LBP	99.31
Gupta et al. [44] 2019	Regression	Renyi entropy	98.6
Subasi et al. [172] 2017	SVM	Wavelet coefficients	99.38
Proposed method (high-pass)	SVM	L^p Norms	99.96
Proposed method (low-pass)	SVM	L^p Norms	99.97

Table 5.5: Performance of various methods for classification of seizure-free and seizure EEG signals from the BONN dataset

Authors and Year	Classifier	Features used	Accuracy (%)
Joshi et al. [38] 2014	SVM	Error and signal energy	95.33
Kaya et al. [162] 2014	Bayes Net	LBP	97.00
Kumar et al. [163] 2015	KNN	LBP	98.33
Pachori et al. [57] 2014	MLPNN	Ellipse area of IMFs	95.75
Tiwari et al. [164] 2017	SVM	LBP	99.45
Raghu et al. [39] 2017	MLPNN	Entropy	84.58
Proposed method (high-pass)	SVM	L^p Norms	99.89
Proposed method (low-pass)	SVM	L^p Norms	99.96

5.3 Results and Discussion

The performance of the proposed classification approach is evaluated by using five performance metrics, i.e., sensitivity, specificity, accuracy, f-measure and ROC area, as discussed in Section

Table 5.6: Performance of various methods while classifying between healthy and seizure EEG signals from the BONN dataset

Authors and Year	Classifier	Features used	Accuracy (%)
Kaya et al. [162] 2014	SVM	LBP	99.50
Tiwari et al. [164] 2017	SVM	LBP	100
Peker et al. [171] 2016	CVANN	Statistical features	100
Fu et al. [60] 2015	SVM	Entropy, sub-band energy	99.85
Subasi et al. [155] 2010	LDA, SVM	Sub-band features	100
Subasi et al. [49] 2007	mixture of experts	Sub-band features	94.5
Proposed method (high-pass)	SVM	L^p Norms	100
Proposed method (low-pass)	SVM	L^p Norms	99.96

Table 5.7: Comparison with existing techniques for seizure detection using the CHB-MIT EEG dataset

Authors and Year	Classifier	Features used	Accuracy (%)
Rafiuddin et al. [52] 2011	LDA	IQR, MAD	99.50
Khan et al. [27] 2012	LDA	Coeff. of variation, energy	91.8
Fergus et al. [189] 2014	kNN	Sub-band features	88
Dash et al. [58] 2019	HMM	PSD, variance, FD	99.60
Proposed method (high-pass)	SVM	L^p Norms	99.94
Proposed method (low-pass)	SVM	L^p Norms	99.71

4.2.4 (Chapter 4). Table 5.1 illustrates the p-values obtained for various FIBFs extracted from the original signal when applying the KW test on healthy and seizure classes, namely Z, O and S. Similarly, p-values for differentiating between seizure-free and seizure classes are listed in Table 5.2. Insignificant p-values are shown in bold letters. The receiver operating characteristic (ROC) curve is obtained by plotting a graph between the true positive rate (TPR) and the false positive rate (FPR). FPR is similar to $1 - specificity$ and TPR is similar to $sensitivity$. Fig. 5.6 depicts the ROC curves of SVM, LDA, RF, NB, DT and kNN classifiers, respectively, for the binary classification between non-seizure and seizure classes using the BONN dataset. It is observed from Fig. 5.6 that AUC is 1, indicating a strong performance of the SVM classifier. Due to this reason, we have studied the SVM classifier for three binary classification problems related to epileptic seizures.

The variation in classification results is also analyzed by varying the window size, i.e., the number of samples considered. As shown in Table 5.3, there is little or no variation in the results indicating the strength of proposed features even for a smaller length of the signal. The results are shown here for the high-pass filtering method and similar trends are observed for the low-pass filtering schemes. A comparative analysis with the existing state-of-the-art methods for two-class problems using the BONN dataset is shown in Tables 5.4-5.6, where

Table 5.8: A comparison of various classifiers in terms of evaluation metrics using the BONN dataset

Evaluation metrics	DT	RF	NB	SVM	kNN	LDA
accuracy (%)	99.50	99.70	99.53	99.96	99.78	95.0
sensitivity (%)	99.78	99.93	99.15	100	99.58	94.33
specificity (%)	99.22	99.48	99.92	99.92	100	98.11
f-measure (%)	99.72	88.87	99.97	99.95	99.83	96.91
ROC area (AUC)	0.99	1	1	1	1	0.96

Table 5.9: A comparison of various classifiers in terms of evaluation metrics using the CHB-MIT EEG dataset

Evaluation metrics	DT	RF	NB	SVM	kNN	LDA
accuracy (%)	99.50	99.35	98.40	99.94	99.68	96.24
sensitivity (%)	99.52	99.42	99.60	99.95	99.72	98.44
specificity (%)	99.49	99.28	97.20	99.93	99.64	94.04
f-measure (%)	99.50	99.19	98.10	99.79	99.50	96.91
ROC area (AUC)	1	1	0.99	1	1	0.98

the results are indicated by the proposed method (high-pass) and the proposed method (low-pass) for high-pass and low-pass filtered versions of the EEG signal, respectively. These results are obtained considering a window size of 2048. A comparison of recent studies for seizure detection using the CHB-MIT EEG dataset is provided in Table 5.7. By applying the high-pass filtering approach, the proposed study has obtained excellent classification performance with an average accuracy of 99.96%, average sensitivity of 100%, f-measure of 99.95%, and an average specificity of 99.92% considering SVM classifier with BONN dataset. Similarly, using a high-pass filtering approach, the proposed study achieved excellent classification performance with an average accuracy of 99.94%, average sensitivity of 99.95%, f-measure of 99.79%, and an average specificity of 99.93% considering SVM classifier with CHB-MIT dataset. Tables 5.8-5.9 compare the performance of six different classifiers, namely, DT, RF, NB, LDA, SVM and kNN in terms of the performance metrics using the BONN and the CHB-MIT EEG datasets.

From the last few decades, various experiments have been performed by researchers for the binary classification of EEG signals. Table 5.4 and Table 5.7 show the results for classifying non-seizure and seizure EEG signals from the BONN dataset and the CHB-MIT EEG dataset, respectively. By applying the high-pass filtering approach, the proposed study has obtained excellent classification performance with an average accuracy of 99.96% considering SVM classifier. In Table 5.4, the classifier 1-NN refers to 1-nearest neighbor, ANN refers to an artificial neural network, CVANN denotes complex-valued ANN, RVM refers to the relevance

vector machine, and MLPNN denotes multi-layer perceptron neural network. Similarly, Table 5.5 shows a comparison of various existing methods with the proposed scheme while comparing seizure-free EEG signals with the seizure EEG signals. Our method produces the best results by attaining average classification accuracy of 99.89%. Lastly, Table 5.6 depicts the third case of two-class problems, i.e., to classify between healthy and seizure EEG signals. The presented scheme produces better results in terms of classification accuracy of 100% when compared with the existing techniques discussed in the literature.

Analyzing the results obtained using the low-pass filtering approach, we have obtained an average classification accuracy of 99.96% for classification between healthy and seizure EEG signals. We have also attained good average classification accuracy of 99.96% while discriminating between seizure-free and seizure EEG signals. The simulation results show excellent performance in terms of classification accuracy of 99.97% when classifying between non-seizure and seizure EEG signals. The high value of accuracy thus obtained indicates that there is no bias or overfit in the model.

The classification results for the CHB-MIT dataset further validate the strength of the proposed method across diverse datasets. The comparison of various schemes provided in Table 5.7 indicates the superior performance of the proposed scheme with classification accuracies of 99.94% and 99.71% considering the high-pass and low-pass filtering approaches, respectively. SVM classifier again produces a strong performance in terms of classification accuracy of 99.94% as shown in Table 5.9.

5.4 Summary

Automatic and accurate detection of epileptic seizures using EEG signals is one of the challenging problems in biomedical engineering. The performance of various methods depends on the strength of the features being extracted. In this work, an efficient approach is proposed for three cases of binary classification problems of EEG signals. FDM technique is a useful tool for decomposing the non-stationary EEG signal into FIBFs, from which appropriate features are extracted using L^p norms. KW statistical test is conducted to select the significant features. Further, the selected feature set is utilized by the SVM classifier to achieve an accuracy of 100% for classifying healthy and seizure EEG signals from the BONN dataset. The proposed

method has also obtained a better classification accuracy of 99.89% and 99.96% when classifying seizure-free versus seizure EEG datasets and non-seizure versus seizure EEG datasets, respectively. Further, accuracy of 99.94% is achieved using the CHB-MIT EEG dataset when classifying seizure and non-seizure events. The pre-processing of EEG signals using high-pass and low-pass filtering produced an excellent performance in comparison to the existing state-of-the-art methods. The future scope of the proposed study is to investigate other physiological conditions of the human brain.

Chapter 6

Identification of epileptogenic zone

6.1 Introduction

Epilepsy is one of the common health issues related to brain disorders after migraine, brain stroke, and Alzheimer's. Epileptic seizures are broadly categorized into two groups: generalized epilepsy and focal (partial) epilepsy. Generalized epilepsy usually originates from one region in the brain and due to widespread neuronal networks, it may extend to other regions of the brain also. In comparison to generalized epilepsy, focal epilepsy is confined to one specific region of the brain. Despite the accessibility of anti-epilepsy drugs, nearly 25% of the patients are not effectively responding to these drugs. It has been revealed that 20% of the patients suffer from generalized epilepsy while 60% of the patients suffer from focal epilepsy [190]. Epileptogenesis, a process by which the working of the neuronal network changes from normal mode to hyper-excitation mode, is the prime cause for inducing seizures in epileptic patients. Such patients might have a high chance of cognitive and physiological disorders that might even lead to death. Therefore, the prime choice the neurologists have for the therapy of these patients is to get rid of the affected brain area (known as epileptogenic foci or zone) prompting the onset of epileptic seizures. Identifying the location of the epileptogenic zone manually by neurologists is a subjective and challenging process that may produce inaccurate results.

Various non-invasive tools, for instance fMRI, CT, EEG and PET have been used for identifying the epileptogenic region [191, 192]. The EEG signals captured from the epileptogenic region, where first ictal EEG changes occurred, are termed focal (F) EEG signals. The signals originated from other parts of the brain are termed as non-focal (NF) EEG signals [193]. There-

fore, differentiating F EEG signals from NF EEG signals is utilized to locate the epileptogenic zone in the brain. In the past few years, several signal processing techniques together with supervised learning algorithms have been explored for searching the exact epileptogenic zone by classifying F and NF EEG signals [194] - [199].

In [194], an efficient method based on Fast Walsh-Hadamard transform (FWHT) is presented to decompose F and NF classes of EEG signals for the detection of the epileptogenic focus. Five entropy features are fed as input to an ANN to assess the potency of the algorithm. This method provides information about the frequency contents of the EEG signals only. In [195], a DFT-based filter bank is utilized for the localization of the epileptogenic region. Two features have been computed from five frequency bands to classify two groups of F and NF EEG signals. Sairamya et al. in [196] presented a comprehensive approach based on WPD for the efficient localization of the epileptogenic zone by identifying F EEG signals from NF EEG signals. Five entropies features together with quad binary pattern features, captured from each sub-band, are applied as input features to the ANN algorithm for classification. However, the performance of wavelet transform based techniques depends on the appropriate selection of the mother wavelet as well as the number of decomposition levels.

In [197], EMD approach is investigated for the detection of F EEG signals. Two features, i.e., sample entropy and variance of IMFs are applied as input features to the LS-SVM classifier for better localization of epileptic events. Das et al. in [198] have investigated an efficient scheme based on the EMD-DWT domain to distinguish between the two classes of EEG signals. Three entropy features, namely Shannon entropy, Renyi entropy and log-energy entropy are computed using a combined approach of EMD-DWT. Rehman et al. in [199] presented another adaptive signal decomposition algorithm based on VMD and DWT for the detection of F EEG signals. Two entropy features along with autoregressive coefficients, computed from the decomposed EEG signals, are utilized as input features to ensemble stacking classifier for the discrimination of EEG signals. Determination of an accurate number of modes and computational time are the major concerns while implementing the VMD technique. Also, these methods [197, 198, 199] are developed on the perception that Fourier-based techniques are not appropriate for the analysis of non-stationary time-series data.

In this chapter, an efficient feature extraction scheme based on the FDM method is presented

for the identification of the epileptogenic zone by classifying F and NF EEG signals. The FDM method divides the given signal into orthogonal FIBFs. Various features are extracted from these FIBFs. Further, the FIBF-based features are applied to various classifiers such as SVM, kNN, DT, RF and LDA to evaluate the efficacy of the proposed scheme.

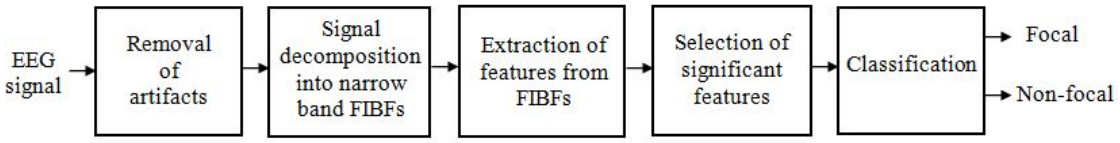

Figure 6.1: Block diagram of the proposed methodology for identification of epileptogenic zone.

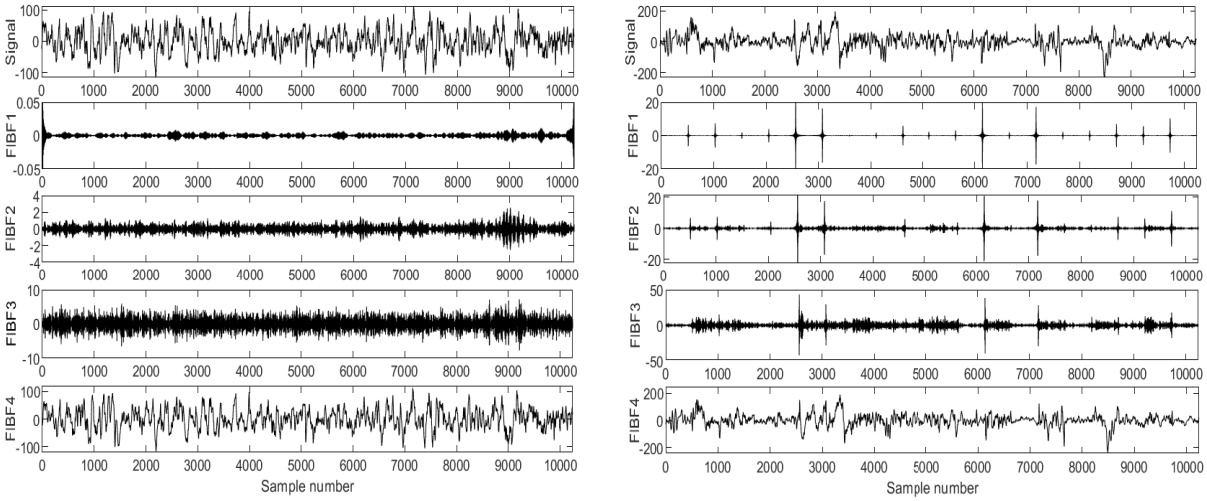

Figure 6.2: (Left) FDM process of focal (F) EEG signals using uniform frequency bands. (Right) FDM process of non-focal (NF) EEG signals using uniform frequency bands. FIBF4: 0-64 Hz, FIBF3: 64-128 Hz, FIBF2: 128-192 Hz, FIBF1: 192-256 Hz.

6.2 Methodology

The block diagram of the proposed work is illustrated in Fig. 6.1. The EEG data set is comprised of two classes, namely, focal (F) and non-focal (NF) obtained from five epileptic subjects who suffered from temporal lobe focal epilepsy. Various artifacts such as eye blinks, body movements are eliminated during the pre-processing of the recorded EEG signals. Thereafter, the FDM technique is applied to segregate the EEG signals into four FIBFs by segmenting the entire bandwidth of EEG signals into equal frequency bands. Fig. 6.2 depicts the FIBFs obtained from the F and NF classes of EEG signals. The FIBF-1 to FIBF-4 illustrate the high to

low frequency components present in the decomposition of EEG signals. The FIBF-1 represents the highest frequency components while FIBF-4 represents the lowest frequency components of the EEG signals. A total of eight features, five features drawn from FIBFs of the original signal and three features drawn from the first derivative of the original signal, are considered to interpret the neurological behavior of the epileptic patients. After feature extraction, the next step is to check the significance level of these extracted features. For this, a statistical test, known as the KW test, is employed to check whether these features are significant or not. Further, the most significant features are employed as input features to various classifiers for the discrimination of F and NF EEG signals.

6.2.1 Dataset

The F and NF sets of EEG signals are obtained from the Bern Barcelona (BB) dataset which is maintained by the Neurology department, Bern University, Switzerland, and is publicly available [193, 200]. The dataset incorporated long-term intracranial EEG recordings obtained from five epileptic patients suffering from drug-resistant temporal lobe epilepsy. There are 3750 pairs of EEG signals which belong to the F and NF classes. Each pair of bivariate EEG signals are denoted by x- and y- time-series recorded from neighboring channels. The sampling frequency of F and NF pairs of EEG signals is 512 Hz having a duration of 20 s, therefore the number of samples is 10240. A bandpass filter with cut-off frequencies of 0.5 Hz and 150 Hz is employed to remove artifacts present in the recorded EEG signals. In this work, 50 F and 50 NF sets of EEG signals are employed to assess the efficacy of the proposed algorithm. The x- time series captured from any one of the five patients which detects the first onset ictal seizure is utilized for F recordings while the y- time series represents any of the neighboring focal channels. The rest of the channels are identified as NF EEG signals.

6.2.2 Feature extraction

Extraction of appropriate features from the EEG signals can provide good classification performance. In this work, five features namely variance, kurtosis, mean frequency, IQR and complexity have been extracted from each FIBF of original F and NF classes of EEG signals, and three features namely mean frequency, IQR and complexity have been computed from the

first derivative of the original F and NF classes. As these features provide better simulation results in various neurological diseases such as epileptic seizure detection [201, 202], identification of alcoholism [203], sleep stage classification [151] as a result, in this study, we endeavor to evaluate the importance of these features to identify epileptic zone by analyzing F and NF classes. These features are defined as follows:

1. Variance indicates how much each sample in a given data set is dispersed from the mean value. An unbiased sample variance is defined as follows:

$$\sigma^2 = \frac{1}{(M-1)} \sum_{i=0}^{M-1} (y[i] - \bar{y})^2 \tag{6.1}$$

where σ^2 represents the variance of the data sample, $y[i]$ denotes the ith sample of a FIBF, $\bar{y}$ represents the average value of all samples in FIBF, and M is the length of the FIBF.

2. Mean frequency(MF) is defined as the sum of the product of the power spectrum and frequency of the FIBF $y[n]$, divided by the total sum of the power spectrum. It is also known as mean power frequency (MPF). It is obtained by the following relation:

$$MPF = \frac{\sum_{k=1}^{N} f_k . P_k}{\sum_{k=1}^{N} P_k} \tag{6.2}$$

where f_k denotes the frequency of EEG power spectrum at frequency bin k, P_k represents the power spectrum at bin k of N with N indicating the total number of frequency bins.

3. Kurtosis is used to evaluate the flatness of a frequency distribution. This parameter helps determine the number of outliers available in the distribution. More outliers residing in the dataset show heavy tails and indicate a high value of kurtosis while fewer outliers correspond to lighter tails and result in a smaller value of kurtosis. In statistics, it is defined as a fourth-order moment and is expressed as:

$$a_4 = \sum_{i=0}^{M-1} \frac{(y[i] - \mu^4)}{M\sigma^4} \tag{6.3}$$

where μ denotes the mean value and σ represents the standard deviation of the signal.

4. One of the Hjorth parameters, known as complexity, represents any changes in the signal frequency. It is expressed as:

$$complexity(y[n]) = \frac{mobility(y_d[n])}{mobility(y[n])} \tag{6.4}$$

where, $y_d[n] = (y[n+1] - y[n-1])/2$ represents the central finite difference approximation of $y[n]$, and $mobility(y[n])$ is the square root of the ratio of variances of $y_d[n]$ and $y[n]$.

5. Interquartile range (IQR) represents the difference between the third quartile and first quartile. The third quartile ($Q3$) corresponds to 75 % percentile of the data and the first quartile ($Q1$) corresponds to 25 % of the data.

$$IQR = Q3 - Q1 \tag{6.5}$$

6.2.3 Statistical analysis using Kruskal-Wallis (KW) test

After obtaining FIBF-based features, the next step is to obtain a subset of the most significant features using statistical analysis. For this purpose, the feature selection approach plays a significant role in machine learning as it offers many advantages for instance (i) avoid overfitting as the classifier is trained with the most significant features, (ii) minimize the execution time, and (iii) enhance the classifier performance. Various feature selection algorithms namely Student t-test, Fisher score, Wilcoxon rank-sum test, and KW test have been applied in the literature for selecting the most discriminating features [151, 149]. In this study, the KW test, a non-parametric test, is exploited for selecting the best discriminating features using MATLAB statistical toolbox by assigning p-value at a 95% significance level. This method has been discussed in detail in chapter 4. Eight FIBFs have been computed from the given EEG signal and the first derivative of the given signal using the FDM technique. Table 6.1 depicts the probability (p)-values acquired for features extracted from FIBFs corresponding to the original signal when implementing the KW test on F and NF classes. Further, Table 6.2 shows the p-values acquired for features pertaining to the first derivative of the original signal. It is evident that most of the features exhibit low p-values and are able to discriminate between the F and NF classes. The values corresponding to features that are statistically less relevant are

indicated in bold letters.

Table 6.1: The p-values obtained for the features computed from the original signal

FIBFs	$Variance$	$Complexity$	$Interquartilerange$	$Kurtosis$	$Meanfrequency$
FIBF1	$6.8061e-04$	$1.0335e-04$	**0.9702**	0.0010	$5.1672e-04$
FIBF2	0.0111	0.0022	**0.8519**	0.0019	0.0040
FIBF3	$2.9316e-04$	0.0017	**0.9405**	$4.4934e-04$	$2.1908e-04$
FIBF4	0.0025	0.0438	**0.9405**	0.0124	$6.8061e-04$

Table 6.2: The p-values obtained for the features computed from the first derivative of the signal

FIBFs	$Complexity$	$Interquartilerange$	$Meanfrequency$
FIBF1	$1.0335e-04$	$5.9342e-04$	$5.1672e-04$
FIBF2	$8.8575e-05$	0.0013	0.0206
FIBF3	$5.1672e-04$	$2.5360e-04$	$8.9180e-04$
FIBF4	$1.0335e-04$	$5.1672e-04$	0.0032

Table 6.3: SVM classifier performance with various levels of FIBFs

No. of FIBFs	4	5	6	8	10	12	15
Classification Accuracy (%)	98.31	97.85	97.38	96.63	95.58	95.28	93.32

6.2.4 Classification

The features obtained from the decomposed EEG signals, as discussed above, are analyzed for the discrimination between two classes using various machine learning algorithms, such as kNN, LDA, RF, DT and SVM. A detailed description of these classifiers is provided in Section 4.2.4 (Chapter 4) and Section 5.2.4 (Chapter 5).

In this work, a m-fold CV is employed to evaluate the efficacy of the proposed algorithm. In a m-fold CV, the entire dataset is randomly divided into m equal partitions. Out of these, $(m-1)$ partitions are utilized to train the models while one partition is used for testing. This procedure is replicated m times, once for each partition being used as the test set. Thereafter, the performance is measured by averaging the classification results. To assess the performance of the proposed classification approach, five evaluation metrics, namely accuracy, recall, precision, f-measure and area under ROC (AUC) have been computed. These performance parameters have been discussed earlier in Section 4.2.4 (Chapter 4).

6.3 Results and Discussion

The classification results are presented in this section, considering a pair of 50 F and NF EEG signals acquired from the Bern-Barcelona dataset, with each signal containing 10240 samples. These results are obtained using MATLAB 2018b software. The FDM technique is employed to decompose F and NF EEG signals into four FIBFs to ascertain time and frequency domain features. Thereafter, statistically relevant features are selected using KW test to differentiate the F class from the NF class of EEG signals using various classifiers.

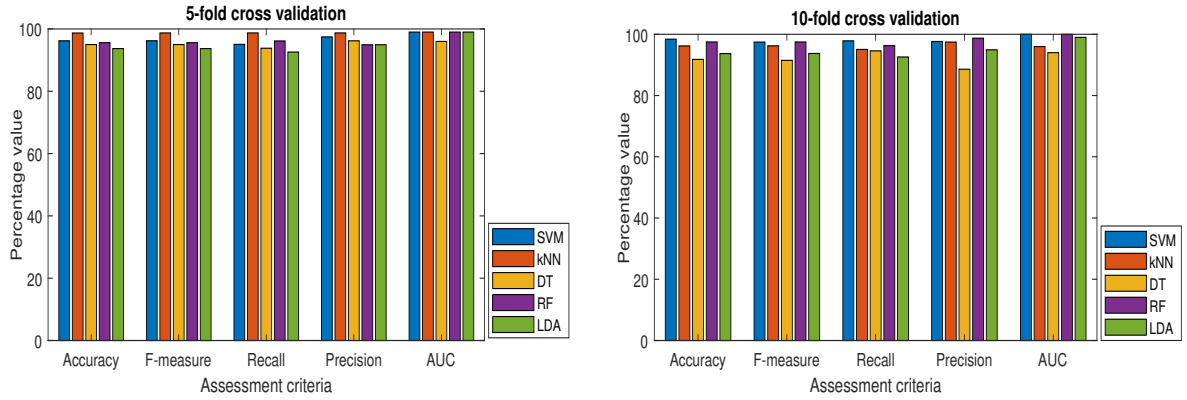

Figure 6.3: Discrimination of F and NF EEG signals using FIBF-based feature extraction from the uniform frequency bands by applying 5 and 10-fold cross validation

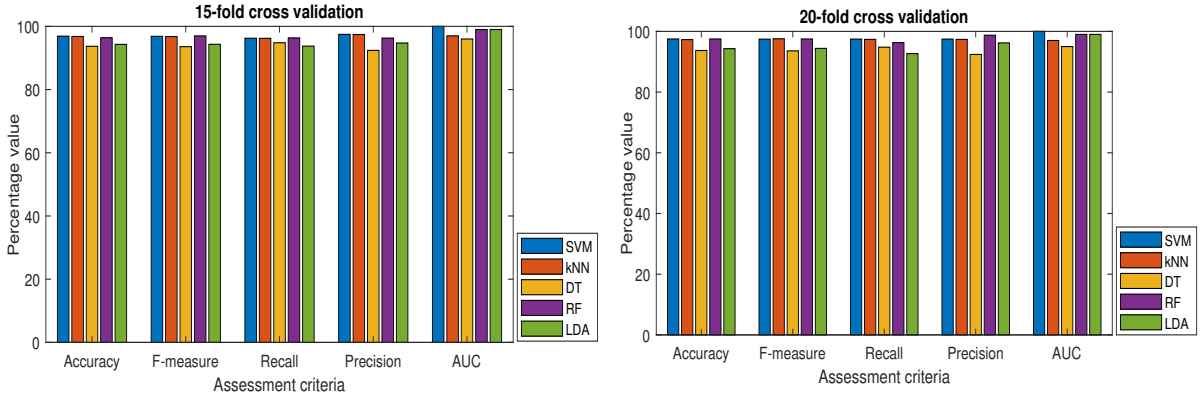

Figure 6.4: Discrimination of F and NF EEG signals using FIBF-based feature extraction from the uniform frequency bands by applying 15 and 20-fold cross validation

The classification accuracies achieved by SVM for different numbers of FIBFs are listed in Table 6.3. The highest accuracy of 98.31% is obtained for 4 FIBFs. Henceforth, all the results are provided considering 4 FIBFs, yielding a total of 32 features, where 20 (5x4) features are computed from the original signal and 12 (3x4) features are computed from the derivative of

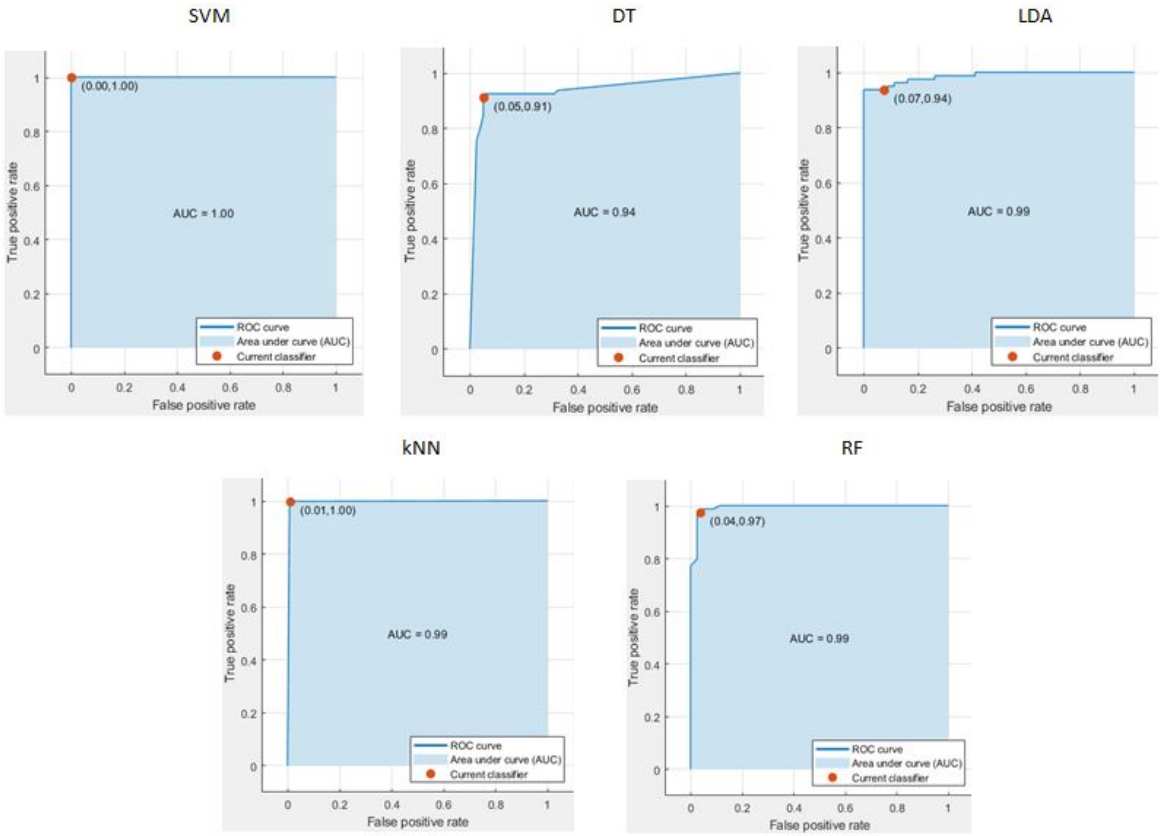

Figure 6.5: Receiver operating characteristic of SVM, DT, LDA, kNN and RF classifiers

the signal. Fig. 6.3 depicts the performance of various classifiers in terms of five evaluation metrics: accuracy, f-measure, recall, precision, and AUC when applying the 5-fold and 10-fold CV schemes. Similar results for 15-fold and 20-fold CV schemes are shown in Fig. 6.4. While comparing different classifiers and CV schemes, it is observed that the highest classification accuracy is obtained by SVM classifier considering a 10-fold CV scheme.

The receiver operating characteristic (ROC) curve illustrates how the sensitivity and 1-specificity vary together. ROC curve is useful in evaluating the classifier performance predicting scarce events such as brain disorders and stroke. Fig. 6.5 illustrates the ROC plots of SVM, DT, LDA, kNN and RF classifiers for the discrimination of F and NF classes. It is observed from Fig. 6.5 that the area under the ROC curve is close to one for the SVM classifier indicating that it predicts the two classes more accurately in comparison to other models.

Recently, many research works have investigated the problem of classifying F and NF EEG signals. Table 4 illustrates the results achieved by various researchers using the Bern-Barcelona dataset as discussed in this work. Sriraam et al. in [149] explored various features extracted from time and frequency domains for the identification of F and NF epileptic seizures. A total

Table 6.4: Comparison of recent studies to discriminate F and NF classes of EEG signals using the Bern Barcelona dataset

Authors and Year	Signal decomposition	Extracted features	Accuracy
Singh et al. [195] 2017	DFT	MF, Root mean square bandwidth	89.7%
Chen et al. [93] 2016	DWT	Sub-band features	83.07%
Gupta et al. [95] 2017	FAWT	entropy-based features	94.41%
Sharma et al. [96] 2017	TQWT	Sub-band features	95%
Sairamya et al. [196] 2020	WPD	entropy-based features	95.74%
Bhattacharyya et al. [131] 2018	EWT	Area measured from phase space rhythms	90%
Sharma et al. [197] 2014	EMD	Sample entropy, variance	85%
Das et al. [198], 2016	EMD-DWT	entropy-based features	89.4%
Sriraam et al. [149] 2017	No	FD, entropy, frequency-based features	92.15%
Raghu et al. [204] 2018	No	Statistical, time, frequency-based features	96.1%
Sharma et al. [205] 2017	OWT	entropy measures	94.25%
Bhattacharyya et al. [207] 2017	TQWT	Sub-band fuzzy entropy	84.67%
Dalal et al. [208] 2018	FAWT	Fractal dimension	90.2%
Arunkumar et al. [209] 2017	No	entropy-based features	98%
Proposed method	FDM	Variance, Complexity, kurtosis, MPF, IQR	98.31%

of twenty six features are drawn out from F and NF EEG signals to achieve a classification accuracy of 92.15% using an SVM classifier considering 10-fold CV. Raghu et al. in [204] applied neighborhood component analysis (NCA) for extracting the significant features from the statistical, time and frequency domains. A classification accuracy of 96.1% is reported using SVM classifier. The authors in [205] employed an orthogonal wavelet transform (OWT) filter bank for the accurate detection of the epileptogenic region by discriminating F and NF events. Using 10-fold CV, they achieved an accuracy of 94.25%. Sharma et al. in [206] computed entropy features from different IMFs obtained by decomposing two classes of EEG signals using the EMD method, and obtained an average accuracy of 87%. In [207], entropy-based features are considered for the identification of epileptic focus with an accuracy of 84.67% using the LS-SVM classifier. On the contrary, Dalal et al. in [208] explored the FAWT approach for decomposing the EEG signals. The fractal dimension is determined from each of the sub-bands to classify F EEG signals, achieving an accuracy of 90.2%. In [209], the authors computed three entropy features from two groups of EEG signals and fed them to six different models to obtain the best accuracy of 98%. It is observed from Table 6.4 that the proposed method achieved the best classification accuracy of 98.31%. Further, the present scheme has utilized less features (variance, complexity, kurtosis, mean frequency and IQR), and hence, the computational complexity gets reduced.

6.4 Summary

In this chapter, an efficient method is presented for accurate detection of epileptogenic focus by discriminating F and NF EEG signals. Each signal is decomposed into a total of eight FIBFs having uniform frequency bands. Thereafter, features such as variance, mean frequency, complexity, kurtosis and inter-quartile range have been extracted from these FIBFs. The Kruskal-Wallis statistical test indicated that most of the extracted features are statistically relevant in distinguishing between F and NF classes. Various classifiers, including SVM, DT, RF, LDA and kNN are applied for training and testing using different cross validation schemes, and the best accuracy is obtained by the SVM classifier considering a 10-fold cross validation scheme. The present study provides better classification performance in comparison to the existing techniques. In future, the proposed method could be employed for detecting temporal lobe focal epilepsy and other neurological abnormalities across a variety of datasets.

Chapter 7

Conclusions and Future Scope

In this chapter, the main contribution of this thesis and future directions of the research are presented.

7.1 Major contributions

Signal processing is an active field of research with applications in various domains such as biomedical engineering and also financial data analysis for the manipulation of real-time data and signals. In this thesis, we have developed and implemented novel and automated algorithms for the accurate diagnosis of various brain abnormalities such as epileptic seizure detection, identification of alcoholism, and recognition of epileptogenic zone by differentiating focal and non-focal EEG signals. The performance of the proposed algorithms is compared with the state-of-the-art methods in terms of various performance metrics such as sensitivity, specificity, accuracy, f-measure and ROC curves. These algorithms are not being developed to completely replace the neuro experts, nonetheless, the prime focus is to reinforce the judgment of the clinical experts and help in making accurate decisions. The proposed study is validated using various publicly available EEG datasets.

The proposed algorithm incorporates the DFT-based zero-phase filter bank for the detection and classification of normal and alcoholic EEG signals. The simulation results revealed the robustness of the time-domain and frequency-domain features. High classification accuracy of 99.98% is achieved using a publically available EEG dataset obtained from the UCI machine learning repository even though the recorded EEG data is greatly contaminated with

ocular artifacts. It is observed that the various features such as kurtosis, Hjorth parameters, interquartile range and median frequency extracted from the signal components obtained using FDM are able to capture discriminative information from the brain signals or EEG. A three-stage automatic alcoholism detection system is developed for the detection and classification of normal and alcoholic EEG signals. In the first stage, the EEG signal is decomposed into various sub-band components. In the second stage, time-domain and frequency-domain features are computed from these frequency sub-bands. Further, an efficient feature selection approach known as KW statistical test is employed to find the most significant features and in the last stage, these significant features are fed as inputs to various classifiers such as kNN, SVM and LDA to discriminate normal and alcoholic EEG signals.

The primary goal of the thesis is to develop efficient automated systems for the diagnosis and classification of various brain disorders with high classification accuracies. The second proposed method incorporates the FDM method by employing the concept of position, velocity, and acceleration on the EEG signals for feature extraction using Lp norms computed from the narrowband signals known as FIBFs. These extracted features are utilized for discriminating seizure events into ictal, interictal, and healthy states with the best accuracy of 99.96% using the BONN dataset and 99.94% using CHB-MIT EEG datasets. The novelty of this work lies is the use of Fourier theory and the generation of the FIBFs that permit efficient implementation using FFT algorithms. The variable amplitudes and frequencies of the FIBFs generate time-frequency-energy (TFE) distribution which demonstrates the embedded structure of the EEG signal. In comparison to the EMD algorithm, the proposed technique does not suffer from a mode mixing problem, end effect artifact as the computation of FIBFs is not dependent on local maxima and minima of the given signal.

7.2 Future directions

It is noticed that the techniques employed in this study would furnish favorable outcomes for the analysis and classification of EEG signals. Still, there are numerous research areas to explore where we can examine the scope of the present study in the analysis of other biomedical signals such as ECG, EMG and EOG. The proposed study is investigated on time series data using generalized Fourier expansion. This creates an issue in the implementation of the proposed

method for the analysis of multidimensional data such as images and videos. Therefore, this work can be further enhanced to develop an efficient method for the analysis of multidimensional data.

References

[1] Callaway, E., Harris, P. R., "Coupling between cortical potentials from different areas," Science, 183(4127), pp. 873–875, 1974.

[2] Mayfieldclinic.com/pe-anatbrain.htm

[3] Merlet, I., Garcia–Larrea, et al., "Simplified projection of EEG dipole sources onto human brain anatomy," Neurophysiol. Clin., 29(1), pp. 9–52, 1999.

[4] Carlson, N. R., "Structure and functions of the nervous system," Foundations of physiological psychology, vol.5, no. 3, 2002.

[5] Chaovalitwongse, W., Pardalos, P., Iasemidis, L. D., Shiau, D. S., Sackellares, J. C., "Dynamical qualitative and quantitative evaluation of EEG signals in epileptic seizure recognition," MECS I.J. intelligent systems and applications, vol. 6, pp. 41–46, 2013.

[6] Dunseath, W. J. R., Kelly, E. F., "Multichannel PC– based data acquisition system for high–resolution EEG," IEEE transactions on biomedical engineering, vol. 42, no. 12, pp. 1212–1217, 1995

[7] Teplan, "Fundamental of EEG measurements," Measurement science review, vol. 2, pp. 1–11, 2002.

[8] Jasper, H. H., "The 10–20 electrode system of the International Federation," Electroencephalography and Clinical Neurophysiology, vol. 10, no. 2, pp. 371–375, 1958.

[9] Palaniappan, R., "Brain computer interface design using band powers extracted during mental tasks," In proceedings of the 2nd international IEEE EMBS conference on neural engineering, 2005.

[10] Qayoom, A., Abdul, W., "Artifact processing of epileptic EEG signals: An overview of different types of artifacts," in International conference on Advanced computer Science Applications and Technologies, pp. 358–361, 2013.

[11] England, M. J., Liverman, C. T., Schultz, A. M., and Strawbridge, L. M., "A reprint from epilepsy across the spectrum: promoting health and understanding," American epilepsy society, pp.245–253, 2012.

[12] World Health Organization, "Fact sheet on epilepsy" [online] Available: http:// www.who.int/mediacentre/fact-sheets/fs999/en/index.html, October 2012.

[13] World Health Organization, "Global Status Report on Alcohol and Health," World Health Organization, Geneva, 2014.

[14] NCRB report, http://ncrb.gov.in/StatPublitions/ADSI/ADSI-2013.pdf, 2013.

[15] Mukherjee, S., "Alcoholism and its effects on the central nervous system," Curr. Neurovascular Res., vol. 10, no. 3, pp. 256–262, 2013.

[16] Alotaiby, T. N., Alshebeli, S. A., El–Samie, F. E., Alabdulrazak, A., Alkhnaian, E., "Channel selection and seizure detection using a statistical approach," in 5th International conference on electronic devices, systems and applications, 2016.

[17] Muhammed Shanir P.P., Khan, Y. U., Farooq, O., "Time domain analysis of EEG for automatic seizure detection," Emerging trends in electrical and electronics engineering, 2015.

[18] Runarsson, T. P., Sigurdsson, S., "On–line detection of patient specific neonatal seizures using support vector machine and half–wave attribute histograms," in International conference on computational intelligence for modelling, control and automation and international conference on intelligent agents, web technologies and internet commerce, pp. 673–677, 2005.

[19] Rana, P., Lipor, J., Lee, H., Drongelen, W. V., Kohrman, M. H., Veen, B. V., "Seizure detection using the phase-slope index and multichannel ECoG," IEEE transactions on biomedical engineering, vol. 59, no. 4, pp. 1125–1134, 2012.

[20] Khamis, H., Mohamed, A., Simpson, S., "Frequency-moment signatures: A method for automated seizure detection from scalp EEG," Clinical Neurophysiology, vol. 124, no. 12, pp. 2317–2327, 2013.

[21] Polat, H., Ozerdem, M. S., "Epileptic seizure detection from EEG signals by using wavelet and Hilbert transform," in 12th International conference on perspective technologies and methods in MEMS design, pp. 66–69, 2016.

[22] Zainuddin, Z., Huong, L. K., Pauline, O., "On the use of wavelet neural networks in the task of epileptic seizure detection from electroencephalography signals," Procedia computer science, vol. 11, pp. 149–159, 2012.

[23] Niknazar, M., Mousavi, S. R., Vahdat, B. V., Sayyah, M., "A new framework based on recurrence quantification analysis for epileptic seizure detection," IEEE journal of biomedical and health informatics, vol. 17, no. 3, pp. 572–578, 2013.

[24] Chen, G., Xie, W., Bui, T. D., Krzyzak, A., "Automatic epileptic seizure detection in EEG using non–subsampled wavelet–Fourier features," Journal of medical and biological engineering, vol. 37, no. 1, pp. 123–131, 2017.

[25] Abbasi, R., Esmaeilpour, M., "Selecting statistical characteristics of brain signals to detect epileptic seizures using discrete wavelet transform and perceptron neural network," International journal of interactive multimedia and artificial intelligence, vol. 4, no. 5, pp. 33–38, 2017.

[26] Panda, R., Khobragade, P. S., Jambhule, P. D., Jengthe, S. N., Pal, P. R., Gandhi, T. K., "Classification of EEG signal using wavelet transform and support vector machine for epileptic seizure diction," in International conference on systems in medicine and biology, Proceedings of international conference on systems in medicine and biology, pp. 405–408, 2010.

[27] Khan, Y. U., Rafiuddin, N., Farooq, O., "Automated seizure detection in scalp EEG using multiple wavelet scales," IEEE international conference on signal processing, computing and control, pp. 1–5, 2012.

[28] Orosco, L., Laciar, E., Correa, A. G., Torres, A., Graffigna, J. P., "An epileptic seizure detection algorithm based on the empirical mode decomposition of EEG," in Annual international conference of the IEEE engineering in medicine and biology society, pp. 2651–2654, 2009.

[29] Alam, S. M. S., Bhuiyan, M. I. H., "Detection of epileptic seizures using chaotic and statistical features in the EMD domain," in Annual IEEE India Conference, 2011.

[30] Bajaj, V., Pachori, R. B., "Epileptic seizure detection based on the instantaneous area of analytic intrinsic mode functions of EEG signals," Biomedical Engineering Letters, vol. 3, pp. 17–21, 2013.

[31] Hyvarinen, A., Ramkumar, P., Parkkonen, L., and Hari, R., "Independent component analysis of short-time Fourier transform for spontaneous EEG/MEG analysis," Neuroimage, vol. 49, pp. 257–271, 2010.

[32] Ingrid, D., Lu, J., and Wu, H. T., "Synchro squeezed wavelet transform: an empirical mode decomposition-like tool," Applied and computational harmonic analysis, pp. 243–261, 2011.

[33] Sharma, R.R., Pachori, R. B., "Eigenvalue decomposition of Hankel matrix-based time-frequency representation of complex signals," Circuits, Systems, and Signal Processing, vol. 37, pp. 3313–3329, 2018.

[34] Dragomiretskiy, K., and Zosso, D., "Variational mode decomposition," IEEE transactions on Signal Processing, vol. 62, no. 3, pp. 531–544, 2014.

[35] Priya, A., Yadav, P., Jain, S., and Bajaj, V., "Efficient method for classification of alcoholic and normal EEG signals using EMD," Journal of Engineering, pp. 166–172, 2018.

[36] Selesnick, I. W., "Resonance–based signal decomposition: A new sparsity-enabled signal analysis method," Signal Processing, vol. 91, no. 12, pp. 2793–2809, 2011.

[37] Liu, A., Hahn, J. S., Heldt, G. P., Coen, R. W., "Detection of neonatal seizures through

computerized EEG analysis," Electroencephalography and Clinical Neurophysiology, vol. 82, no. 1, pp. 30–37, 1992.

[38] Joshi, V., Pachori, R. B., Vijesh, A., "Classification of ictal and seizure-free EEG signals using fractional linear prediction," Biomedical Signal Processing and Control, vol. 9, pp. 1–5, 2014.

[39] Raghu, S., Sriraam, N., "Optimal configuration of multilayer perceptron neural network classifier for recognition of intracranial epileptic seizures," Expert Systems with Applications, vol. 89, pp. 205–221, 2017.

[40] Singh, P., Joshi, S. D., Patney, R. K., Saha, K, "Fourier-based feature extraction for classification of EEG signals using EEG rhythms," Circuits System Signal Process, vol. 35, pp. 3700–3715, 2015.

[41] Boashash, B., Mesbah, M., Colditz, P. B., "Time-frequency detection of EEG abnormalities," Time-frequency signal analysis and processing: A comprehensive Reference, pp. 663–670, 2003.

[42] Pachori, R. B., Sircar, P., "EEG signal analysis using FB expansion and second–order linear TVAR process," Signal Processing, vol. 88, no. 2, pp. 415–420, 2008.

[43] Tzallas, A. T., Tsipouras, M. G., Fotiadis, D. I., "Automatic seizure detection based on time-frequency analysis and artificial neural network," Computational Intelligence and Neuroscience, pp. 1–13, 2007.

[44] Gupta, V., Pachori, R. B., "Epileptic seizure identification using entropy of FBSE based EEG rhythms, Biomedical Signal Processing and Control," vol. 53, pp. 1–11, 2019.

[45] Srinivasan, V., Eswaran, C., Sriraam, N., "Artificial neural network based epileptic detection using time-domain and frequency-domain features," Journal of Medical Systems, vol. 29, no. 6, pp. 647–660, 2005.

[46] Tzallas, A. T., Tsipouras, M. G., Fotiadis, D. I., "Epileptic seizure detection in EEGs using time-frequency analysis," IEEE transactions on information technology in biomedicine, vol. 13, no. 5, pp. 703–710, 2009.

[47] Ocak, H., "Optimal classification of epileptic seizures in EEG using wavelet analysis and genetic algorithm," Signal processing, pp. 1858–1867, 2008.

[48] Wang, D., Ren, D., Li, K., Feng, Y., Ma, D., Yan, X., and Wang, G, "Epileptic seizure detection in long-term EEG recordings by using wavelet-based directed transfer function," IEEE transactions on biomedical engineering, vol. 65, no. 11, pp. 2591–2599, 2018.

[49] Subasi, A. "EEG signal classification using wavelet feature extraction and a mixture of expert model," Expert systems with applications, vol. 32, pp. 1084–1093, 2007.

[50] Satapathy, S. K., Dehuri, S., Jagadev, A. K., "EEG signal classification using PSO trained RBF neural network for epilepsy identification," Informatics in Medicine Unlocked, 2016.

[51] Mursalin, M.,Zhang, Y., Chen, Y., and Chawla, N.V., "Automated epileptic seizure detection using improved correlation-based feature selection with random forest classifier," Neurocomputing, 2017.

[52] Rafiuddin, N., Khan, Y. U., Farroq, O., "Feature extraction and classification of EEG for automatic seizure detection," in International conference on multimedia, signal processing and communication technologies, pp. 184–187, 2011.

[53] Guo, L., Rivero, D., Pazos, A., "Epileptic seizure detection using multiwavelet transform based approximate entropy and artificial neural network," Journal of neuroscience methods, vol. 193, no. 1, pp. 156–163, 2010.

[54] Alam, S. M. S., Bhuiyan, M. I. H., "Detection of seizure and epilepsy using higher order statistics in the EMD domain," IEEE journal of biomedical and health informatics, vol. 17, no. 2, pp. 312–318, 2013.

[55] Riaz, F., Hassan, A., Rehman, S., Niazi, I. K., Dremstrup, K., "EMD-based temporal and spectral features for the classification of EEG signals using supervised learning," IEEE transactions on neural systems and rehabilitation engineering, vol. 24, no. 1, pp. 28–35, 2016.

[56] Sharma, R., Pachori, R. B., "Classification of epileptic seizures in EEG signals based on

phase space representation of intrinsic mode functions," Expert systems with applications, vol. 42, no. 3, pp. 1106–1117, 2015.

[57] Pachori, R. B., Patidar, S., "Epileptic seizure classification in EEG signals using second order difference plot of intrinsic mode functions," Computer methods and programs in biomedicine, vol. 113, no. 2, pp. 494–502, 2014.

[58] Dash, D. P., Kolekar, M. H., Jha, K., "Multichannel EEG based automatic epileptic seizure detection using iterative filtering decomposition and hidden Markov model," Journal of computers in biology and medicine, 2019.

[59] Hassan, A. R., Subasi, A. Zhang, Y., "Epileptic seizure detection using complete ensemble empirical mode decomposition with adaptive noise," Knowledge-based systems, 2019.

[60] Fu, K., Qu, J., Chai, Y., Dong, Y., "Classification of seizure based on the time-frequency image of EEG signals using HHT and SVM," Biomedical Signal Processing and Control, vol. 13, pp. 15–22, 2015.

[61] Oweis, R. J., Abdulhay, E. W., "Seizure classification in EEG signals utilizing Hilbert-Huang transform," Biomedical engineering online, vol. 10, no. 1, pp. 1–15, 2011.

[62] Alickovic, E., Kevric, J., Subasi, A., "Performance evaluation of empirical mode decomposition, discrete wavelet transforms, and wavelet packet decomposition for automated epileptic seizure detection and prediction," Biomedical Signal Processing and Control, vol. 39, pp. 94–102, 2018.

[63] Wu, Z., Huang, N. E., "Ensemble empirical mode decomposition: a noise-assisted data analysis method," Advances in adaptive data analysis, vol. 1, no. 1, pp. 1–41, 2009.

[64] Hassan, A. R., Haque, M. A., "Epilepsy and seizure detection using statistical features in the complete ensemble empirical mode decomposition domain," IEEE conference, pp. 1–6, 2015.

[65] Singh, P., Joshi, S. D., Patney, R. K., Saha, K., "The Hilbert spectrum and the energy preserving empirical mode decomposition," arXiv preprint arXiv: 1504.04104, 2015.

[66] Rehman, N., Mandic, D. P., "Multivariate empirical mode decomposition," Proceeding of the Royal Society A, vol. 466, pp. 1291–1302, 2010.

[67] Enoch, M. A., Goldman, D., "Problem drinking and alcoholism: diagnosis and treatment," Am. Fam. Phys., 65(3), pp. 441–448, 2002.

[68] Prince, J., "Substance use disorder and suicide attempt among people who report compromised health," Substance Use Misuse, vol. 53, no. 1, pp. 9–15, 2018.

[69] Schuckit, M.A., "Drug and Alcohol Abuse: A Clinical Guide to Diagnosis and Treatment," Springer Science and Business Media, 2006.

[70] Han, D. X., Zhou, C. D., Liu, Y. H., "Application of brain state related EEG complexity measure in mental workload evaluation," Space Med. Eng., vol. 14, no. 2, pp. 102–106, 2001.

[71] Arns, M., Gunkelman, J., Olbrich, S., Sander, C., Hegerl, U., "EEG vigilance and phenotypes in neuropsychiatry: Implications for intervention," pp. 79–123, 2011.

[72] Son, K., Choi, J., Lee, J., Park, S., Lim, J., "Neurophysiological features of Internet gaming disorder and alcohol use disorder: a resting–state EEG study,"Transl Psychiatry, 2015.

[73] Alhassoon, O. M., Sorg, S. F., Stern, M. J., Hall, M. G., Wollman, S. C., "Neuroimaging in alcohol-use disorders: clinical implications and future directions," Future Neurology, pp. 345–56, 2015.

[74] Tessy, E., Muhammed Shanir, P. P., Manafuddin, S., "Time domain analysis of epileptic EEG for seizure detection," International conference on next generation intelligent system, 2016.

[75] Bhople, A. D., Tijare, P. A., "Fast Fourier transform based classification of epileptic seizure using artificial neural network," Int. J. Adv. Res. Comput. Sci. Softw. Eng., vol. 2, no. 4, pp. 228–231, 2012.

[76] Upadhyay, R., Padhy, P., Kankar, P., "Alcoholism diagnosis from EEG signals using continuous wavelet transform," Annual IEEE India Conference, 2014.

[77] Patidar, S., Pachori, R.B., Upadhyay, A., Acharya, U.R., "An integrated alcoholic index using tunable–Q wavelet transform based features extracted from EEG signals for diagnosis of alcoholism," Appl. Soft Comput. vol. 50, 71–78, 2017.

[78] Faust, O., Yu, W., Kadri, N.A., "Computer-based identification of normal and alcoholic EEG signals using wavelet packets and energy measures," J. Mech. Med. Biol., vol. 13, no. 3, 2013.

[79] Acharya, U. R., Sree, S. V., Chattopadhyay, S., Suri, J. S., "Automated diagnosis of normal and alcoholic EEG signals," International journal of neural systems, vol. 22, no. 3, pp. 1250011–1–1250011–11, 2012.

[80] Palaniappan, R., "Discrimination of alcoholic subjects using second order autoregressive modelling of brain signals evoked during visual stimulas perception," Proceedings of world academy of science, engineering and technology, vol. 7, 282–287, 2005.

[81] Faust, O., Archarya, R. U., Allen, A. R., Lin, C. M., "Analysis of EEG signals during epileptic and alcoholic states using AR modeling techniques," IRBM, vol. 29, no. 1, pp. 44–52, 2008.

[82] NG, E. P., LIM, T. C., Chattopadhyay, S., and Bairy, M., "Automated identification of epileptic and alcoholic EEG signals using recurrence quantification analysis," Journal of mechanics in medicine and biology, vol. 12, no. 5, pp. 1240028(1–17), 2012.

[83] Guntaka, R., Tcheslavski, G. V., "On the EEG–based automated detection of alcohol dependence," Int. J. Bio. Automation, vol. 17, no. 3, pp. 167–176, 2013.

[84] Mumtaz, W., Vuong, P. L., Xia, L., Malik, S. A., Rashid, R. B. A., "Automatic diagnosis of alcohol use disorder using EEG features," Knowledge-based systems, vol. 105, pp. 48–59, 2016.

[85] Faust, O., Yanti, R., Yu, W., "Automated detection of alcohol related changes in electroencephalograph signals," Journal of medical imaging and health informatics, vol. 3, pp. 333–339, 2013.

[86] Raymond, D. P., Gotman, J., "Asymmetry in delta activity in patients with focal epilepsy," Electroencephalography and clinical neurophysiology, vol. 75, no. 6, pp. 474–481, 1990.

[87] Zhu, G., Li, Y., Wen, P., Wang, S., Xi, M., "Epileptogenic focus detection in intracranial EEG based on delay permutation entropy," AIP conference proceedings, pp. 31–36, 2013.

[88] Yadav, R., Swamy, M. N. S., Agarwal, R., "Rapid identification of epileptogenic sites in the intracranial EEG," International conference of the IEEE Engineering in Medicine and Biology Society, pp. 7553–7556, 2011.

[89] Gutierrez, J., Alcantara, R., Medina, V., "Analysis and localization of epileptic events using wavelet packets," Medical Engineering and Physics, vol. 23, no. 9, pp. 623–631, 2001.

[90] Akbari, H., Sadiq, M. T., "Detection of focal and non–focal EEG signals using non-linear features derived from empirical wavelet transform rhythms," Physical and Engineering Science in Medicine, pp. 1–15, 2020.

[91] Chen, D., Wan, S., Bao, F. S., "Epileptic focus localization using EEG based on discrete wavelet transform through full-level decomposition," IEEE international workshop on machine learning for signal processing, pp. 1–6, 2015.

[92] Deivasigamani, S., Senthilpari, C., Yong, W. H., "Classification of focal and non-focal EEG signals using ANFIS classifier for epilepsy detection," International journal of imaging systems and technology, vol. 26, no. 4, pp. 277–283, 2016.

[93] Chen, D., Wan, S., Bao, F. S., "Epileptic focus localization using discrete wavelet transform based on interictal intracranial EEG," IEEE Transactions on neural systems and rehabilitation engineering, 2016.

[94] Acharya, U. R., Sree, S. V., Alvin, A. P. C., Suri, J. S., "Use of principal component analysis for automatic classification of epileptic EEG activities in wavelet framework," Expert systems with applications, vol. 39, pp. 9072–9078, 2012.

[95] Gupta, V., Priya, T., Yadav, A. K., Pachori, R. B., U. R. Acharya, U. R., "Automated detection of focal EEG signals using features extracted from flexible analytic wavelet transform," Pattern recognition letters, 2017.

[96] Sharma, R., Kumar, M., Pachori, R. B., Acharya, U. R., "Decision support system for Focal EEG signals using tunable-Q wavelet transform," Journal of computational science, 2017.

[97] Gratton, G., Coles, M. G., Donchin, E., "A new method for off-line removal of ocular artifact," Electroencephalography and Clinical Neurophysiology, vol. 55, no. 4, pp. 468–484, 1983.

[98] Woestenburg, J. C., Verbaten, M. N., Slangen, J. L., "The removal of the eye-movement artifact from the EEG by regression analysis in the frequency domain," Biological Psychology, vol. 16, pp. 127–147, 1983.

[99] Jung, T. P., Humphries, C., Lee, T.W., Makeig, S., Mckeown, M. J., Iragui, V., Sejnowski, T. J., "Extended ICA removes artifacts from electroencephalographic recordings," Advances in neural information processing systems, vol. 10, pp. 894–900, 1998.

[100] Jung, T. P., Makeig, S., Humphries, C., Lee, T.W., Mckeown, M. J., Iragui, V., Sejnowski, T. J., "Removing electroencephalographic artifacts by blind source separation," Psychophysiology, vol. 37, pp. 163–178, 2000.

[101] Vigario, R. N., "Extraction of ocular artifacts from EEG using independent component analysis," Electroencephalography, and clinical neurophysiology, vol. 103, pp. 395–404, 1997.

[102] Romero, S., Mananas, M. A., Clos, S., Gimenez, S., Barbanoj, M. J., "Reduction of EEG artifacts by ICA in different sleep stages," Proceedings of the 25th annual international conference of the IEEE EMBS, pp. 2675–2678, 2003.

[103] Kher, R., Gandhi, R., "Adaptive filtering-based artifact removal from electroencephalogram (EEG) signals," International conference on Communication and Signal Processing, pp. 561–564, 2016.

[104] Mosquera, C. G., Vazquez, A. N., "Automatic removal of ocular artifacts using adaptive filtering and independent component analysis for electroencephalogram data," IET Signal Processing, vol. 6, no. 2, pp. 99–106, 2012.

[105] Chen, Y., Zhao, Q., Hu, B., Li, J., Jiang, H., Lin, W., Li, Y., Zhou, S., Peng, H., "A method of removing ocular artifacts from EEG using discrete wavelet transform and Kalman filtering," IEEE International conference on Bioinformatics and Biomedicine, pp. 1485–1492, 2016.

[106] Ghandeharion, H., Noubari, H. A., "Detection and removal of ocular artifacts using independent component analysis and wavelets," Proceedings of the 4th international IEEE EMBS conference on Neural Engineering, pp. 653–656, 2009.

[107] Sharma, H., Sharma, K. K., "Baseline wander removal of ECG signals using Hilbert vibration decomposition," Electronics letters, vol. 51, no. 6, pp. 447–449, 2015.

[108] Keshtkaran, M. R., Yang, Z., "A fast, robust algorithm for power line interference cancellation in neural recording," Journal of neural Engg., 11(2), 026017, 2014.

[109] Astle, J. A., Schilder, T., "Removal of baseline wander and power line interfernce from the ECG by an efficient FIR filter with a reduced number of taps," IEEE trans. Biomed. Engg., vol. 12, pp. 1052–1060, 1985.

[110] Huang, N.E. Shen, Z., Long, S., Wu, M., Shih, H., Zheng, Q., Yen, N., Tung, C., Liu, H., "The empirical mode decomposition and Hilbert spectrum for non-linear and non-stationary time series analysis," Proceedings of The Royal Society A, 454, pp. 903–995, 1988.

[111] Huang, N. E., Wu, M. L. C., Long, S. R., Shen, S. S. P., Qu, W., Gloersen, P., Fan, K. L., "A confidence limit for the empirical mode decomposition and Hilbert spectral analysis," Proceedings of The Royal Society A, 459, pp. 2317–2345, 2003.

[112] Bansod, P., Lambhate, R., "A new approach for removal of baseline wander in ECG signal using empirical mode decomposition and hurst exponent," IEEE international conference on recent advances and innovations in engineering, pp. 1–6, 2016.

[113] Anapagamini, S. A., Rajavel, R., "Removal of artifacts in ECG using empirical mode decomposition," in International conference on communication and signal processing, pp. 288–292, 2013.

[114] Rakshit, M., Das, S., "An improved EMD based ECG denoising method using adaptive switching mean filter," in International conference on signal processing and integrated networks, pp. 251–255, 2017.

[115] Singhal, A., Singh, P., Fatimah, B., and Pachori, R. B., "An efficient removal of power-line interference and baseline wander from ECG signals by employing Fourier decomposition technique," Biomedical Signal Processing and Control, 57, 101741, 2020.

[116] Singh, P., Joshi, S.D., Patney, R. K., Saha, K., "The Fourier decomposition method for nonlinear and non-stationary time series analysis," Proceeding of The Royal Society A, 20160871, 2017.

[117] Singh, P., "Novel Fourier quadrature transforms and analytic signal representations for nonlinear and non-stationary time series analysis," Royal Society Open Science, vol. 5, no. 11, 2018.

[118] Singh, P., "Breaking the Limits: Redefining the Instantaneous Frequency," Circuits Syst Signal Process, vol. 37, pp. 3515–3536, 2018.

[119] Fatimah, B., Singh, P., Singhal, A., Pachori, R. B., "Detection of apnea events from ECG segments using Fourier decomposition method," Biomedical Signal Processing and Control, vol. 61, 102005, 2020.

[120] Gupta, A., Joshi, S. D., Singh, P., "On the approximate discrete KLT of fractional Brownian motion and applications," Journal of the Franklin Institute, vol. 355, no. 17, pp. 8989–9016, 2018.

[121] Singh, P., Joshi, S. D., "Some Studies on Multidimensional Fourier Theory for Hilbert Transform, Analytic Signal and AM-FM Representation," Circuits, Systems, and Signal Processing, vol. 38, pp. 5623–5650, 2019.

[122] Kapoor, E., Johnson, V., Pati, S., and Chakka, V. K., "Fourier decomposition method based descriptor of EEG signals to identify Dementia," IEEE Proceeding of the International Conference, pp. 2474–2478, 2016.

[123] Singhal, A., Singh, P., Lall, B., Joshi, S. D., "Modeling and prediction of COVID-19 pandemic using Gaussian mixture model," Chaos, Solitons and Fractals, vol. 138, 110023, 2020.

[124] Singh, P., Singhal, A., Joshi, S.D., "Time-frequency analysis of gravitational waves," in International Conference on Signal Processing and Communications (SPCOM), pp. 197–201, 2018.

[125] Bhler, M., Mann, K., "Alcohol and the human brain: a systematic review of different neuroimaging methods," Alcohol Clin. Exp. Res., vol. 35, no. 10, 1771–1793, 2011.

[126] Mumtaz, W., Vuong, P. L., Malik, A. S., Rashid, R. B. A., "A review on EEG–based methods for screening and diagnosing alcohol use disorder," Cognitive Neurodynamics, pp. 141–156, 2018.

[127] Camprodon, J. A., Stern, T. A., "Selecting neuroimaging techniques: A review for the clinician," The primary care companion for CNS disorders, 2012.

[128] Bajaj, V., Guo, Y., Sengur, A., Siuly, S., and Alcin, O. F., "A hybrid method based on time-frequency images for classification of alcohol and control EEG signals," Neural Computing and Applications, pp. 3717–3723, 2016.

[129] Sharma, M., Sharma, P., Pachori, R. B., Acharya, U. R., "Dual–tree complex wavelet transform-based features for automated alcoholism identification," Int. J. Fuzzy Stst., vol. 20, no. 4, pp. 1297–1308, 2018.

[130] Sharma, M., Acharya, U. R., and Pachori, R. B., "A new approach to characterize epileptic seizures using analytic time-frequency flexible wavelet transform and fractal dimension," Pattern Recognition Letters, vol. 94, pp. 172–179, 2017.

[131] Bhattacharya, A., Sharma, M., Pachori, R. B., Sircar, P., and Acharya, U. R., "A novel

approach for automated detection of focal EEG signals using empirical wavelet transform," Neural Computing and Applications, pp. 47–57, 2018.

[132] Gilles, J., "Empirical wavelet transform," IEEE Transactions on signal processing, vol. 61, no. 16, pp. 3999–4010, 2013.

[133] Bhattacharya, A., Singh, L., and Pachori, R. B., "Fourier-Bessel series expansion based empirical wavelet transform for analysis of non–stationary signals," Digital Signal Processing and Control, vol.78, pp. 185–196, 2018.

[134] Anuragi, A., Sisodia, D. S., and Pachori, R. B., "Automated alcoholism detection using Fourier-Bessel series expansion based empirical wavelet transform," IEEE Sensors Journal, 2020.

[135] Feldman, M., "Time-varying vibration decomposition and analysis based on the Hilbert transform," Journal of Sound and Vibration, vol. 295, issue 3–5, pp. 518–530, 2006.

[136] Agrawal, S., and Gupta, A., "Fractal and EMD based removal of baseline wander and powerline interference from ECG signals," Computers in Biology and Medicine, vol. 43, issue 11, pp. 1889–1899, 2013.

[137] Bajaj, V., and Pachori, R. B., "Classification of seizure and non-seizure EEG signals using empirical mode decomposition," IEEE Transactions on Information Technology in Biomedicine, pp. 1135–1142, 2011.

[138] Zou, S., Qiu, T., Huang, P., Bai, X., and Liu, C., "Constructing multi-scale entropy based on the Empirical Mode Decomposition(EMD) and its application in recognizing driving fatigue," Journal of Neuroscience Methods, 341, 108691, 2020.

[139] Hassan, A. R., and Bhuiyan, M. I. H., "Automatic sleep scoring using statistical features in the EMD domain and ensemble methods," Biocybernetics and Biomedical Engineering, vol. 36, issue 1, pp. 248–255, 2016.

[140] Hassan, A. R., and Bhuiyan, M. I. H., "Computer-aided sleep staging using complete ensemble empirical mode decomposition with adaptive noise and bootstrap aggregating," Biomedical Signal Processing and Control, vol. 24, pp. 1–10, 2016.

[141] Taran, S., Bajaj, V., "Rhythm-based identification of alcohol EEG signals," The institute of Engineering and Technology, vol. 12, issue 3, pp. 343–349, 2018.

[142] Thilagaraj, M., and Rajasekaran, M. P., "An empirical mode decomposition based scheme for alcoholism identification," Pattern Recognition Letters, vol. 125, pp. 133–139, 2019.

[143] Labate, D., Foresta, F. L., Morabito, G., Palamara, I., and F. C. Morabito, F. C., "On the use of empirical mode decomposition for Alzheimer's disease diagnosis," Advances in Neural Netwroks: Computational and Theoretical Issues, pp. 121–128, 2015.

[144] Singh, P., "Some studies on a generalized Fourier expansion for nonlinear and nonstationary time series analysis," PhD thesis, Department of Electrical Engineering, IIT Delhi, India, 2016.

[145] UCI, "EEG Database, UCI Knowledge Discovery in Databases Archive" [Online]. https://kdd.ics.uci.edu/databases/eeg/eeg.data.html, 2018.

[146] Acharya, J. N., Hani, A., Cheek, J., Thirumala, P., and Tsuchida, T. N., "American Clinical Neurophysiology Society Guideline 2: Guidelines for Standard Electrode Position Nomenclature," J. Clin. Neurophysiol. vol. 33, no. 4, pp. 308–311, 2016.

[147] Snodgrass, J. G., and Vanderwart, M. A., "A standardized set of 260 pictures: Norms for the naming agreement, familiarity, and visual complexity," J. Exp Psychol: Human Learning and Memory, vol. 6, pp. 174–215, 1980.

[148] Acharya, U. R., Hagiwara, Y., Deshpande, S. N., Suren, S., Koh, J. E. W., Oh, S. L., Arunkumar, N., Ciaccio, E. J., and Lim, C. M., "Characterization of focal EEG signals: A review," Future Generation Computer Systems, 2018.

[149] Sriraam, N., Raghu, S., "Classification of focal and non focal epileptic seizures using multi–features and SVM classifier," Journal of Medical Systems, pp. 1–14, 2017.

[150] Bedeeuzzaman, M., Fatima, T., Khan, Y. U., and Farroq, O., "Seizure prediction using statistical dispersion measures of intracranial EEG," Biomedical Signal Processing and Control, vol. 10, pp. 338–341, 2014.

[151] Sen, B., Peker, M., Cavusoglu, A., Celebi, F. V., "A comparative study on classification of sleep stage based on EEG signals using feature selection and classification algorithms," Journal of medical systems, vol. 38, no. 18, 2014.

[152] Vapnik, V., "The nature of statistical learning theory," New York: Springer–Verlag, 1995.

[153] Chandel, G., Upadhyaya, P., Farooq, O., and Khan, Y. U., "Detection of seizure event and its onset/offset using orthonormal triadic wavelet based features," IRBM, vol. 40, pp. 103–112, 2019.

[154] Esa, N. E. M., Amir, A., IIyas, M. Z., and Razalli, M. S., "The performance analysis of k-nearest neighbors algorithm for motor imagery classification based on EEG signal," MATEC Web of conferences, vol. 140, 01024, 2017.

[155] Subasi, A., M. I. Gursoy, M. I., "EEG signal classification using PCA, ICA, LDA and support vector machines," Expert Systems and Applications, vol. 37, pp. 8659–8666, 2010.

[156] Prabhakar, S. K., Rajaguru, H. K., "Epilepsy classification using discriminant and implementation with space time trellis coded MIMO–OFDM system for telemedicine applications," in International conference on the development of biomedical engineering in Vietnam, pp. 493–497, 2017.

[157] Adeli, H., Zhou, Z., Dadmehrc, N., "Analysis of EEG records in an epileptic patient using wavelet transform," Journal of Neuroscience Methods, vol. 123, no. 1, pp. 69–87, 2003.

[158] Anuragi, A., and Sisodia, D. S., "Alcohol use disorder detection using EEG signal features and flexible analytical wavelet transform," Biomedical Signal Processing and Control, 2018.

[159] Sharma, M., Deb, D., and Acharya, U. R., "A novel three-band orthogonal wavelet filter bank method for an automated identification of alcoholic EEG signals," Applied Intelligence, pp. 1368–1378, 2017.

[160] Shah, S., Sharma, M., Deb, D., and Pachori, R. B., "An automated alcoholism detection

using orthogonal wavelet filter bank," Machine Intelligence and Signal Analyis, Singapore: Springer, pp. 473–483, 2019.

[161] Bavkar, S., Iyer, B., and Deosarkar, S., "Detection of alcoholism: An EEG hybrid features and ensemble subspace kNN based approach," International conference on distributed computing and internet technology, pp. 161–168, 2019.

[162] Kaya, Y., Uyar, M., Tekin, R., Yildirim, S., "1-D local binary pattern–based feature extraction for classification of epileptic EEG signals," Applied Mathematics and Computation, vol. 243, pp. 209–219, 2014.

[163] Kumar, T. S., Kanhangad, V., Pachori, R. B., "Classification of seizure and seizure-free EEG signals using local binary pattern," Biomedical Signal Processing and Control, vol. 15, pp. 33–40, 2015.

[164] Tiwari, A. K., Pachori, R. B., Kanhangad, V., Panigrahi, B. K., "Automated diagnosis of epilepsy using key-point-based local binary pattern of EEG signals," IEEE Journal Biomed. Health Inform., vol. 21, no. 4, pp. 888–896, 2017.

[165] Gupta, A., Singh, P., Karlekar, M., "A novel signal modeling approach for classification of seizure and seizure-free EEG signals," IEEE Transactions on Neural Systems and Rehabilitation Engineering, vol. 26, no. 5, pp. 925–935, 2018.

[166] Alam, M. Z., Rahman, M. S., Parvin, N., Sobhan, M. A., "Time-frequency representation of a signal through non-stationary multipath fading channel," in International conference on informatics, electronics and vision, pp. 1130–1135, 2012.

[167] Subbarao, M. V., Samundiswary, P., "Time-frequency analysis of non-stationary signals using frequency slice wavelet transform," in International conference on intelligent systems and control, pp. 1–6, 2016.

[168] Bhati, D., Gadre, V. M., Pachori, R. B., "A novel approach for time-frequency localization of scaling functions and design of three-band biorthogonal linear phase wavelet filter banks," Digital Signal Processing, vol. 69, pp. 309–322, 2017.

[169] Bhati, D., Sharma, M., Gadre, V. M., Pachori, R. B., "Time-frequency localized three-band biorthogonal wavelet filter bank using semidefinite relaxation and nonlinear least squares with epileptic seizure EEG signal classification," Digital Signal Processing, vol. 62, pp. 259–273, 2017.

[170] Wang, L., Xue, W., Li, Y., Luo, M., Huang, J., Cui, W., Huang, C., "Automatic epileptic seizure detection in EEG signals using multi-domain feature extraction and non-linear analysis," Entropy, vol. 19, no. 6, pp. 1–17, 2017.

[171] Peker, M., Sen, B., Delen, D., "A novel method for automated diagnosis of epilepsy using complex-valued classifiers," IEEE Journal of Biomedical and Health Informatics, vol. 20, no. 1, pp. 108–118, 2016.

[172] Subasi, A., Kevric, J., Canbaz, M. A., "Epileptic seizure detection using hybrid machine learning methods," Neural Computing and Applications, 2017.

[173] Tuncer, T., Dogan, S., Ertam, F., Subasi, A., "A novel ensemble local graph structure based feature extraction network for EEG signal analysis," Biomedical Signal Processing and Control, vol. 61, 102006,2020.

[174] Vidyaratne, L. S., Iftekharuddin, K. M., "Real-time epileptic seizure detection using EEG," IEEE Transactions on Neural System and Rehabilitation Engineering, vol. 25, no. 11, pp. 2146–2156, 2017.

[175] Fu, K., Qu, J., Chai, Y., Zou, T., "Hilbert marginal spectrum analysis for automatic seizure detection in EEG signals," Biomedical Signal Processing and Control, vol. 18, pp. 179–185, 2015.

[176] Kaleem, M., Guergachi, A., Krishnan, S., "EEG seizure detection and epilepsy diagnosis using a novel variation of empirical mode decomposition," proceedings of the 2013 35th annual international conference of the IEEE engineering in Medicine and Biology Society, pp. 4314–4317, 2013.

[177] Torres, M. E., Colominas, M. A., Schlotthauer, G., Flandrin, P., "A Complete ensemble empirical mode decomposition with adaptive noise," in IEEE International Conference on Acoustics, Speech, and Signal Processing, pp. 4144–4147, 2011.

[178] Andrzejak, R. G., Lehnertz, K., Mormann, F., Rieke, C., David, P., Elger, C. E., "Indications of nonlinear deterministic and finite–dimensional structures in time series of brain electrical activity: Dependence on recording region and brain state," Physical Review E, vol. 64, no. 6, 061907, 2001.

[179] CHB–MIT Scalp EEG Database, [Online]. Available: http://physionet.org/physiobank/database/chbmit/.

[180] Shoeb, A., "Application of machine learning to epileptic seizure detection," in International Conference on Machine Learning (ICML), pp. 975–982, 2010.

[181] Zhang, Z., Xu, Y., Yang, J., Li, X., Zhang, D., "A survey of sparse representation: algorithms and applications," IEEE Access, vol. 3, pp. 490–530, 2015.

[182] Koopmans, L. H., "The Spectral Analysis of Time Series," Academic Press, 1995.

[183] Oppenheim, A. V., Willsky, A. S., "Signals & Systems," Prentice Hall India, 1997.

[184] Guyon, I., Weston, J., Barnhill, S., Vapnik, V., "Gene selection for cancer classification using support vector machines," Machine Learning, vol. 46, pp. 389–422, 2002.

[185] Khandoker, A. H., Lai, D. T. H., Begg, R. K., Palaniswami, M., "Wavelet–based feature extraction for support vector machines for screening balance impairments in the elderly," IEEE transactions on neural systems and rehabilitation engineering, vol. 15, no. 4, pp. 587–597, 2007.

[186] Jukic, S., Saracevic, M., Subasi, A., and Kevric, J., "Comparison of ensemble machine learning methods for automated classification of focal and non–focal epileptic EEG signals," MDPI, 2020.

[187] Hussain, MD. S., Sarfraz, M., Rukhsar, S., "Epileptic seizure detection using temporal based measures in EEG signal," International Conference on Communication and Electronics Systems, pp. 743–748, 2018.

[188] Sharma, N., "Classification using Naive bayes classifer: A survey," International journal of engineering science invention research and development, vol. 2, no. 8, pp. 1–6, 2016.

[189] Fergus, P., Hignett, D., Hussain, A. J., and Al-Jumeily, D., "An advanced machine learning approach to generalized epileptic seizure detection," International Conference on Intelligent Computing, pp. 112–118, 2014.

[190] Pati, S., and Alexopoulos, A. V., "Pharmacoresistant epilepsy: from pathogenesis to current and emerging therapies," Cleveland Clinic Journal of Medicine, vol. 77, no. 7, pp. 457–467, 2010.

[191] Savic, I., Thorell, J. O., Roland, P., "Flumazenil positron emission tomography visualizes frontal epileptogenic regions," Epilepsia, vol. 36, no. 12, pp. 1225–1232, 1995.

[192] Seeck M et al., "Non-invasive epileptic focus localization using EEG-triggered functional MRI and electromagnetic tomography," Electroencephalogram Clin Neurophysiology, vol. 106, no. 6, pp. 508–512, 1998.

[193] Andrzejak, R. G., Schindler, K., Rummel, C., "Nonrandomness, nonlinear dependence, and nonstationarity of electroencephalographic recordings from epilepsy patients," Phys. Rev. E, vol. 86, no. 4, 2012.

[194] Prasanna, J., Subathra, M. S. P., Mohammed, M. A., Maashi, M. S., Sairamya, N. J., George, S. T., and Zapirain, B. G., "Detection of focal and non-focal electroencephalogram signals using fast Walsh-Hadamard transform and artificial neural network," Sensors, MDPI, 2020.

[195] Singh, P., Pachori, R. B., "Classification of focal and nonfocal EEG signals using features derived from Fourier-based rhythms," Journal of mechanics in medicine and biology, vol. 17, no. 7, 1740002, 2017.

[196] Sairamya, N. J., Subathra, M. S. P., Suviseshamuthu, E. S., George, S. T., "A new approach for automatic detection of focal EEG signals using wavelet packet decomposition and quad binary pattern method," Biomedical signal processing and control, vol. 63, 2020.

[197] Sharma, R., Pachori, R. B., "Empirical mode decomposition based classification of focal and non-focal EEG signals," in International conference on medical biometrics, pp. 135–140, 2014.

[198] Das, A. B., Bhuiyan, M. I. H., "Discrimination and classification of focal and non-focal EEG signals using entropy-based features in the EMD–DWT domain," Biomedical signal processing and control, vol. 29, pp. 11–21, 2016.

[199] Rahman, M. M., Bhuiyan, M. I. H., Das, A. B., "Classification of focal and non-focal EEG signals in VMD-DWT domain using ensemble stacking," Biomedical signal processing and control, vol. 50, pp. 72–82, 2019.

[200] Bern–Barcelona Database: http://ntsa.upf.edu/downloads/andrzejak-rg-schindler-k-rummel-c-2012-nonrandomness-nonlinear-dependence-and nonstationarity of electroencephalographic recordings from epilepsy patients, Phys. Rev. E 86, 046206, 2012.

[201] Gill, A. F., Fatima, S. A., Nawaz, A., Nasir, A., Akram, M. U., Khawaja, S. G., and Ejaz, S., "Time domain analysis of EEG signals for detection of epileptic seizure," IEEE Symposium on Industrial Electronics and Applications (ISIEA), pp. 32–35, 2014.

[202] Thomas, E. M., Temko, A., Marnane, W. P., Boylan, G. B., and Lightbody, G., "Discriminative and generative classification techniques applied to automated neonatal seizure detection," IEEE journal of biomedical and health informatics, vol. 17, no. 2, pp. 297–304, 2013.

[203] Mehla, V. K., Singhal, A., and Singh, P., "A novel approach for automated alcoholism detection using Fourier decomposition method," Journal of neuroscience methods, vol. 346, 2020.

[204] Raghu, S., Sriraam, N., "Classification of focal and non-focal EEG signals using neighborhood component analysis and machine learning algorithm," Expert systems with applications, 2018.

[205] Sharma, M., Dhere, A., Pachori, R. B., and Acharya, U. R., "An automatic detection of focal EEG signals using new class of time-frequency localized orthogonal wavelet filter banks," Knowledge–based systems, 2017.

[206] Sharma, R., Pachori, R. B., Acharya, U. R., "Application of entropy measures on intrinsic mode functions for the automated identification of focal electroencephalogram signals," MDPI, Entropy, 2015.

[207] Bhattacharyya, A., Pachori, R. B., and Acharya, U. R., "Tunable-Q wavelet transform based multivariate sub-band fuzzy entropy with application to focal EEG signal analysis," MDPI, Entropy, 2017.

[208] Dalal, M., Tanveer, M., and Pachori, R. B., "Automated identification system for focal EEG signals using fractal dimension of FAWT-based sub-bands signals," Machine intelligent and signal analysis, pp. 583–596, 2018.

[209] Arunkumar, N., Ramkumar, K., Venkatraman, V., "Classification of focal and non–focal EEG using entropies," Pattern recognition letters, 2017.

List of publications

Journal Publications

1. **Mehla, V. K.**, Singhal, A., Singh, P., "A Novel Approach for Automated Alcoholism Detection Using Fourier Decomposition Method," Journal of Neuroscience Methods, vol. 346 (108945), 2020. https://doi.org/10.1016/j.jneumeth.2020.108945. (Impact Factor: 2.21)

2. **Mehla, V. K.**, Singhal, A., Singh, P., Pachori, R. B., "An Efficient Method for Identification of Epileptic Seizures From EEG Signals Using Fourier Analysis," Physical and Engineering Sciences in Medicine, pp. 1–14, 2021. https://doi.org/10.1007/s13246-021-00995-3. (Impact Factor: 1.15).

Conference

1. **Mehla, V. K.**, Singhal, A., Singh, P., "EMD-based Discrimination of Mental Arithmetic Tasks From EEG signals," in Proceedings of IEEE India Council International Conference (INDICON), Delhi, India, December 2020, pp. 1–4. https://doi.org/10.1109/INDICON49873.2020.9342095

Book Chapters

1. **Mehla, V. K.**, Kumar, A., Singhal, A., Singh, P., Kumar, M., and Komaragiri, R. S., "Classification of Epileptic Seizure in EEG Signal Using Support Vector Machine and EMD," in Handbook of Research on Advancements of Artificial Intelligence in Healthcare Engineering, pp. 80–95, IGI Global. https://doi.org/10.4018/978-1-7998-2120-5.ch005.

2. **Mehla, V. K.**, Kumar, A., Singhal, A., and Singh, P, "Noise removal and classification of EEG signals using the Fourier decomposition method," in Modelling and Analysis

of Active Bio-potential Signals in Healthcare, vol. 1, pp. 6.1–6.27, IOP Science, 2020. https://doi.org/10.1088/978-0-7503-3279-8ch6.

Under communication

1. **Mehla, V. K.**, Singhal, A., Singh, P., "An Efficient Classification of Focal and Non-focal EEG signals Using Adaptive DCT Filter Bank Method," (submitted).

Biography of Virender Kumar Mehla

Virender Kumar Mehla received his B.Tech degree (first class with Honors) in Electronics and Instrumentation Engineering from M. M. Engineering College, Ambala, India in 2004, and M.E. degree in Instrumentation and Control Engineering from NITTTR Chandigarh in 2011. From August 2004 to June 2013, he worked as a lecturer and senior lecturer in the Electronics and Communication Engineering Department of N. C College of Engineering, Panipat. From October 2013 to August 2014, he worked as an assistant professor in the Department of Instrumentation and Control Engineering at JMIT, Radaur. He has worked for four years as an assistant professor and HOD in the Department of Electronics and Electrical Engineering at Asia Pacific Institute of Information Technology, SD INDIA, Panipat. He is currently pursuing Ph. D. degree in Electronics and Communication Engineering from the Bennett University, Greater Noida, Uttar Pradesh. His areas of interest are signal processing, biomedical signal processing, machine learning, etc.